



THE HONG KONG
POLYTECHNIC UNIVERSITY

香港理工大學

Pao Yue-kong Library

包玉剛圖書館

Copyright Undertaking

This thesis is protected by copyright, with all rights reserved.

By reading and using the thesis, the reader understands and agrees to the following terms:

1. The reader will abide by the rules and legal ordinances governing copyright regarding the use of the thesis.
2. The reader will use the thesis for the purpose of research or private study only and not for distribution or further reproduction or any other purpose.
3. The reader agrees to indemnify and hold the University harmless from and against any loss, damage, cost, liability or expenses arising from copyright infringement or unauthorized usage.

IMPORTANT

If you have reasons to believe that any materials in this thesis are deemed not suitable to be distributed in this form, or a copyright owner having difficulty with the material being included in our database, please contact lbsys@polyu.edu.hk providing details. The Library will look into your claim and consider taking remedial action upon receipt of the written requests.

**FUNDAMENTALS OF SELECTIVE ULTRASONIC BRAIN
STIMULATION**

ZHIHAI QIU

PhD

The Hong Kong Polytechnic University

2019

The Hong Kong Polytechnic University
Department of Biomedical Engineering

Fundamentals of selective ultrasonic brain stimulation

Zhihai Qiu

**A thesis submitted in partial fulfillment of the requirements
for the
degree of Doctor of Philosophy
August 2018**

Certificate of Originality

I hereby declare that this thesis is my own work and that, to the best of my knowledge and belief, it reproduces no material previously published or written, nor material that has been accepted for the award of any other degree or diploma, except where due acknowledgement has been made in the text.

(Signed)

Zhihai Qiu

(Name of Student)

Abstract

Ultrasonic brain stimulation is well recognized as an encouraging method for probing brain function and treating brain disorders with the advantages of non-invasiveness, fine spatial control, and deeper tissue penetration. The focal spot can be steered dynamically in brain wide with high spatiotemporal resolution. Recently, various studies have shown that ultrasound can be utilized to modulate neuronal activity and signaling in animal and human brain effectively without damaging brain tissues. However, the mechanism is unclear. In addition, the minimum focal spot of a low frequency ultrasound beam is still much larger than a single neuron or a specific small set of neurons, so it is difficult to probe the complex neural circuits entangled with interdependent different neurons. The stimulation outcome of current approach is not easy to be predicted and even controversial. Therefore, understand the mechanism of ultrasound brain stimulation and engineering the ability to stimulate a selected subset of neurons is a key issue for precise ultrasound neuro-modulation for future application and translation.

Ultrasound is a mechanical wave which can insert various mechanical perturbations onto the tissue. Recently, mechanical perception of the cells has gain momentum with the discovery of various mechanosensitive ion channels with wide spectrum of mechanosensing properties. It has been hypothesized that ultrasound could activate mechanosensitive ion channels. It is emergent to test in mammalian cells. In addition, inspired by optogenetics, to achieve targeted ultrasound stimulation, one can rely on altering neuronal sensitivity by inserting artificial ultrasonic sensitive ion channels to chosen neurons. The targeting ability of such ultrasonic sensitivity could be achieved either by genetic approach or biochemical targeting technology. The discovery of the

underlying mechanism will make it possible to develop a analogue strategy to optogenetics, for selective neural activation and inhibition in deep brain regions non-invasively. The selectivity of such method relies on altering neuronal ultrasound sensitivity by inserting mechanosensitive proteins which will transduce ultrasonic energy into electrochemical signaling and induce neural activity and subsequent downstream intracellular signaling to chosen neurons using genetic modification method. To achieve, it is emergent to discover the effective ion channels for initiate ultrasound neuron stimulation and obtain solid knowledge about the biophysical mechanism. In addition, toolkits should be validated *in vivo* and its application should be developed and well-characterized.

The present thesis explored the mechanism of ultrasound brain stimulation and the way to develop toolkits for achieving selective ultrasound stimulation in *in vivo* rodent model. This thesis is a summary of the past three-years exploration in ultrasound brain stimulation. The output of these thesis provides a critical approach for selective brain stimulation with a non-invasive, deep brain targeted and selective stimulation technique, with or without genetic modification and invasive procedure. I also envision that the outcome of this thesis could provide an invaluable tool for screening mechanosensitive proteins as well.

Keywords: Ultrasound brain stimulation, mechanosensitive ion channels, selective brain stimulation, neuroscience, brain diseases, optogenetics, sonogenetics, acoustic mechanogenetics

PUBLICATIONS ARISING FROM THE THESIS

- [1] **Zhihai Qiu**, Jinghui Guo,and Lei. Sun* et. al. Selective ultrasound brain stimulation via activation of Piezo1. *In submission.*
- [2] **Zhihai Qiu**, andLei Sun et. al. Noninvasive ultrasonic selective brain stimulation, *In submission.*
- [3] **Zhihai Qiu**, Jinghui Guo,.... Hairong Zheng, Lei Sun*. Towards precise manipulation of neuron activity by ultrasound: via modulating ion channels to beyond. *In submission*
- [4] **Zhihai Qiu**, Quanxiang Xian, ...Lei Sun*. Ultrasound stimulation on C.elegans. *In submission*
- [5] **Zhihai Qiu**, ...et al. Ultrasonic sensitivity of neurons enabled by gene encoded ultrasound responsive gas nano vesicles. **In submission**

Patent

- [1] Lei Sun, **Zhihai Qiu** et al, Non-invasive and selective brain stimulation, US patent, Pending.
- [2] Lei Sun, **Zhihai Qiu** et al, Ultrasonic mechnogenetics enabled by biogenic nano gas vesciles. US patent, pending.

Conference presentations

- [1] **Zhihai Qiu**, Lei Sun et al. Ultrasound brain stimulation by activating Piezo1, IUS, IEEE, Kobe, Japan, 2018

- [2] **Zhihai Qiu**, Lei Sun et al. Non-invasive and selective brain stimulation by ultrasound via activation of mechanosensitive ion channels, SfN, San Diego, USA 2018
- [3] **Zhihai Qiu**, Lei Sun et al. Non-invasive and selective brain stimulation by ultrasound, CSHL, New York, USA, 2018
- [4] **Zhihai Qiu**, Lei Sun et al. Precise control of neuronal activity by ultrasound: Fundamentals and toolkits, IUS, IEEE, Washington DC, USA, 2017
- [5] **Zhihai Qiu**, Lei Sun et al. Sonogenetics by ultrasound activation of mechanosensitive ion channels, Mechanobiology, Singapore, 2017
- [6] **Zhihai Qiu**, Lei Sun et.al. selective ultrasound neuron stimulation, HHMI, Janelia conference: From light to sound, frontiers in deep tissue imaging, 2017. Travel scholarship.
- [7] **Zhihai Qiu**, Lei Sun et.al. Control of neuron activity by sonogenetics. Sfn2016, San Diego, 2016 (Nanosymposium)
- [8] **Zhihai Qiu**, Lei Sun at. al. Fundamentals of precise ultrasonic brain stimulation, CSHA, Suzhou, China, 2017
- [9] **Zhihai Qiu**, Lei Sun et al. Acoustic mechnogenetics: a non-invasive tool for probing brain function.CSHA, Suzhou, China, 2016 (Oral)
- [10] **Zhihai Qiu**, Lei Sun et al. Control of neuron activity by mechanogenetics. Mechanobiology of Disease, Singapore, 2016 (Poster)
- [11] **Zhihai Qiu**, Lei Sun et al. Sensing ultrasound promotes axon growth during development, 2nd Brain stimulation, Barcelona, Spain, 2017 (Poster)

- [12] **Zhihai Qiu**, Lei Sun et al. Imaging of ultrasound stimulation on zebrafish neural development with light-sheet microscopy, 2nd Brain stimulation conference, Barcelona, Spain, 2017 (Poster)
- [13] **Zhihai Qiu**, Lei Sun et al. Acoustic mechanogenetics: a promising tool for probing brain function, 2nd Brain stimulation conference, Barcelona, Spain, 2017 (Poster)
- [14] Puxiang Lai, Tianting Zhong, **Zhihai Qiu**, et al. Temporal evolution optogenetics enabled by wavefront shaping technology. Photonics Asia, Beijing, China, 2018
- [15] Rui Zhang, **Zhihai Qiu** et al. Study of Piezo1 Localization and Transportation Dynamics by Light-sheet Microscopy. PIBM, 2017
- [16] Fei Cao, **Zhihai Qiu** et al. Non-linear photoacoustic imaging by Pump-Probe Excitation. PIMB, 2017
- [17] Yaoheng Yang, **Zhihai Qiu**, et al. Enhanced sonodynamic therapy using oxygen-rich nano gas vesicle. 17th International Symposium on Therapeutic Ultrasound, Najing, China, May 31- June 2, 2017
- [18] Yaoheng Yang, **Zhihai Qiu**, Lei Sun. Biogenic nano gas vesicle- An active probe for cellular biophysics. Cold Spring Harbor Asia conference on New Advances in Optical Imaging of Live Cells and Organisms. Suzhou, China, Dec 7-11 2015

ACKNOWLEDGEMENTS

First and foremost, I would like to express my sincere gratitude to Dr. Lei Sun, my supervisor, for being my advisor, mentor and launching my academic career. His profound knowledge and wisdom lead me to think smart differently not only in academic but also in daily maybe boring life. I still remember the first talk with him in his office, he told me that do not limit myself by any unnecessary assumptions. Besides, he created a wonderful scientific environment for me, providing an incomparable opportunity for shaping my career and personal integrity.

I also like to thank my mother. She is a traditional farmer in a small country yard. She is kind, wise, and love this world. I also thank my elder sister and her husband, without their support, it is impossible for me to go out for my dream as I was supposed to run the entire family. She has always had confidence in me and supported me all the time. My research life is full of cheerfulness because of their accompanying.

I would like to thank Prof. Hsiao Chang Chan, Dr. Mo Yang, Dr. Guofeng Li, Prof. Ming Zhang, Prof. Ed X. Wu, for assessing my proposal, confirmation report, and dissertation, providing valuable suggestions and pointing out problems existing in my work and presentations. I am also grateful to many colleagues, who learned along with me, for maintaining a stimulating and flexible working environment, most notably Dr. Jinghui Guo, Ms. Rui Zhang, Mr. Yaoheng Yang, Ms. Jiejun Zhu, Ms. Quanxiang Xian, Ms. Shashwati Kala, Mr. Xuandi Hou, Ms. Ting Zhu, and Dr Chunlong Fei from Xi'dian University, I would like to thank them for helping me in both technical assistance and living aspects.

My special thanks go to Mr. Yaoheng Yang. He is a good friend not only in academic but also in my daily life.

Finally, the financial support from the Hong Kong Research Grant Council (RGC) General Research Fund (GRF) (PolyU 5301/09E), and The Hong Kong Polytechnic University (A-PJ84) are gratefully acknowledged.

ACADEMIC AWARD

- [1]. Biophysical Journal Outstanding Poster Award in the student category at the Mechanobiology of Disease, Biophysical society, Singapore, 2016
- [2]. Young Investigator Travel Award, 2nd International Brain Stimulation Conference, Barcelona, Spain, 2017
- [3]. Travel Scholarship, Janelia conference: From light to sound, frontiers in deep tissue imaging, Washington. DC, 2017
- [4]. Third Prize of Tianqiao and Chrissy Chen Fellowship, Cold Spring Harbor Asia, Francis Crick Symposium- Transforming Neuroscience: Questions and Experiments. Suzhou, China, 2017
- [5]. Talent Development Scholarship, HKSAR Government Scholarship Fund, 2016/17
- [6]. Noninvasive brain stimulation session Chair, SfN, Wanshington DC. 2017
- [7]. Best Student Oral Presentation Award, The 8th WACBE World Congress on Bioengineering, Hong Kong, 2017
- [8]. Travel Award for IEEE International Ultrasonics symposium, Washington, DC. 2017.
- [9]. 1st Runner-up, The Hong Kong Medical and Healthcare Device Industries Association Student Research Award, Hong Kong, 2017
- [10]. Tianqiao and Chrissy Chen Fellowship, Cold Spring Harbor Laboratory, NY, USA, 2018

TABLE OF CONTENTS

Certificate of Originality	III
Abstract.....	IV
PUBLICATIONS ARISING FROM THE THESIS	VI
ACKNOWLEDGEMENTS.....	IX
ACADEMIC AWARD.....	XI
TABLE OF CONTENTS.....	XII
LIST OF FIGURES	XIV
LIST OF TABLES	XXII
Chapter 1: Towards precise manipulation of neuron activity by ultrasound via modulating ion channels to beyond	1
1. Introduction	2
2. Basics of ultrasonic physical effects.....	8
3. Mechanism of ultrasound neuron stimulation: theories, evidences and controversies	13
4. Strategies towards selective ultrasound brain stimulation.....	19
5. Challenge and future perspectives.....	25
6. Summary.....	26
Chapter 2: Proof-of concept:.....	28
Brain stimulation via ultrasonic activation of Piezo1	28
1. Introduction	29
2. Results and discussion	32
3. Materials and Methods:.....	47
Chapter 3: Toolkit for non-invasive brain stimulation by ultrasound	59
Sonogenetics enabled by MscL	59
1. Introduction	60
2. Materials and Methods:.....	76
Chapter 4: Toolkit for non-invasive brain stimulation by ultrasound	86

Biogenetic acoustic actuator for mediating neuronal activity..... 86

- 1. Introduction** 87
- 2. Results and discussion** 89
- 3. Materials and methods** 100

Chapter 5: Conclusion and outlook..... 104

- 1. Applications** 109
- 2. Challenges** 112
- 3. Philosophy** 116

References 119

LIST OF FIGURES

Figure 1 Ultrasound brain stimulation. Ultrasound at lower frequency can penetrate through the skull and be focused into a small region to modulate the neurons. The interaction of ultrasound waves with neurons is still unclear. Several mechanisms have been proposed but without strong evidence to support.	3
Figure 2 the existed brain stimulation methods are based on the nature of the brain. Although, brains are considered as electrical and chemical in nature, there are more and more evidences showing that brains are mechanical, thermal sensitive. There is several theory pointing out mechanics could be the really nature of an action potential, and there are mechanical waves accompanying with an action potential which is an electrical wave. In addition, artificial photosensitivity has been created in CNS neurons in addition to retinal.	5
Figure 3 Key concerning for brain stimulation	6
Figure 4 Wave-front shaping for (a) engineering the spatial pattern [5], (b) unique acoustic field generated by 3D printed masks [7], and (c) engineered electrical wave for deep brain stimulation [11].	11
Figure 5 Different ultrasound transducers: (a) various ultrasound transducers; (b) focused ultrasound field and (c) Fresnel ultrasound beam generated by the Fresnel lens based transducer in (a)	12
Figure 6 Evidences showing ultrasound modulation on mechanosensitive ion channels [31]	16
Figure 7 Intramembrane cavitation coupling with H&H model as mechanism of ultrasound neurons stimulation [15].	18
Figure 8 Strategies towards selective ultrasound neuron stimulation. A) Ultrasound pressure/intensity lower down to which act on untargeted neuron no obvious effects can be observed while B) ultrasound sensitive ion channel overexpressed neurons, C) ultrasonic mechanogenetics; D) Piezoelectric nanoparticle mediated ultrasound brain stimulation.....	20
Figure 9 Publication of non-invasive and selective brain stimulation (Optogenetics) each year	26

Figure 10 Functional validation of Piezo1 expression in 293T cells. Yoda1, a Piezo1 agonist, induces significantly higher calcium influx in 293T cells overexpressing Piezo1 than in control cells. 32

Figure 11 Ultrasound induces intracellular calcium influx by Piezo1 activation. (A) The experimental scheme for this study. Cells are sensitized to ultrasound stimulation by inducing the expression of mechanosensitive ion channels, such as Piezo1. Treatment by ultrasound can hence open Piezo1, allowing Ca^{2+} into the cell and setting into motion calcium-related signaling. (B) Piezo1 overexpression in 293T cells transfected with the Piezo1-containing plasmid, as evaluated by Western blot and RT-qPCR. Graphs show mean \pm SEM from three independent experiments, * $P < 0.05$, unpaired t-test. (C) Ultrasound induces dose-dependent calcium influx in 293T cells overexpressing Piezo1. Ultrasound stimulating mode: each stimulus contained 200 tone bursts of 500 kHz ultrasound at 1 kHz RPF, 200 cycles, and 0.1 MPa, 0.2 MPa, and 0.3 MPa. *** $P < 0.001$, unpaired t-test. (D) Ultrasound induces dose-dependent calcium influx in primary cortical neurons through Piezo1. Piezo1 expression in primary cortical neurons was confirmed by immunocytochemical staining; Green: Piezo1; Red: MAP2; DAPI: Blue. Ultrasound stimulation induced significant increase of intracellular calcium of the neuron, comparable to the effect of Yoda1, a chemical agonist of Piezo1. * $P < 0.05$, *** $P < 0.001$, one-way ANOVA with post-hoc Tukey test. (E) Primary neurons made to overexpress Piezo1 by plasmid transfection accumulate more intracellular calcium when treated with ultrasound than do neurons treated with a control plasmid..... 34

Figure 12 Ultrasound regulates the activity of calcium-related signaling and downstream gene expression profile. (A) The expression of Piezo1 in mouse primary cortical neurons was examined in two ways. Left: Representative images of Piezo1 and MAP2 immunocytochemical staining of primary neurons at DIV 10. Right: (B) Ca^{2+} imaging of primary neurons stimulated with Piezo1 agonist Yoda1, including cells pre-treated with Piezo1 blocker GsMTx-4. Top: Representative Ca^{2+} imaging time-course for cells treated with either 10 μ M Yoda1 alone, or pre-treated with 40 μ M GsMTx-4 respectively. Bar charts show the mean \pm SEM of 3 independent experiments. $n = 15$, *** $P < 0.001$, unpaired two-tailed t-test. (C) Ca^{2+} imaging of primary neurons stimulated with ultrasound, including cells pre-treated with GsMTx-4. Top: Representative Ca^{2+}

imaging time-course of primary neurons treated with 0.45 MPa ultrasound, or pre-treated with 40 μ M GsMTx-4 and then with ultrasound. Bottom: Bar chart represents mean \pm SEM of 3 independent experiments treating primary neurons with varying intensities of ultrasound and GsMTx-4. n = 9, * P < 0.05, ** P < 0.01, *** P < 0.001, one-way ANOVA with post-hoc Tukey test. (D) An illustration of the ultrasound setup used to treat cells placed inside a cell culture incubator for immunofluorescence or Western blots. The ultrasound was illuminated from the bottom and there a coupling waveguide between the ultrasound transducer and dish. (E) Left: Representative IF images of c-Fos and MAP2 staining, in cells that were untreated, treated with 0.3 MPa ultrasound, or with 20 μ M GsMTx-4 followed by ultrasound. Right: Bar chart represents the mean \pm SEM of 3 independent experiments. n = 3, * P < 0.05, ** P < 0.01, one-way ANOVA with post-hoc Tukey test. 37

Figure 13 Ultrasound induces mouse body movement in vivo mediated by Piezo1 (A)

The levels of Piezo1 in a mouse neuronal cell line, CLU199, evaluated in two ways. Left: PCR results of Piezo1 expression in multiple samples of CLU199 cells, with HeLa cells for comparison. Right: Western blot of Piezo1 expression in multiple samples of CLU199. (B) Western blot for expression levels of p-CaMKII, p-CREB and c-Fos, in CLU199 cells treated with varying ultrasound intensities. Left: Representative Western blot images. Right: Bar charts show the levels of each protein as a fold change compared to the untreated control. Results are mean \pm SEM of 3 independent experiments. n = 3, * P < 0.05, unpaired two-tailed t-test. (C) Piezo1 was knocked down in CLU199 cell using non-targeting ('Ctrl') or Piezo1 siRNA ('Piezo1 KD'). Left: qRT-PCR was performed for Piezo1, normalized to β -actin and expressed as a fold change. Bar charts represent mean \pm SEM of 3 independent experiments. n = 3, ** P < 0.01, unpaired two-tailed t-test.. Also shown are representative IF images of Piezo1 staining in CLU199 cells. Middle: Representative Ca²⁺ imaging time-course for Ctrl and Piezo1 KD cells treated with Yoda1. Right: Bar chart shows the mean \pm SEM of 3 independent Ca²⁺ imaging experiments. n = 9, *** P < 0.001, unpaired two-tailed t-test with Holm-Sidak correction. (D) Western blot for levels of p-CaMKII, p-CREB and c-Fos in CLU199 cells treated with siRNA and ultrasound. Left: Representative Western blot images. Right: Bar charts show the levels of each protein as a fold change compared to the untreated control. Results

are mean \pm SEM of 3 independent experiments. n = 3, * P < 0.05, unpaired two-way ANOVA with post-hoc Tukey test..... 40

Figure 14 Selective brain stimulation via activation of Piezo1 in vivo. Top: The in vivo experimental scheme for this study. Mouse brains were made to overexpress Piezo1 by injecting plasmid locally into the M1 region. 3 days later mice were treated with ultrasound, in either an anesthetized or free-moving state; Bottom: Piezo1 was successfully expressed in M1 of mouse brains, 3 days after plasmid injection. (B) A higher rate of tail flicks is induced by ultrasound stimulation (0.1 - 0.6 MPa) in Piezo1-transfected mice than that of control mice under anesthesia. No significance found by a two-tailed unpaired t-test, n = 3. (C) Ultrasound (0.3 MPa) induces a higher rate of head movement in Piezo1-transfected mice than in control mice when moving freely, n was labelled in the columns, *P < 0.05, two-tailed unpaired t-test. (D) c-Fos expression after ultrasound stimulation is significantly higher in Piezo1-transfected mice than in control mice. *P < 0.05, two-tailed unpaired t-test, n = 3. 43

Figure 15 In vitro experimental system. *This setup combines a calcium imaging system and an ultrasound stimulation system.* 50

Figure 16 Strategies for probing brain function. To dissect the neural circuits, it is required established a behavior model and then detect the structural, functional changes correlated to the behavior. However, to get causal information, it still needs an external stimulation modality to excite or inhibit neural activity. This stimulation modality can also translate as a treatment technique. 60

Figure 17 Ultrasound induces intracellular calcium influx by MscL activation in 293T cells. (A). Schematic representation of our experimental plan. Briefly, this involves sensitizing cells to ultrasound by heterologously expressing a mechanosensitive ion channel, MscL-G22S, in their cell membranes. Thereafter, these channels will react to ultrasound stimulation by opening, and allow the entry of cations such as Ca²⁺. (B) The expression of MscL-G22S in transfected cells was assessed by qRT-PCR and microscopy, in comparison with a mock-transfection control. Left: The bar chart of qPCR results represents mean \pm SEM of three independent experiments, n = 3, *** P < 0.001. Right: Representative images of GFP fluorescence and phase contrast are shown. (C) An illustration of our patch clamp recording setup. The ultrasound stimulation system is

composed of a needle transducer incorporated into a patch clamping system. **(D)** Left: Current clamp recording of inward-flowing current in cells stimulated by 0.05 MPa ultrasound (US). Right: t voltage clamp experiments, $n = 4$ * $P < 0.05$, unpaired two-tailed t-test. **(E)** A schematic illustration of the combined ultrasound stimulation and calcium imaging system used. **(F)** Left: A representative time-course of ratiometric Ca^{2+} imaging comparing ultrasound stimulation of Control and MscL-transfected cells at 0.15 MPa. Right: The bar chart shows the mean \pm SEM of 3 independent Ca^{2+} imaging experiments. $n = 9$, * $P < 0.05$, *** $P < 0.001$, two-tailed unpaired t-test with Holm-Sidak correction. 64

Figure 18 Ultrasound regulates the neural activity of calcium signaling and electrophysiology. (A) Representative immunocytochemical staining of primary neurons transduced with rAAV/9-hSyn-EYFP-pA and rAAV/9-hSyn-MscL-G22S-EYFP-pA viruses at DIV 12. Cells were imaged for MAP2 (red) staining and EYFP fluorescence (green) to confirm the virus' ability to preferentially transduce neurons. (B) (Upper) Voltage clamp recordings of virus-transduced primary neurons treated stimulated with 0.05 MPa ultrasound. (Lower) Bar charts show the mean \pm SEM spike frequencies and amplitudes of 3 independent experiments. * $P < 0.05$. *** $P < 0.001$, unpaired two-tailed t-tests. (C) (Left) Representative Ca^{2+} imaging result of primary neurons transduced with rAAV/9-hSyn-GCaMP6S-pA and rAAV/9-hSyn-MscL-G22S-GCaMP6S-pA viruses, and stimulated with 0.15 MPa ultrasound at DIV 12. (Middle) Representative time-course of Ca^{2+} imaging of transduced neurons stimulated with ultrasound. (Right) Bar charts represent mean \pm SEM of neurons stimulated with ultrasound at varying intensities from 3 independent experiments. $N = 6$, *** $P < 0.001$, unpaired 2-tailed t-tests with Holm-Sidak correction. 66

Figure 19 Resting membrane potentials of transduced primary neurons. Resting membrane potentials of primary neurons transduced with Ctrl-EYFP or MscL-EYFP viruses. Bar chart represents mean \pm SEM of at least 3 independent experiments, n for Ctrl = 4, n for MscL = 6. Differences are non-significant according to an unpaired 2-tailed t-test..... 68

Figure 20 Additional data from mice. A. (Left) Representative images of M1 areas of mouse brains in the sham group, with and without ultrasound, stained for c-Fos. (Right)

Bar charts represent mean \pm SEM, n = 3. Differences are non-significant according to an unpaired 2-tailed t-test. B. Body weight measurements of mice with sham transduction, and transduced with the Ctrl-EYFP and MscL-EYFP viruses. Scatter plot shows body weights of different mice and mean \pm SD are shown. Differences are non-significant according to one-way ANOVA with post-hoc Tukey test. 70

Figure 21 Ultrasound induces c-fos expression in MscL expressing neurons. (A) Schematic illustration of our in vivo neuron sensitization and ultrasound stimulation plan. Mice at 8 weeks were injected with viruses in their M1 regions and were treated with ultrasound 5 weeks later. The mice were tested for motor responses to ultrasound and their M1 regions stained for c-Fos expression. (B) (Left) Representative images of transduced M1 regions stained for c-Fos and EYFP expression, with or without 0.3 MPa ultrasound. Bars represent 100 μ m. (Right) Bar charts represent mean \pm SEM of c-Fos+ cells per stained slice. n for Ctrl groups = 3 and n for MscL groups = 6. * P > 0.05, ** P > 0.01, unpaired 2-tailed t-test with Holm-Sidak correction. (C) Schematic illustration of the motor response assay used. The mice were stimulated with ultrasound and various intensities, and the movement considered a ‘response’ is shown here. The ratio of responses per ultrasound stimulus was recorded as a ‘success rate’. (D) Success rates of motor response per ultrasound stimulus at varying ultrasound intensities. Results are mean \pm SEM, n = 3, * P > 0.05, unpaired 2-tailed t-test with Holm-Sidak correction. 72

Figure 22 Ultrasound stimulation of anesthetized mice 85

Figure 23 GVs mediated ultrasound neural stimulation (A) scheme of nano-bubbles mediated neuron stimulation by interacting with membrane surface proteins upon ultrasound illuminating; (B) calcium imaging of neurons with and without GVs before and ultrasound stimulation. There is no difference between GCaMP6s fluorescence imaging with and without GVs before ultrasound stimulation while GVs group shows significant higher GCaMP6s fluorescence after ultrasound stimulation; (C) temporal profile of ultrasound induced calcium change with and without GV. Upon ultrasound stimulation, there is a fast activation of GCaMP6s at 30; D) time-resolved stimulation induced calcium responses. Neurons were stimulated with different interval time, and induced precise calcium responses from 60s, 30s, 20s, 10s, 5s, to 3s. The subsecond

stimulation were characterized with a fast dopamine sensor as indicated in other sessions.
..... 90

Figure 24 Characterization of ultrasound effects on CLU199 neural cell line. Calcium imaging of CLU199 before (A); and after (B) ultrasound stimulation; (C) the statistics of fluorescence differences before and after ultrasound stimulation; (D)The dependence of calcium responses as a function of the concentration of GVs; 91

Figure 25 intracellular release and calcium influx induced by ultrasound in: A) CHO cells and B) CLU199 cells. The most significant responses were observed in the normal condition with calcium ions that are like physiological conditions. Movement of calcium ions in extracellular solution reduced the effects dramatically, indicating there were intracellular calcium release as confirmed by using TG to chelate the intracellular calcium store. On the other hand, blockage of mechanosensitive ion channels by RR also reduced the calcium responses. In these conditions, the calcium responses are significantly different with the control group which without any GVs. Comparing the CHO and CLU199 Cells, it is found that the CLU199 has much larger responses as there are more mechanosensitive ion channels expression. 93

Figure 26 Temporal calcium responses upon ultrasound stimulation for different cell types. Different cell lines are utilized in this case studies. The amplitude of the responses was normalized. The calcium response shows great synchronizations with ultrasound stimulation..... 94

Figure 27 Ultrasound is a non-invasive and selective brain stimulation modality. There are various selective neuromodulation technologies from DREAD, optogenetics, to other analogical modalities. However, there isn't any method that can targeted neural stimulation non-invasively. Now, we add ultrasound stimulation to this list. 105

Figure 28 summary of the different strategies include in this thesis; A) sonogenetics enabled by MscL-G22s; B) acoustic mechanogenetics mediated by biogenic gas vesicles. The first strategy is a genetics-based technology which requires genetic modifications in CNS. This procedure could raise the safety concern. The second strategy with NGV mediated 106

Figure 29 the road to biophysical mechanisms. A) Cell membranes are lipid bilayer which can be stretched, bended under different conditions. There were varied ion channels

embedded in cell membranes. Upon ion channels opening, the cell membrane will be polarized or depolarized to give rise to neural activates. The wavelength of ultrasound at mm range are much longer than the size of an ion channel protein. Thus, the biophysical mechanism is underlying the interaction among ultrasound, cell membranes, and ion channels:

B) Membrane dynamics under ultrasound stimulation..... 108

Figure 30 one of the possible future development of ultrasound based closed loop stimulation system for targeting Dopaminergic neurons. 112

Figure 31 Road map to clinical translation..... 114

Figure 32 Single neuron activation by high frequency ultrasound 115

LIST OF TABLES

Table 1 Ultrasonic physical effects. The relationship with different parameters and the physical conditions are summarized. The scales of these effects are estimated. 10

Chapter 1: Towards precise manipulation of neuron activity by ultrasound via modulating ion channels to beyond

Ultrasound neuromodulation methodology could enable possible way of stimulation of specific brain region for inhibition or excitation while treating neurodegenerative disease. Although the impact of this temporal versatility has been greater for clinical research due to its non-invasive advantage, it is however, lacks understanding on how it works. In addition, it is natural to ask its accuracy for treating disease and whether it can be a tool for precise probing the dynamic patterns of neural circuit activity to revealing causal information of brain function. Here, we consider the landscape of ideas related to precise control of neuron activity by using ultrasound. Specifically, we highlight the possible mechanism including interaction of ultrasound with ion channels, and the chemo-, electrical, and thermal- cues. Finally, we discuss the strategies towards precise neuron stimulation based on these possible mechanisms.

1. Introduction

In the brain, billions of neurons work together as an intricately organized, interconnected circuit, supporting the vast diversity of animal behavior, up to advanced functions like consciousness, cognition, and emotion (1-4). These neural circuits are both extremely complex and exquisitely specific, and the connectivity motifs used to build these circuits vary widely across the whole brain (5, 6). Understanding the brain function requires testing hypotheses with precise control of the circuits operation to determine the behaviorally relevant dynamics circuits (7, 8). Achieve precise stimulation of specific types or sub-types of neurons involved in each circuit to identify its role in the brain function as well as to modulate brain dysfunctions are major goal in neuroscience (9, 10).

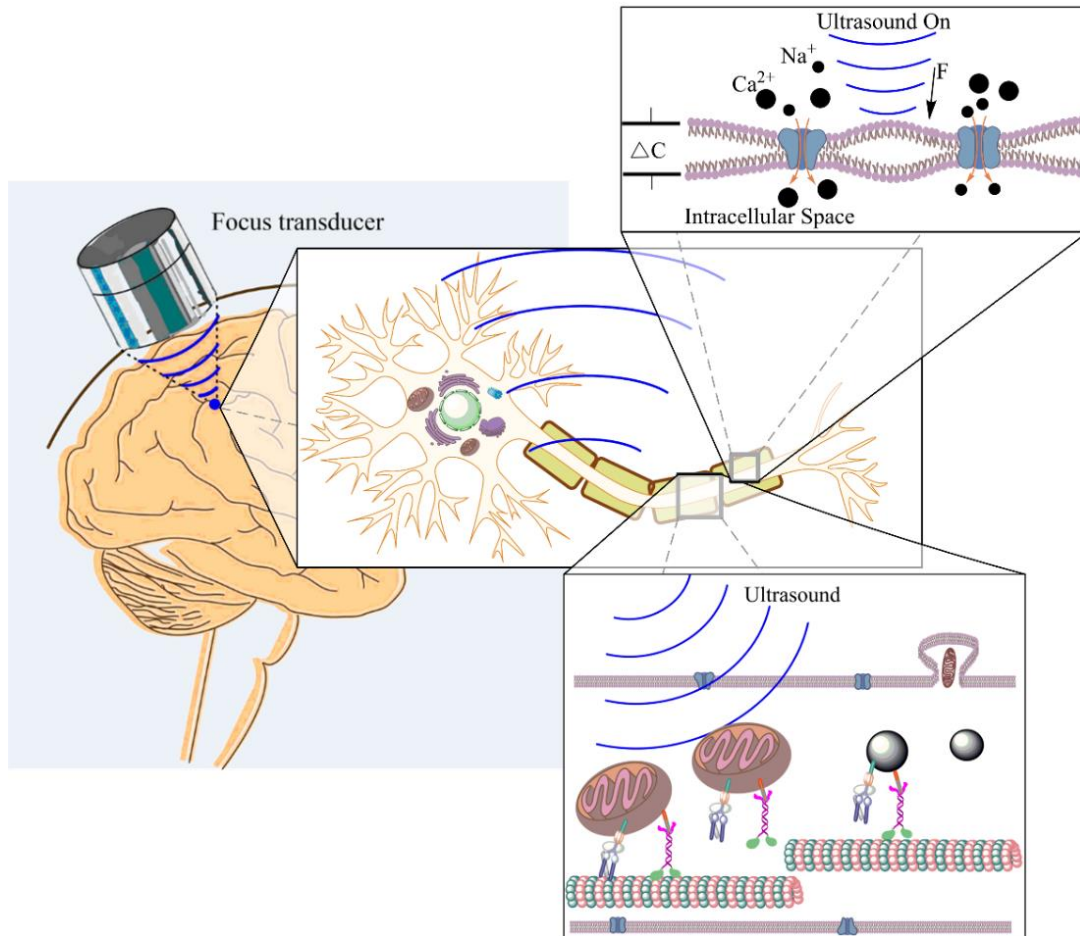


Figure 1 Ultrasound brain stimulation. *Ultrasound at lower frequency can penetrate through the skull and be focused into a small region to modulate the neurons. The interaction of ultrasound waves with neurons is still unclear. Several mechanisms have been proposed but without strong evidence to support.*

The development of non-invasive, precise stimulation modality with high spatiotemporal resolution is an open challenge in the scientific society(4, 6). Based on the neuron sensitivity (Fig. 2) to different physical factors, varied stimulation strategies for neuromodulation and brain stimulation have been proposed and developed. Last decade has witness rapid advances of understanding brain function with the development of novel brain stimulation toolkits, for example optogenetics, which can selectively label and

stimulate given neuron types (11-25). More and more neural circuits for advanced brain functions, such as cognition, social behavior and learning and memory etc., are being discovered (23, 26-32). Optogenetics are based on artificial inserted well-characterized light sensitive proteins (e.g. opsins) to the chosen neurons, which are enabled to respond to light stimulation, while leaving other cells silent with the same dose of light stimulation (12, 14, 15, 18, 20, 23). However, the limited penetration depth of light in brain tissue makes it invasive and the stimulation are constrained in a small region. The stimulation thus is mechanically invasive which could cause severer side-effects and it is possible to miss the circuits in deep brain with long range projection (15, 19, 21). The invasiveness nature of optogenetics makes it challenge to be translated into clinical application.

On the other hand, there are some other stimulation modalities with less invasiveness or non-invasiveness, such as transcranial magnetic stimulation (TMS), transcranial direct current stimulation (tDCS) etc., that have been utilized to treat brain disease and dysfunction (33-35) in clinical conditions. They showed various advantages and have great values in clinical practice, but lack spatiotemporal resolution, nor can they pinpoint to single neurons or neuron types in a small region. In such a complex environment in brain, the stimulation could be canceled out or even cause undefined side effects.

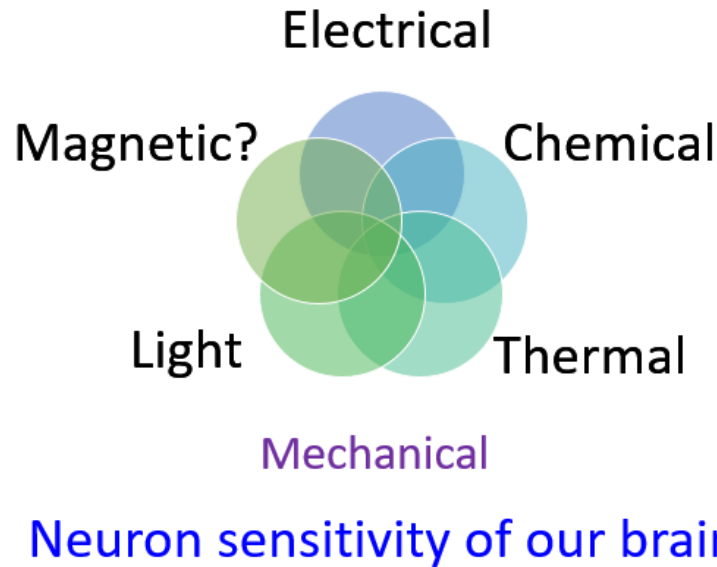


Figure 2 the existed brain stimulation methods are based on the nature of the brain.

Although, brains are considered as electrical and chemical in nature, there are more and more evidences showing that brains are mechanical, thermal sensitive. There is several theory pointing out mechanics could be the really nature of an action potential, and there are mechanical waves accompanying with an action potential which is an electrical wave. In addition, artificial photosensitivity has been created in CNS neurons in addition to retinal.

To achieve precise neuro-stimulation with high spatiotemporal resolution noninvasively, various strategies have been explored to improve the performance of the existing methods by either extending the penetration depth or improving targeting ability and spatiotemporal resolution. For example, to extend the penetration of optogenetics, longer wavelength photosensitive ion channels and up-conversion nanoparticles for converting longer wave light to blue light have been developed, as longer wavelength light can penetrate deeper into the brain (19, 36, 37)[15-16] for minimal optogenetics. But

brain tissues are highly scattering, even longer wavelength has limited penetration depth, and it is difficult to be focused in deep brain tissues while the up-conversion nanoparticles are suffered from the low efficiency of converting longer wavelength to blue light. With complicated wave front-shaping techniques, it is possible to generate better focus of waves, e.g. electromagnetic wave or electrical wave, in deep brain(38-41). Most recently, a good example is by temporal interfered electrical field to achieve focal stimulation in deep brain as a great potential for treating brain disease (38). Collectively, great efforts have been conducted towards the goal of non-invasive, precise stimulation with high spatiotemporal resolution which could have significant impact on the fundamental neuroscience research and may become a good tool for probing brain functions and treating brain diseases (Fig. 3).

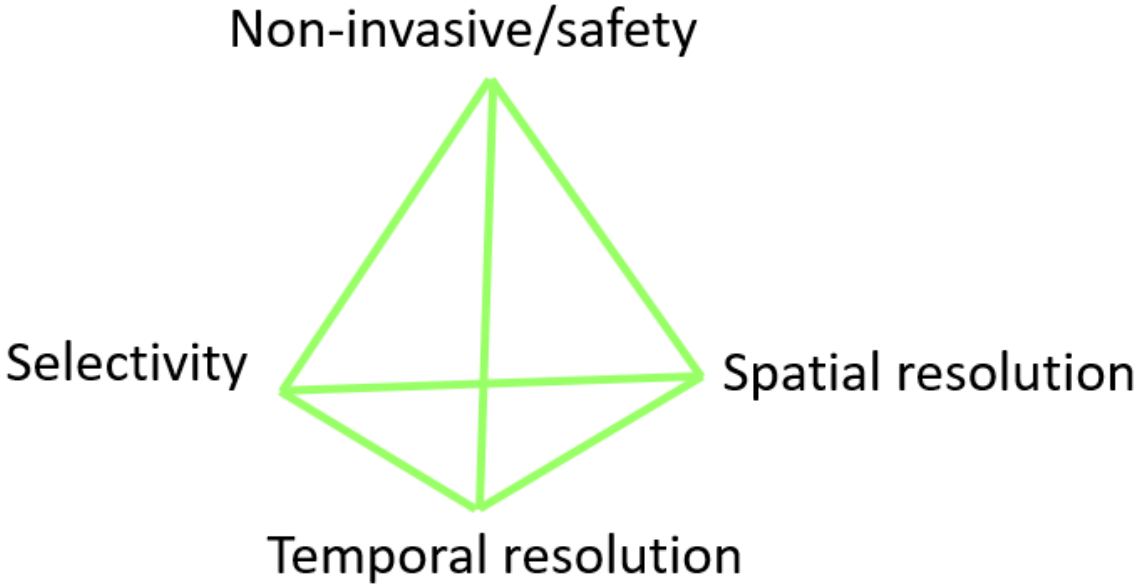


Figure 3 Key concerning for brain stimulation

Among these methods, low intensity low frequency ultrasonic brain stimulation has made great advances in the last few years. Ultrasound beam can be focused into a small region in deep brain tissues without any observable damage to the brain tissues. It has been demonstrated capable of stimulating prefrontal cortex and improving task in human without side effects (24, 42-56). It has also been shown that ultrasound can be used to stimulate visual cortex in monkeys (52). Ultrasound stimulation has good spatiotemporal resolution and neurons could be either activated or suppressed depending on different ultrasound parameters and different stimulation locations(57) (48, 58, 59). People are also trying to use ultrasound to treat Parkinson's disease, epilepsy, as well as mental diseases like depression (58). Recently, it is found that being incorporated with circulating microbubbles, ultrasound can treat Alzheimer's disease(60).

Because of these encouraging results, it is considered as one of the most promising techniques for neuroscience research and clinical translation. Currently, great efforts are being spent on technology development and mechanism understanding for the improvement in stimulation accuracy and outcome predictability (55-57, 59, 61). Remarkably, it is feasible to combine ultrasound stimulation with MRI techniques for probing brain function(62). However, there are technical and practical challenges in the following aspects: first, governed by diffraction limit of acoustic wave, ultrasound at current applied frequencies can only be focused into a millimeter size spot(45, 48, 54). By using novel beam focusing and image-guided technology, it can compensate the heterogeneity of brain tissue to form sub-diffraction pattern(53, 62), but the focal spot is still too large for single neuron or neuron type stimulation. On the other hand, the underlying mechanism of ultrasound neuro-stimulation is still unclear, thus it is hard to

make it controllable and optimize the stimulation outcome. It lacks enough selectivity to pinpoint to a specific target to stimulate the chosen neurons involved in specific circuits.

The effectiveness of ultrasound neuromodulation and brain stimulation has been explored and demonstrated intensively recently (48, 49, 61, 63-71). In this session, the diverse physical effects of ultrasound were summarized. In addition, the mechanisms of ultrasound neuromodulation and brain stimulation were discussed. Based on these understanding, I am going to discuss various possible strategies towards selective ultrasound brain stimulation.

2. Basics of ultrasonic physical effects

Ultrasound, generated by piezoelectric effects, is a mechanical pressure wave beyond the audible range with frequency above 20 KHz. Ultrasound imaging make use of low intensity output with controlled safety margin, has provided incredible wealth of deep tissue structural and functional knowledge in medicine(72-79). Recently, more and more evidence shown that there are abundant bio-effects in the low-level range(80-88), suggesting a new possibility and utilities of ultrasound for cancer treatment, bone hilling, gene and drug delivery, and neuromodulation. In this session, we revisit the physical effects of ultrasound along with its parameter relationship and physical conditions. Table. 1, listed the representative ultrasound physical effects such as radiation force, particle displacement, thermal effects, microstreaming, cavitation, and sonochemistry. The propagation of ultrasound was accompanied by various mechanical, thermal, and chemical effects. First, in ultrasound field, the particles in the media are oscillated driven by the ultrasound wave. The particle displacement can up to ~10 nm which could induce

elastic forces on cellular compartment. In addition, the propagation of ultrasound can induce radiation force which could be generated at acoustic pressure gradient by standing wave, absorption, and tissue acoustic properties gradient, introducing a non-zero average net force to the media [8]. Moreover, for the low frequency ultrasound, there could be other effects like cavitation, and the consequent streaming and sonochemistry [9]. There is no clear boundary of the parameters to generate each of those effects suggesting that it is difficult to control the effects by using different parameters.

Table 1 Ultrasonic physical effects. *The relationship with different parameters and the physical conditions are summarized. The scales of these effects are estimated.*

	Physical condition	Frequency dependency	Scale	Ref
Particle displacement (μ)	Propagation of ultrasound	$\sqrt{\frac{8\pi I(x,y)}{\rho c f^2}}; \frac{2\pi v}{f}$	~10nm	[11]
Radiation force	Acoustic pressure gradient; non-zero average net force; absorption; Standing wave	$\frac{2af^b I(x,y)}{c}$	pN- nN	[12]
Cavitation	High intensity, e.g. 1.9 MPa/MHz ^{0.5}	$\frac{PNP}{f}; MI: \frac{PNP}{\sqrt{f}}$	\	[13]
Acoustic streaming/Microstreaming	Fluid environment/cavitation	\	\	[14]
Sonochemistry	Cavitation, ultrasound sensitive compound	\	ROS	[10]
Heat	Tissue absorption	$\rho C \frac{\partial T}{\partial t} = 2af^b I(x,y)$	0.1 °C	[30]

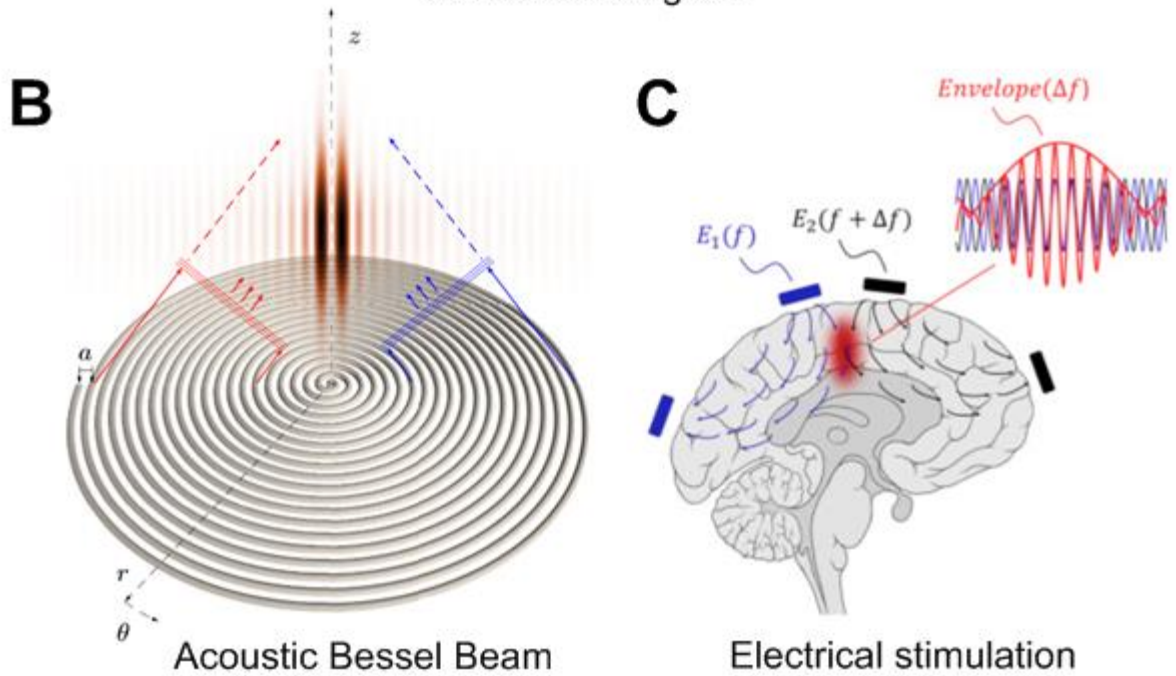
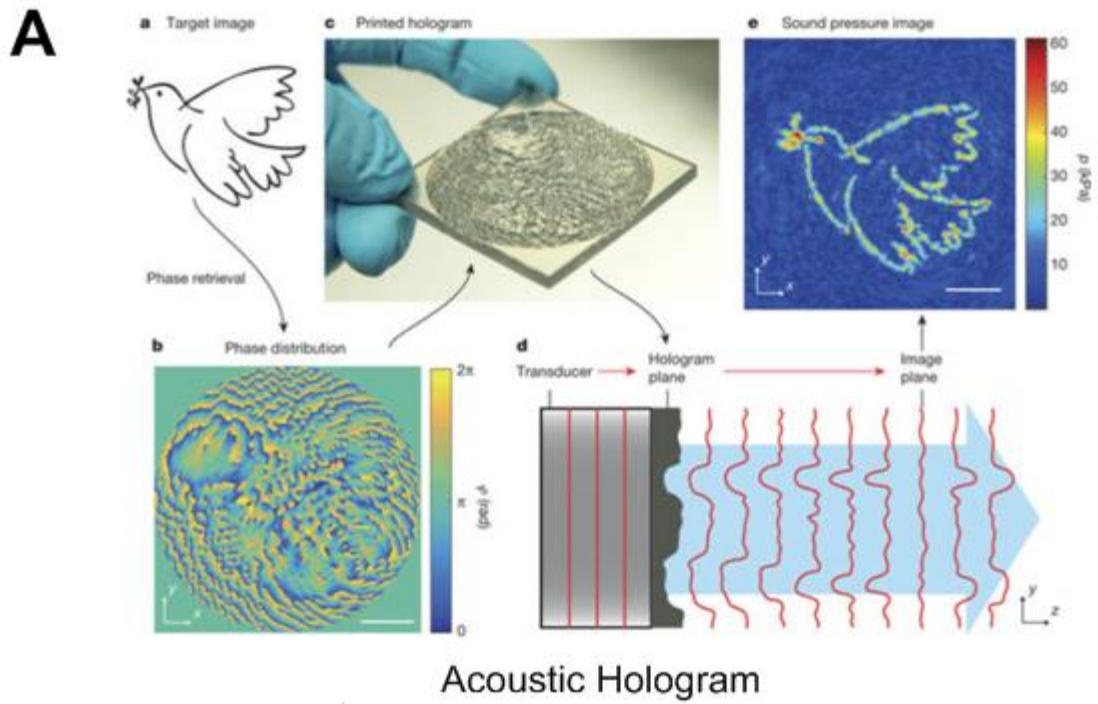


Figure 4 Wave-front shaping for (a) engineering the spatial pattern [5], (b) unique acoustic field generated by 3D printed masks [7], and (c) engineered electrical wave for deep brain stimulation [11].

On the other hand, as a pressure wave, its propagation can be engineered to generate different focal patterns (Fig. 4). By modulating the phase of the driving function, ultrasound beam can be shaped. The phased transducer array, which can be incorporated into MRI system, can generate and direct ultrasound accessing to deep brain region neuron stimulation. Interestingly, complex 3D pattern can be generated cost-effectively by using 3D printed phase mask. As outstanding examples, it can produce a bird like focal pattern and a Bessel beam with 3D printed phase mask (89-93).

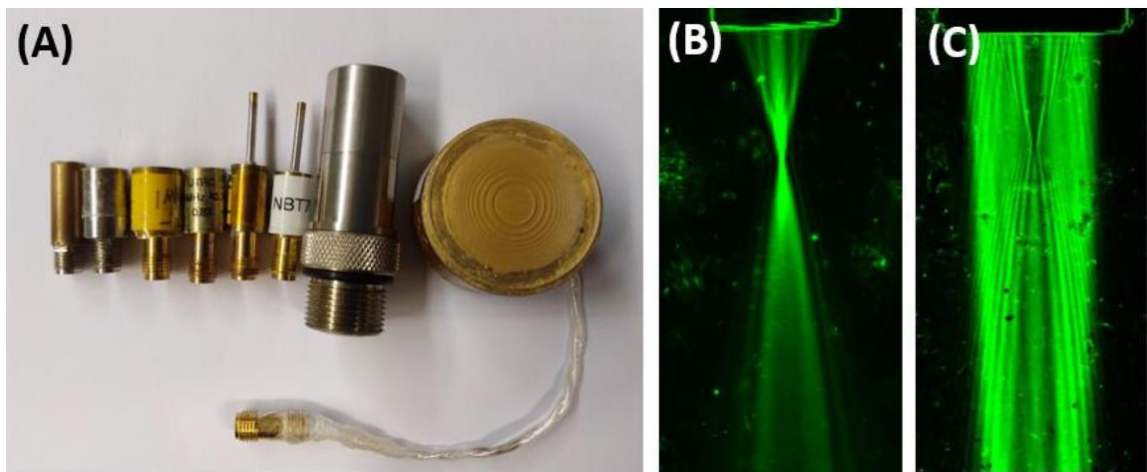


Figure 5 Different ultrasound transducers: (a) various ultrasound transducers; (b) focused ultrasound field and (c) Fresnel ultrasound beam generated by the Fresnel lens-based transducer in (a)

In my studies, I have included various ultrasound transducers as demonstrated in Fig. 4 (a) and the unique ultrasound field in Fig. 5 (a) and (b) In addition to the spatial flexibility, the frequency of the ultrasound inserted force can also be modulated. For example, the superposition of two ultrasound beam with different high frequency ultrasound can generate low beat frequency. The development of transient interference electrical brain stimulation has gain lots of attention and inspiring for ultrasound brain

stimulation. The potential of temporal interference of ultrasound in ultrasound stimulation remains to be demonstrated. These wave-front shaping, however, is diffraction limited that is at millimeter range for the typical frequency used in vivo (~MHz). Thus, it is emergent to develop cell type selective modalities which should be based on a better understanding of ultrasound neuron stimulation. In the following sessions, we will summarize the recent advances of the understanding and the possible strategies for developing selective ultrasound brain stimulation methods.

3. Mechanism of ultrasound neuron stimulation: theories, evidences and controversies

Currently, the effective ultrasound parameters being utilized in different labs are varied, and the models tested on were also different. It is not surprisingly that the results reported weren't convergent to a certain mechanism or even controversial, as the physical effects of ultrasound is diverse and strongly depends on the parameters being utilized. As very example, Prieto et.al, using model lipid membrane to test the ultrasound effects on the electrical activity suggesting a radiation force-based mechanism(94). While the *in vivo* experiments shown that the mechanism could be cavitation or particle displacement related (57). In the following sessions, we summarized the recent advances in understanding the ultrasound neuron stimulation.

However, the bio-effects induced by ultrasound are diverse, thus the mechanism is still unclear. One major hypothesis of LILFUS ultrasound neural stimulation is that ultrasonic wave activates mechanosensitive ion channels located on cell membrane (55, 95-100). To confirm this hypothesis, various experiments have been conducted from cells

and *C. elegans*. It was shown that higher frequency ultrasound (10MHz, 43 MHz, 200 MHz) can activate mechanosensitive ion channels such as MEC-4 and Piezo1, while microbubbles were required to facilitate the activation of mechanosensitive ion channels (Piezo1, TRP-4) in lower frequency range (1 MHz, 2MHz)(55, 101-104). Similarly, Zhou et al demonstrated the activation of ASH neuron in *C. elegans* by a surface acoustic wave device at 26MHz (105). In addition, the surface acoustic wave device was also shown able to activate MscL to generate neural activity (99). However, whether ultrasound can activate neurons in vivo directly at low frequency hasn't been approved yet. The protocol used in studies are not clinical relevant because higher frequency ultrasound is unable to access to deep brain regions or incorporated with different physical mechanisms, therefore lead us to wonder whether lower frequency ultrasound at 1 MHz or below without the presence of microbubble can activate neurons in vivo, that may be more likely to be translated to clinic.

1.1 Ultrasound effects on ion channels

As demonstrated in Table. 1, mechanical effects of ultrasound, including radiation forces, streaming, particle displacement and stable cavitation are the profound phenomenon. Recently, growing evidence shown that cellular activity and signaling are well regulated by mechanosensitive ion channels which is a machinery that link the cellular epigenetics and its microenvironment (106). For these reasons, it could induce rich mechanical effects which could act on neurons(107). It is rational to hypotheses that ultrasound can induce neuron activity through interacting with mechanosensitive ion

channels in the brains. Neurons reserved some mechanosensitive nature from revolution (107). The forces for activation of these mechanosensing compartment is at tens of Pico Newton level. Recently, lots of efforts have been spent on testing the ultrasound effects on mechanosensitive ion channels. S Ibsen, et al, (108)demonstrated that ultrasound can induce neuron activity and behavior change of *Caenorhabditis elegans* mediated by TRP-4 in the presence of microbubbles. The use of microbubbles is deviated from the ultrasound neuron stimulation and the mechanism could be different. Zhou et. al., (105) utilized surface acoustic chip to activate mechanosensing neuron in *C elegans*. However, they have not ruled out which mechanosensitive ion channels involved, and the experimental scheme is hard to translate to in vivo application. Direct evidence demonstrated by Kubanek et al. (55) by using different ion channels overexpressed *Xenopus* Oocyte cell model for testing ultrasound effects by measuring ion current. It is demonstrated that ultrasound can modulate K⁺ currents of K2P channels and Na⁺ currents of NaV1.5. However, the cell model is typical, and the effects are moderate, whether it is physiological relevant or not is unclear. These data in Fig. 6 support the idea that ultrasound can gate mechanosensitive ion channels but there still lacks direct evidence in mammalian cells and in vivo systems. The detailed biophysical mechanism of how mechanosensitive ion channels are gated by ultrasound is still unclear as ion channels are in nanometer scale which is much smaller than ultrasound wavelength in KHz to MHz range.

Ultrasonic thermal effect is also well-known and has been explored as a cancer treatment modality in the past several decades. The tissue heating by ultrasound are attributed to absorption of the energy. Afterwards, the energy is diffusively transfer to the

surrounding tissue. It has been proposed that thermal perturbations can induce neuron firing by opening thermos sensitive ion channels like TRPV1 or by changing the capacitance of the membrane(109). Some results on *C. elegans* shown that thermal effects in not necessary but obviously, it can easily get involved.

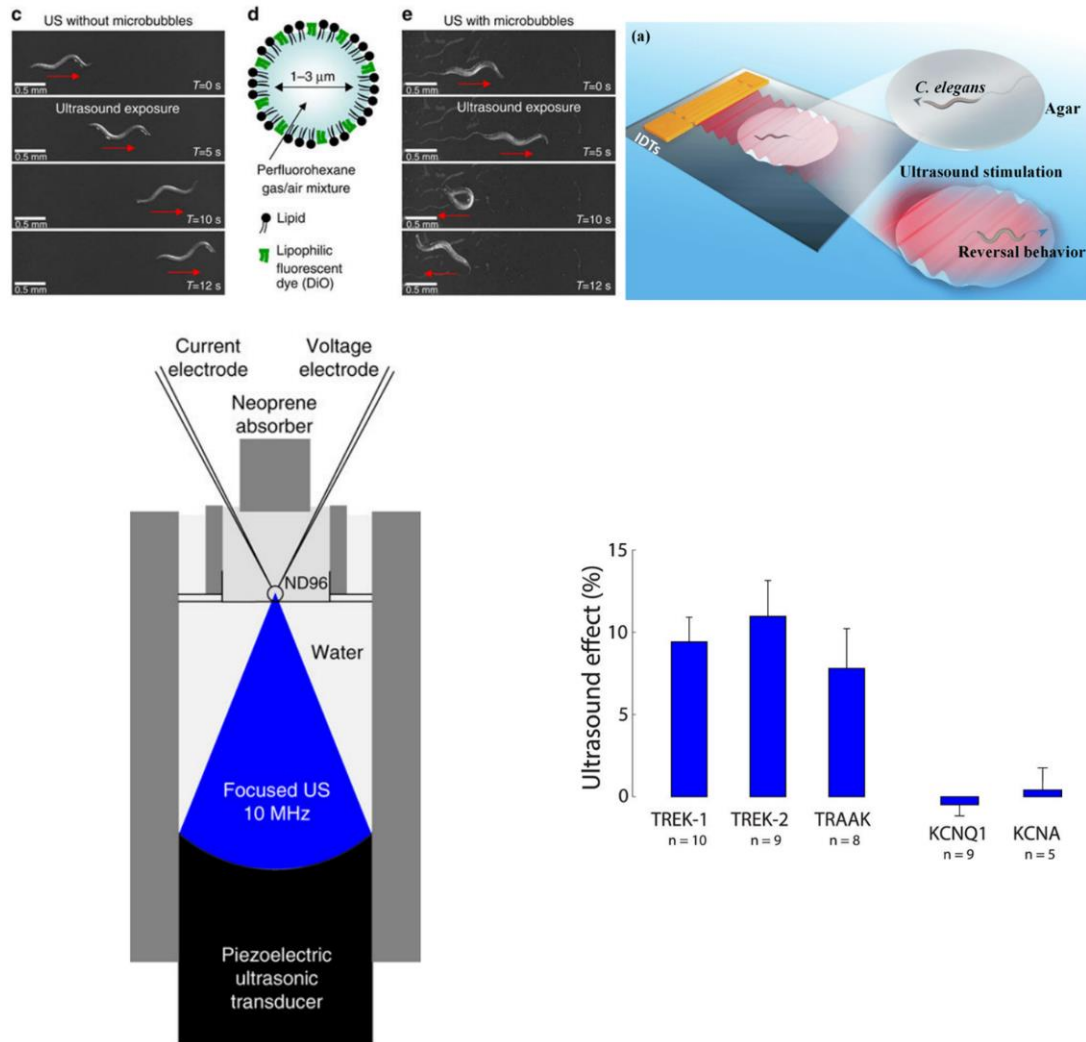


Figure 6 Evidences showing ultrasound modulation on mechanosensitive ion channels [31]

1.2 Mediate neuron activity by piezoelectrical effects

The generation and detection of ultrasound is based on piezoelectric effects. One elegant theory proposed a piezoelectric mechanism that converse ultrasound oscillation into electrical perturbation. Intramembrane cavitation defined as off-phase oscillations of the lipid bilayers which was proposed as a mechanism for mediating ultrasound bio-effects(110) . Consider cell membrane which is a bilayer lipid membrane with changeable capacitance when its thickness or total area were changed by stretching or compressing as a tunable capacitor, Plaksin et.al, extended this concept in ultrasound neuron stimulation coupling with Hodgkin-huxley model as shown in Fig. 7. (111, 112). This model for transducing mechanical vibrations into electrical signal and then triggering the action potential. This mechanism is success to interpret ultrasound neuron activation and suppression supported by some *in vivo* experiments. But it still lacks direct evidence to support. It is important to come up with testable predictions to validate this mechanism. Also, it is noted that intramembrane cavitation also predicted a ~ 10 mN/m membrane tension (T) under ultrasound irradiation which means even this mechanism is true, the mechanosensitive ion channels could also be activated simultaneously.

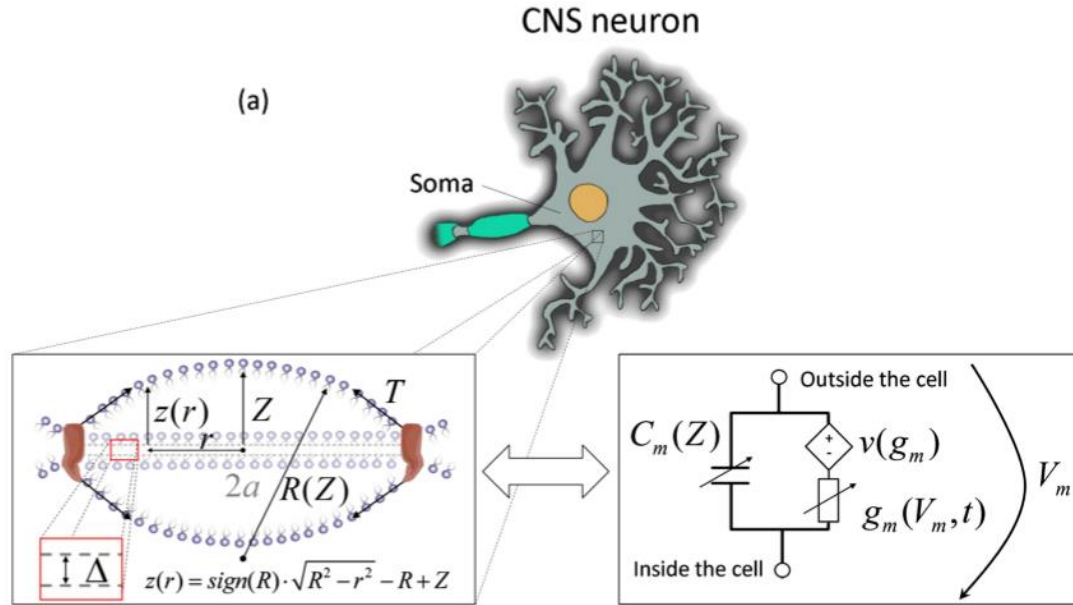


Figure 7 Intramembrane cavitation coupling with H&H model as mechanism of ultrasound neurons stimulation [15].

1.3 Subthreshold mechanical and sonochemical perturbation

Despite electrical firing, neurons can also undergo Neurons are polarized cell with long axons(113-115). The axon transportation and signaling are rely on the well-functioning cytoskeletons and its related motor proteins. It is known that cytoskeleton can transfer mechanical induced ECM signaling into nucleus(116, 117) Theories have been proposed that cytoskeleton can resonance at 3.5 MHz with evidence on cell line model showing that ultrasound could induce cytoskeleton rearrangement and effects on the cellular signaling [11-13]. On the other hand, there are lots of interaction between ion channels and cytoskeleton(118). Cytoskeletons are act as a preventer for ion channel opening(119). There are evidence from the osteoblast stem cells that ultrasound can

modulate the cytoskeletons. But ultrasound has unique morphology with extremely long axon. The cytoskeleton is critical for maintaining the axon functions. It has been shown that ultrasound can modulate cytoskeleton functions in OA cells but there still lacks for key and detailed evidences to support the cytoskeleton hypothesis in ultrasound neuron stimulation.

The reactive oxygen species (ROS) are important intracellular signaling molecules (120). Sonochemical effects can generate ROS (121) which can be utilized to kill cells as a cancer treatment modality (122, 123). Some drugs can sensitizer targeted cells for generating large amount of ROS which is name sonodynamic therapy. Although the mechanism is unclear, it is widely accepted that during the sonodynamic process, there are ROS generated. On the other hand, the low intensity ultrasound can induce the ROS generation in cells.

4. Strategies towards selective ultrasound brain stimulation

The key to achieve precise and selective stimulation is to inscribe ultrasound sensitivity into targeted neurons (Fig. 8). Afterwards, low level ultrasound could activate those targeted neurons while leave the untargeted neurons silent. The mechanism of ultrasound stimulation is unclear, and it is believed to be diverse. The development and verification of toolkits that based on each specific proposed mechanism would separate those diverse factors providing us an opportunity to test those mechanism one by one.

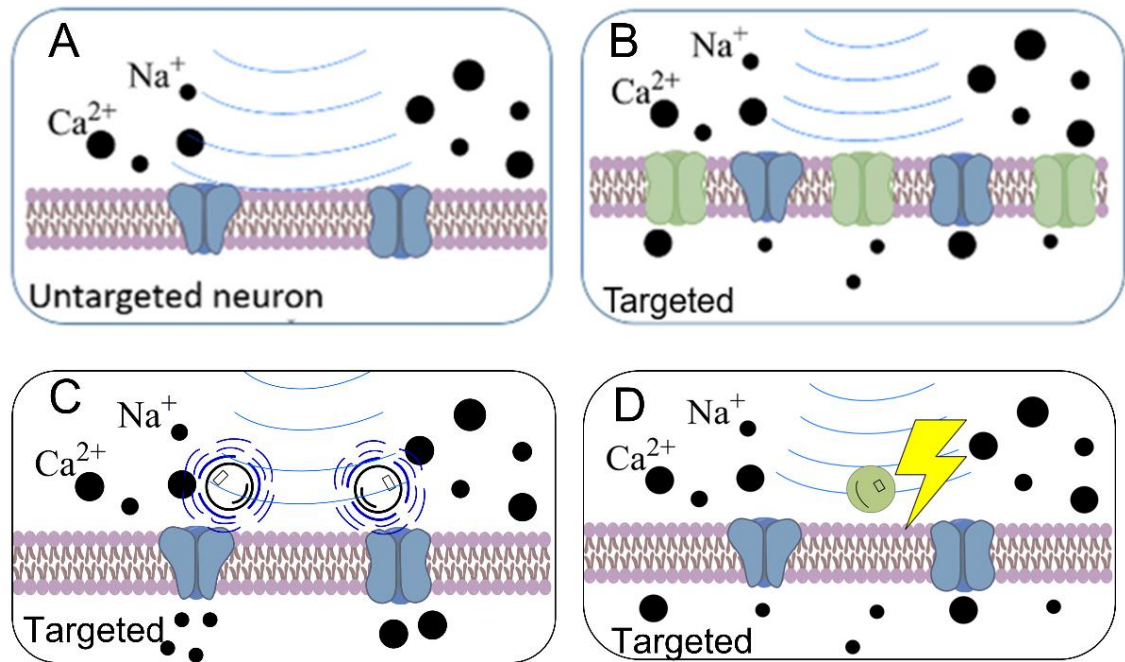


Figure 8 Strategies towards selective ultrasound neuron stimulation. A) *Ultrasound pressure/intensity lower down to which act on untargeted neuron no obvious effects can be observed while B) ultrasound sensitive ion channel overexpressed neurons, C) ultrasonic mechanogenetics; D) Piezoelectric nanoparticle mediated ultrasound brain stimulation*

1.4 Sonogenetics

Based on the evidence discussed in Session 3.1, sonogenetics has been proposed (108). It is simple analogous to optogenetics while the activation is achieved by ultrasound with deep penetration. The implementation includes: 1) make the targeted neurons overexpress with mechanosensitive ion channels by genetic modification. Well-established gene delivery technologies are available even with minimal invasiveness or

non-invasiveness. After the expression of the mechanosensitive ion channels, ultrasound from 2) dedicate ultrasound beam for activate these ion channels are administrated into the brain region non-invasively through the skull. However, due to the unclear mechanism the effectiveness is hard to optimize. It is emergent to screen ultrasound sensitive ion channels and engineer the ion channels to be more sensitive to ultrasound. Moreover, it is remained to be validate in rodent model in vivo. mechanosensitive in channels, screening effective optimal ion channels, in addition, is the ultrasound induced current are able to initiate cellular activity and signal is remains testing, toolkits for delivery mechanosensitive ion channels and ultrasound for free moving animal are under developing;

Alternatively, we proposed to use ultrasound responsive protein holly nano structure (124) to amplify and localize the acoustic energy as a targeting brain stimulation strategy. Since Bubbles are highly ultrasound responsive which is widely used as contrast agent (125, 126). However, the convention bubbles used as contrast agent are in micro-size. It is unable to go through the blood vessel. Nano-size bubbles are being developed but those nano-bubbles are not stable. Recently, nano-gas vesicles are demonstrated with unique acoustic properties. It is considered as NGV, gene encoded, was considered as GFP for ultrasound; generating enough force for probing cellular mechanics.

1.5 Ultrasound thermal genetics

Ultrasound can heat up the tissue easily in a controllable way (127). The thermal effects have been utilized to treat various diseases and its heat transfer process could be

controlled by shifting the pulse width and duty circles. As Magneto-thermal genetics have been reported feasible *in vivo* mouse model (128). The results demonstrated that the elevation of 6 degree by alternating magnetic field is sufficient to initiate neuron activity. Thus, it is also rational to proposed ultrasonic thermal genetics. As shown in Fig. 8 (B), the targeted neuron can be overexpressed with thermal sensitive ion channels like TRPV1. Once the region of focus being heated with 2 degrees, those neurons can be activated. The concern is that the thermal diffusion could be slow. Thus, the temporal resolution of this methods should be well characterized. Assuming the thermal diffusion is quite slow, it can still benefit some research like learning and memory.

1.6 Piezoelectric transducer as electrical stimulation.

The intramembrane cavitation mechanism suggested a ‘piezoelectrical’ model that to convert acoustic pressure into electricity to stimulate neurons in an electrical stimulation manner. It acts as an electric stimulation. It is suggested that selective stimulation on neuron types with distinct expression level of voltage gated ion channels could be with different acoustic wave front suggesting a mechanism that ultrasound field into electric current for stimulation (129). It is not easier to achieve selective neuron stimulation by changing the expression level of ion channels, because the voltage gated ion channels are explicit involved in neuron activity, manipulation of voltage gated ion channels for alternating the ultrasound sensitivity could alter the neuron circuits without the control of ultrasound.

Alternatively, using nanomaterials to convert ultrasound energy into electricity for generating local microcurrent for electrical stimulation on neurons is proposed shown in Fig. 8D. This strategy has been tested under different conditions recent years. Elegant review [22] has summarized the development of this methods. Briefly, these methods have been tested on neuron like cell lines. Further experiments are needed to characterize different materials (Table 2) and clarify the mechanism. In addition, its feasibility in neurons and in vivo model remains validation. The challenges are how to deliver the nanoparticles into the specific brain region and targeted to specific neurons as well as improving efficiency to generating micro-current.

1.7 Ultrasound induced drug uncaging and chemogenetics.

In addition to control the electrical activity of given neurons directly, it is also desired to modulate neural activity and signaling by chemical drugs as brains are also chemical in nature. In this aspect, ultrasonic drug control release has been widely studied in cancer treatment and there are varied strategies to control mostly based on ultrasonic contrast agents. As an example, chemogenetics (130), expressing specific ligand in chosen neurons followed by systematic administration of small molecules to activate or inhibit targeted neurons, has been widely used to probing brain functions which are limited by its poor temporal resolution. The ultrasonic drug uncaging will allow us to control the release molecules to improving the temporal resolution of such application(131).

On the other hand, for some large molecules, it is hardly to access to neurons as there were blood brain barrier in mammalian CNS. Transiently open the BBB to deliver

the large molecules and even virus to the CNS neuron could have lots of application (132, 133). As an example, it is demonstrated that by using ultrasound BBB opening to deliver rAAV virus to CNS make neurons expressing designer receptors can eliminate the viral injection process making chemogenetics a purely non-invasive modality.

1.8 Subthreshold modulation

The cytoskeleton has its own intrinsic oscillation frequency. Its oscillation is depending on many factors like the orientation, length, etc. The external stimulus at resonance frequency could insert specific force on the chosen cytoskeleton. As mentioned above, after identifying the resonance frequency of cytoskeleton can be used to selective perturbation on the structure and thus induce force stimulation to the cell even transduce directly into cytoplasm. During neuron development and functioning, stem cell differentiation, migration and each neuron extends an axon, which is the dominant cell process, and several fiber, branched dendrites. Accumulative evidence showed that Generally, the mechanosensitive ion channels, the extracellular matrix, the cellular cytoskeleton and its associated proteins like acto-myosin which plays important role in neuron development, and nuclear are the major compartments for neuronal mechanosensing (134).

On the other hand, considering the ROS signaling, we can use low intensity ultrasound sensitized with sonosensitizer to generate low level ROS for triggering cascade signaling. Varied sonosensitizer with different cell targeting capability and subcellular

localization are available for the application. The selectivity can achieve by the selective accumulation of sonosensitizer.

5. Challenge and future perspectives

As shown here that the effects of ultrasound are diverse and thus the possible mechanism is also complex. It is emergent to test the hypothesis mentioned above. The testing of the selective neuron stimulation strategy will not only provide a useful tool but also give us insight into the possible mechanisms. The diversity of bioeffects of ultrasound make it challenge to separate and quantify biophysical mechanism and come up testable biophysical models of the interactions between ultrasound and cellular/subcellular compartment. On the other hand, it also provides us an opportunity to multiplex the stimulation which could be a useful feature for future development.

Recent years have witnessed the dramatic advances in basic neuroscience understanding of brain function by optogenetics and clinical application by non-invasive brain stimulation. In terms of the development of the tools for application. Efforts should be spent on the developing of novel ultrasonic stimulation system for free moving and circuits level stimulation. Advanced wave-front control and beam shaping like Bessel Beam, or other types of ultrasound beams could also very useful for improving the performance. On the other hand, it is notable that the non-invasive delivery of ultrasonic sensitive proteins, nano-particles are also important to the development of the tools.

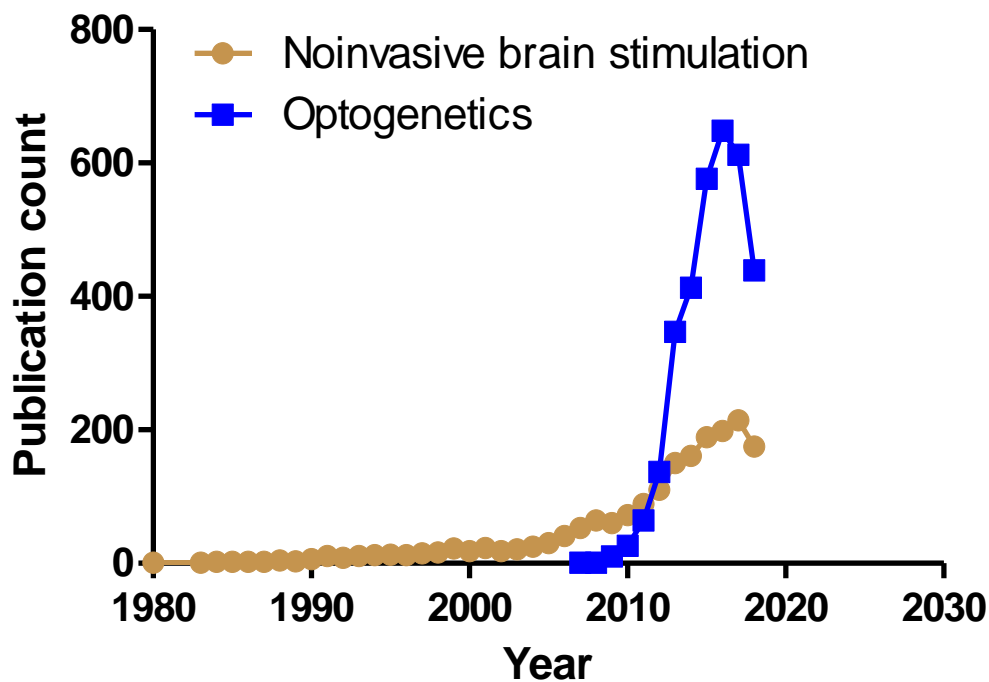


Figure 9 *Publication of non-invasive and selective brain stimulation (Optogenetics) each year*

6. Summary

Ultrasound brains stimulation is a promising technology for clinical and basic neuroscience. In summary, the mechanism of ultrasound neurons stimulation remains elusive as the ultrasonic bio-effects are diverse. Various possible mechanisms of ultrasound brain stimulation have been proposed and discussed. One of the most possible mechanisms are gating mechanosensitive ion channels. In the following sessions, session, we are going to test this mechanism and develop precise brain stimulation toolkits. The efforts of the development of precise ultrasound neuron stimulation will not only provide us a non-invasive, safe, capable of high spatiotemporal control of neuron activity across

the whole brain, but also give us insight into the mechanisms of ultrasound neuron stimulation.

Chapter 2: Proof-of concept:

Brain stimulation via ultrasonic activation of Piezo1

As aforementioned, one of the possible mechanisms for ultrasound brain stimulation is gating mechanosensitive ion channels. Mechanosensitive ion channels can sense various mechanical perturbations and induce physiological changes to adapt its microenvironment. Understanding brain functions and treating brain disorders requires modulating the activity of well-defined neuronal populations with high spatiotemporal resolution. Here we demonstrate control of neural activity and signaling by opening the piezo-type mechanosensitive ion channel component 1 (Piezo1) using non-invasive ultrasonic stimulation. Our results show that Piezo1, when triggered by ultrasound, was activated to induce reversible neural activity in the form of calcium influx and elicit significant modifications in calcium signaling pathways, including the levels of the proteins p-CREB, p-CaMKII and *c-Fos*. Ultrasonic stimulation in the primary motor cortex (M1) of mouse brains induced activity of targeted neurons, resulting in increased movement in both anesthetized and free-moving mice. Thus, we demonstrate a proof-of-concept for targeting ultrasound into deep brain structures non-invasively, allowing selective neuronal control.

1. Introduction

Understanding brain function has been a perennial goal of scientists, and efforts to this end over the past few decades have led to a trove of knowledge in this area(135-137). The primary factor behind this is the growing number of modalities that can probe brain activity both inside a living brain as well as in ex vivo settings. Billions of neurons form interconnected circuits across the brain and make possible the diversity of complex animal behavior, from cognition, to learning to emotion (138, 139). New technologies can stimulate neuronal activity, with varying degrees of spatiotemporal resolution, so that downstream effects may be studied at any level from the genetic to the behavioral(137).

Optogenetics is one such influential technology, which relies on making some neurons express light-sensitive ion channels (opsins) and then stimulating them with light (137). This approach is being used to study disparate complex phenomena in animal models, such as the neural circuitry of fear (140) and how this may be turned off or on at will (141), the relationship between sexual behavior and violence (142, 143) and psychiatric disease in rodents (144). However, this technique is limited by the inability of light to penetrate tissue even using longer-wavelength light (145-147), requiring significant surgical invasion, and the limited area and depth in which such stimulation can be achieved (148). Transcranial magnetic stimulation (TMS) (149) and transcranial direct current stimulation (tDCS) are alternative methods that have been applied therapeutically in the brain (150). These methods have direct clinical application but lack spatiotemporal resolution and cannot target a small region or specific cell types in the brain, which could dilute the treatment's effects or even lead to side-effects.

Ultrasound-based brain stimulation is another choice which is being actively studied, and it offers some advantages compared to the abovementioned techniques. Ultrasound beams can be focused on small region in deep brain tissues without any observable damage to the surrounding region (151). It has been demonstrated to stimulate the prefrontal cortex and improving task in human without side effects (53) and to stimulate visual cortex in monkeys (152). Ultrasound stimulation has good spatiotemporal resolution and neurons can be either activated or suppressed depending on different ultrasound parameters and different stimulation locations (153, 154). Attempts have also been made to use ultrasound therapeutically for conditions like Parkinson's disease, epilepsy and depression (155). It was recently reported that scanning ultrasound in the brain, combined with administration of microbubbles, were able to open the blood-brain-barrier and relieve symptoms of Alzheimer's disease in a mouse model (60), although the mechanism for this is as yet unclear.

Indeed, the mechanism for ultrasound is still unclear, and this make it more difficult to control and optimize treatments or target them to only desired cell types. Understanding the molecular machinery that mediates the effect of ultrasound would be a significant aid in improving therapeutic procedures. Insofar as the response to ultrasound treatment is purely due to mechanical effects (and not owing to any consequent thermal effects) "mechanosensitive" ion channels, a component of the cellular force-sensation machinery, likely play an important role. These are ion channels whose opening is controlled by disparate signals and phenomena like sound, pressure, shear forces, membrane stretch, cell volume, gravitropism, proprioception, and touch/pain sensation., which effectively "translates" physical force into chemical messages (156).

Among the better-known mammalian mechanosensitive ion channels are members of the TREK family (157), the TRP family (158), and the Piezo family (159). Of these, Piezo1 and Piezo2 were most recently discovered to be mechanosensitive cation-selective channels (160), capable of conferring mechanosensitivity to cells in heterologous expression systems. These are very large proteins composed of around 2500 amino acids which form 25- 40 transmembrane domains. Piezo1 is among the mechanosensitive proteins most sensitive to physical force (160), responding quickly and dynamically (161) to forces estimated to be as low as 10 pN (161, 162). While it allows cations to permeate cells in general, it is reported to exhibit a preference for calcium ions (Ca^{2+}) (162). These properties of Piezo1 makes it the potential candidate of ultrasonic sensitive ion channels regarding the sensitivity and temporal responses to external forces.

2. Results and discussion

In the present study, we demonstrate that low-frequency can open the Piezo1 channel and initiate Ca²⁺ influx. for the first time the non-invasive stimulation of cells with ultrasound, by specifically opening the Piezo1 channel to allow Ca²⁺ into the cell. Ultrasound caused significant Piezo1-mediated changes in calcium-regulated signaling, and a marker of neuronal activation.

We first overexpressed Piezo1 in 293T cells, known to have minimal expression of Piezo1 (163) by transfecting a plasmid encoding a Piezo1-EGFP fusion protein (as described in (163)). The expression of Piezo1 in 293T cells was verified by Western blot and qPCR (Fig. 10).

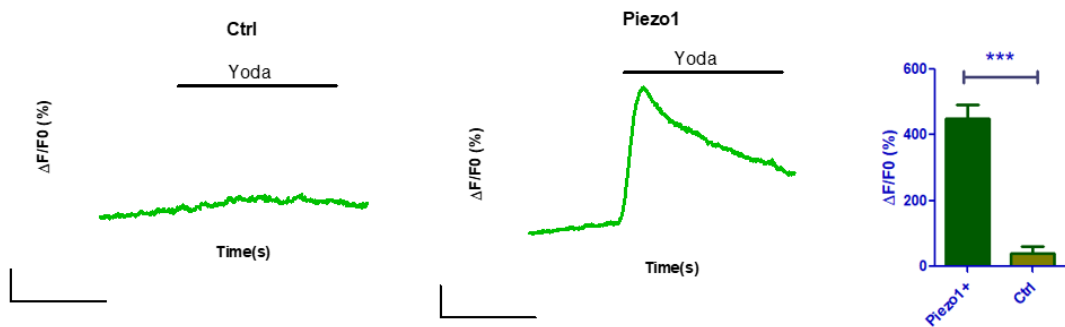


Figure 10 Functional validation of Piezo1 expression in 293T cells. Yoda1, a Piezo1 agonist, induces significantly higher calcium influx in 293T cells overexpressing Piezo1 than in control cells.

Using our in vitro setup (Fig. 15), we treated cells with 500 kHz ultrasound of 200 cycles, at 1 kHz pulse repetition frequency (PRF) with 200 tone bursts at 0.1, 0.2, and 0.3 MPa, respectively. We applied ultrasound at acoustic pressures corresponding to a range previously reported to have elicited responses (95, 164). A fluorescent calcium indicator was used to measure intracellular Ca²⁺. In response to US, dose-dependent Ca²⁺ influx was seen in cells treated with the Piezo1 plasmid, but not with the control plasmid. Significant Ca²⁺ increase was observed in response to 0.3 MPa ultrasound (Fig. 11C), as well as to Yoda1 (Fig. 11), a chemical agonist of Piezo1(165). Ultrasound stimulation can, therefore, specifically activate Piezo1. On the other hand, we tested the ultrasound effects by using patch clamping techniques. It is shown that upon ultrasound stimulation, inward current can be observed on the 293T cells expressing Piezo1 while no effects were found on the 293T cells transfected by control plasmids (Fig. 11 D). These results set solid foundation that expression of mechanosensitive ion channels can gain ultrasound sensitivity in 293T cells for cellular activity control.

We next tested the effects of ultrasound on primary cortical neurons harvested from embryonic mouse brains to test the feasibility of stimulating live neurons with ultrasound. Primary neurons at day in vitro (DIV) 10 were seen to express Piezo1 endogenously and accumulated intracellular Ca²⁺ in response to ultrasound in a dose-dependent manner. Acoustic pressures of 0.2 and 0.3 MPa elicited significant responses, comparable to that produced by Yoda1 (Fig. 11). When blocked by GsTMx-4 a Piezo1 blocker, primary neurons showed an decreased level of Ca²⁺ influx compared to control neurons (Fig. 11E), revealing that the US-induced Ca²⁺ response is through activation of Piezo1. In addition, we also tested *c-Fos* expression after ultrasound stimulation as shown

in Fig. 1F, the ultrasound can activate *c-fos* expression while the GsMTx-4 treated group can reduce the *c-Fos* expression significantly.

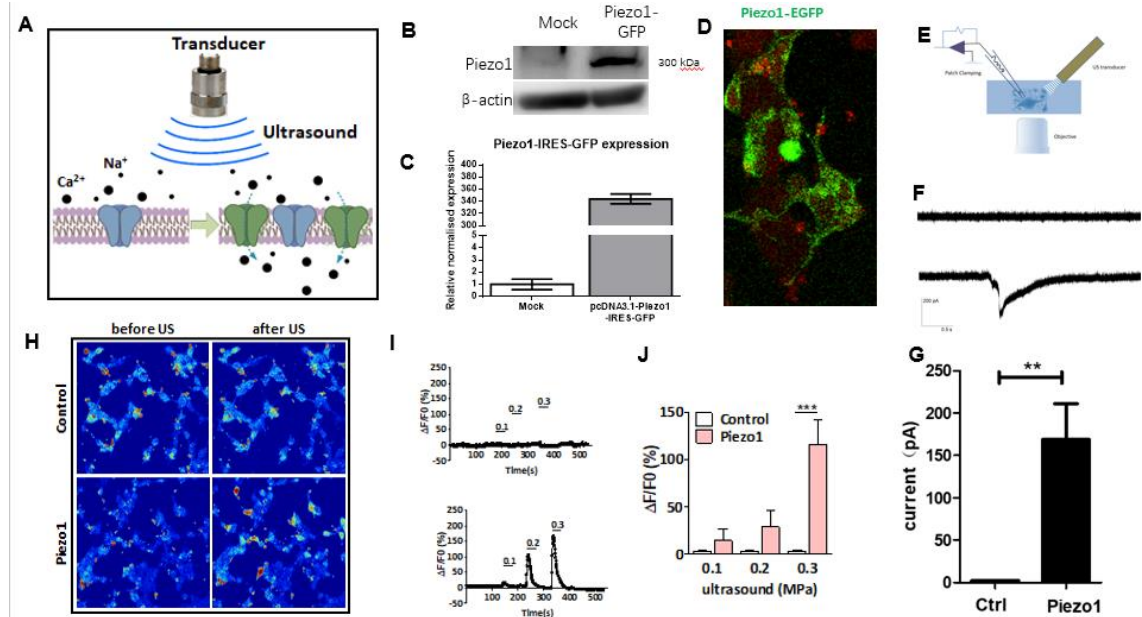


Figure 11 *Ultrasound induces intracellular calcium influx by Piezo1 activation.* (A) The experimental scheme for this study. Cells are sensitized to ultrasound stimulation by inducing the expression of mechanosensitive ion channels, such as *Piezo1*. Treatment by ultrasound can hence open *Piezo1*, allowing Ca^{2+} into the cell and setting into motion calcium-related signaling. (B) *Piezo1* overexpression in 293T cells transfected with the *Piezo1*-containing plasmid, as evaluated by Western blot and RT-qPCR. Graphs show mean \pm SEM from three independent experiments, * $P < 0.05$, unpaired *t*-test. (C) Ultrasound induces dose-dependent calcium influx in 293T cells overexpressing *Piezo1*. Ultrasound stimulating mode: each stimulus contained 200 tone bursts of 500 kHz ultrasound at 1 kHz RPF, 200 cycles, and 0.1 MPa, 0.2 MPa, and 0.3 MPa. *** $P < 0.001$, unpaired *t*-test. (D) Ultrasound induces dose-dependent calcium influx in primary cortical neurons through *Piezo1*. *Piezo1* expression in primary cortical neurons was

*confirmed by immunocytochemical staining; Green: Piezo1; Red: MAP2; DAPI: Blue. Ultrasound stimulation induced significant increase of intracellular calcium of the neuron, comparable to the effect of Yoda1, a chemical agonist of Piezo1. * $P < 0.05$, *** $P < 0.001$, one-way ANOVA with post-hoc Tukey test. (E) Primary neurons made to overexpress Piezo1 by plasmid transfection accumulate more intracellular calcium when treated with ultrasound than do neurons treated with a control plasmid.*

We next tested the effects of ultrasound on primary cortical neurons harvested from embryonic mice to test the feasibility of stimulating live neurons with ultrasound. Immunofluorescent staining revealed that primary neurons at day in vitro (DIV) 10 expressed Piezo1 endogenously (Figure 12A). Treating these cells with 10 μM Yoda1 stimulated Ca^{2+} influx, while pre-treatment with 40 μM GsMTx-4 significantly reduced it (Figure 12B). The inhibitory effect of GsMTx-4 upon Yoda1-induced Ca^{2+} influx was consistent with the known mechanism of its action as a Piezo1 gating modifier (166-171). Thus, primary neurons at DIV 10 were expressed functional Piezo1, and we proceeded to evaluate the effects of ultrasound on these cells.

Ultrasound stimulation resulted in dose-dependent Ca^{2+} influx into the neurons, and this influx was abrogated when the cells were pre-treated with 40 μM GsMTx-4 (Figure 12C). Ultrasound of 0.3 MPa and above was able to induce significant Ca^{2+} influx, so we evaluated the effects of ultrasound on neuron activation by immunofluorescent staining of c-Fos, a well-established molecular marker of neuronal activation that is responsive to Ca^{2+} influx (172). Untreated cells, cells treated with 0.3 MPa ultrasound for 20 minutes inside a standard cell culture incubator (setup illustrated in Figure 12D), and cells pre-treated with 20 μM GsMTx-4 before ultrasound were compared. We found

that c-Fos expression in the nuclei of neurons (identified by MAP2 staining) significantly increased upon US treatment compared to the untreated control and reduced significantly when GsMTx-4 pre-treatment was applied (Figure 12E). Hence, ultrasound could trigger Ca^{2+} influx into primary neurons and activate them, in a manner dependent on Piezo1's activation.

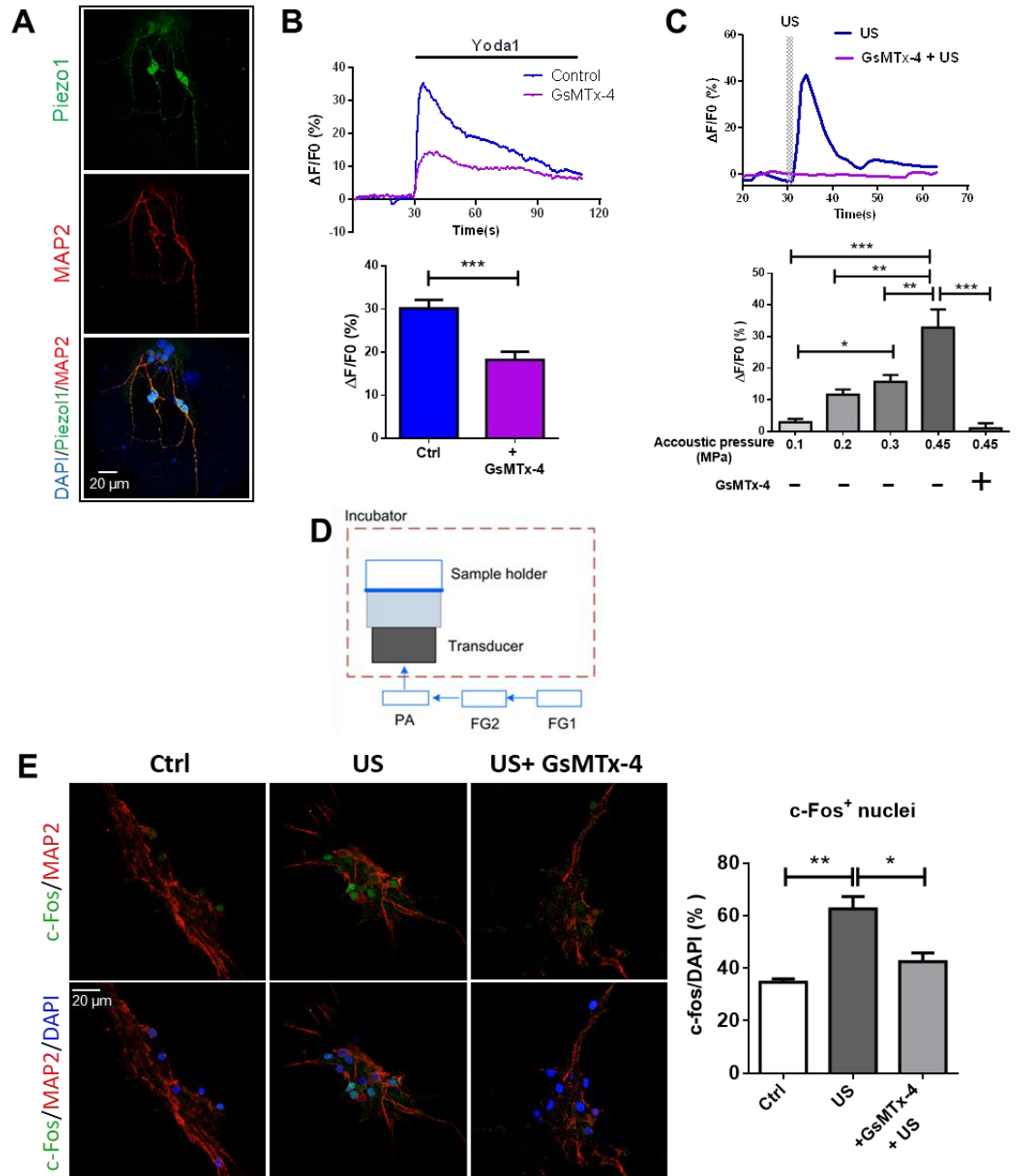


Figure 12 Ultrasound regulates the activity of calcium-related signaling and downstream gene expression profile. (A) The expression of Piezo1 in mouse primary cortical neurons was examined in two ways. Left: Representative images of Piezo1 and MAP2 immunocytochemical staining of primary neurons at DIV 10. Right: (B) Ca^{2+} imaging of primary neurons stimulated with Piezo1 agonist Yoda1, including cells pre-

treated with Piezo1 blocker GsMTx-4. Top: Representative Ca²⁺ imaging time-course for cells treated with either 10 μ M Yoda1 alone, or pre-treated with 40 μ M GsMTx-4 respectively. Bar charts show the mean \pm SEM of 3 independent experiments. $n = 15$, *** $P < 0.001$, unpaired two-tailed t -test. (C) Ca²⁺ imaging of primary neurons stimulated with ultrasound, including cells pre-treated with GsMTx-4. Top: Representative Ca²⁺ imaging time-course of primary neurons treated with 0.45 MPa ultrasound, or pre-treated with 40 μ M GsMTx-4 and then with ultrasound. Bottom: Bar chart represents mean \pm SEM of 3 independent experiments treating primary neurons with varying intensities of ultrasound and GsMTx-4. $n = 9$, * $P < 0.05$, ** $P < 0.01$, *** $P < 0.001$, one-way ANOVA with post-hoc Tukey test. (D) An illustration of the ultrasound setup used to treat cells placed inside a cell culture incubator for immunofluorescence or Western blots. The ultrasound was illuminated from the bottom and there a coupling waveguide between the ultrasound transducer and dish. (E) Left: Representative IF images of c-Fos and MAP2 staining, in cells that were untreated, treated with 0.3 MPa ultrasound, or with 20 μ M GsMTx-4 followed by ultrasound. Right: Bar chart represents the mean \pm SEM of 3 independent experiments. $n = 3$, * $P < 0.05$, ** $P < 0.01$, one-way ANOVA with post-hoc Tukey test.

We were interested in exploring the signaling implications of Piezo1-mediated ultrasound effects on neurons in greater depth. For this we chose the mouse hippocampal cell line mHippoE-18 (CLU199) as an *in vitro* representation of normal neuronal cells that could help elucidate the possible downstream effects of Ca²⁺ influx through ultrasound-activated Piezo1 channels. Expression of Piezo1 in CLU199 cells was confirmed through semi-quantitative RT-PCR, with HeLa cells as a positive control (173)

and Western blot (Figure 13A). To evaluate the treatment's effects on downstream cell signaling, we looked for the phosphorylated (activated) forms of the Ca²⁺/calmodulin-dependent protein kinase type II (p-CaMKII), and the transcription factor CREB (p-CREB), both of which are crucial players in Ca²⁺ signaling. CaMKII is directly regulated by calmodulin, a good indicator of the level of Ca²⁺ inside the cell, and both it and CREB are involved in critical neuronal functions like neurotransmitter secretion, plasticity, transcription regulation, learning and memory (174, 175). We observed the levels of these activated proteins along with c-Fos using Western blots, to gauge whether ultrasound may affect aspects of neuronal function downstream from Ca²⁺ influx. Ultrasound treatment (performed using the setup shown in Figure 12E) increased the levels of p-CaMKII, p-CREB and c-Fos in a dose-dependent manner, with 0.3 and 0.5 MPa inducing significant increases (Figure 13B). We then evaluated Piezo1's contribution to these effects by knocking it down using siRNA. We were able to achieve over 50% knockdown of Piezo1 and found that this significantly reduced the 1 μ M Yoda1-induced Ca²⁺ influx compared to cells treated with non-targeting siRNA (Figure 13C). CLU199 cells with Piezo1 knockdown also displayed significantly reduced upregulation of p-CaMKII, p-CREB and c-Fos than the control when treated with 0.3 MPa ultrasound compared to (Figure 13D). Thus, we determined that ultrasound stimulation significantly affects the levels of important proteins in CLU199 neuronal cells, and these effects were dependent upon Piezo1.

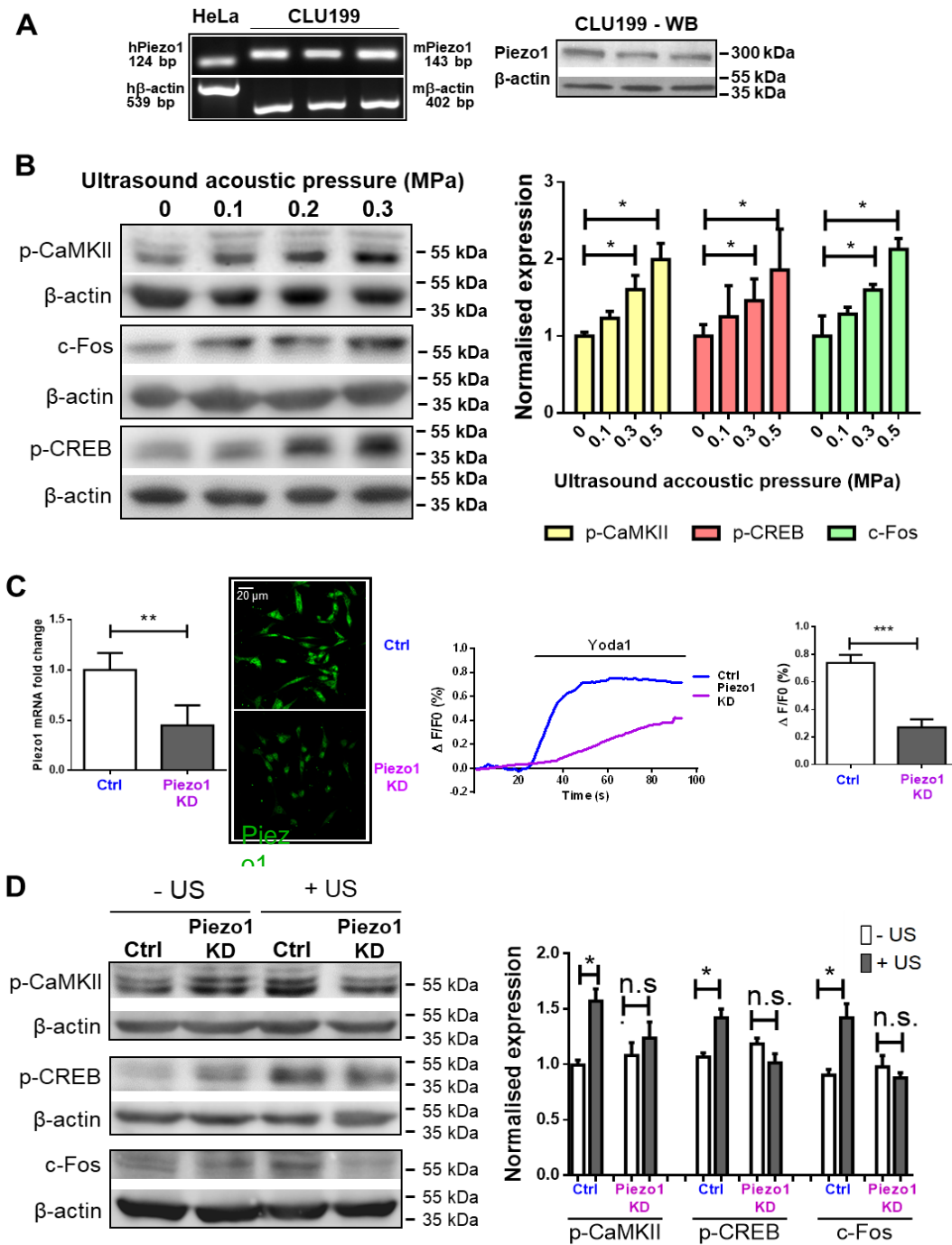


Figure 13 Ultrasound induces mouse body movement *in vivo* mediated by Piezo1 (A)
 The levels of Piezo1 in a mouse neuronal cell line, CLU199, evaluated in two ways. Left: PCR results of Piezo1 expression in multiple samples of CLU199 cells, with HeLa cells for comparison. Right: Western blot of Piezo1 expression in multiple samples of CLU199.

(B) Western blot for expression levels of p-CaMKII, p-CREB and c-Fos, in CLU199 cells treated with varying ultrasound intensities. Left: Representative Western blot images. Right: Bar charts show the levels of each protein as a fold change compared to the untreated control. Results are mean \pm SEM of 3 independent experiments. $n = 3$, * $P < 0.05$, unpaired two-tailed t-test. (C) Piezo1 was knocked down in CLU199 cell using non-targeting ('Ctrl') or Piezo1 siRNA ('Piezo1 KD'). Left: qRT-PCR was performed for Piezo1, normalized to β -actin and expressed as a fold change. Bar charts represent mean \pm SEM of 3 independent experiments. $n = 3$, ** $P < 0.01$, unpaired two-tailed t-test.. Also shown are representative IF images of Piezo1 staining in CLU199 cells. Middle: Representative Ca^{2+} imaging time-course for Ctrl and Piezo1 KD cells treated with Yoda1. Right: Bar chart shows the mean \pm SEM of 3 independent Ca^{2+} imaging experiments. $n = 9$, *** $P < 0.001$, unpaired two-tailed t-test with Holm-Sidak correction. (D) Western blot for levels of p-CaMKII, p-CREB and c-Fos in CLU199 cells treated with siRNA and ultrasound. Left: Representative Western blot images. Right: Bar charts show the levels of each protein as a fold change compared to the untreated control. Results are mean \pm SEM of 3 independent experiments. $n = 3$, * $P < 0.05$, unpaired two-way ANOVA with post-hoc Tukey test.

Lastly, we applied our scheme in vivo to further confirm whether Piezo1 could increase neuron sensitization to ultrasound (Fig. 14A, top). With well-characterized projections, like muscle in tail, paw and neck, the primary motor cortex (M1) is an established region in which to demonstrate the effects of a new neural control modality. Piezo1 or control plasmids were injected into M1, and 3 days later this region was checked

for Piezo1 expression (Fig. 14A, bottom), showing higher Piezo1 expression in Piezo1-transfected mice. The anesthetized mice were exposed to ultrasound in a range of 0.1 – 0.6 MPa, and the motor responses were recorded and quantified with the number of tail flicks per ultrasound stimulus. Motor responses were found to be affected by the acoustic pressure of the ultrasound and were increased in the Piezo1-transfected mice compared to the control mice. At 0.3 MPa, tail flicks increased from 11% to 39% between the control and Piezo1-transfected mice, and this pattern increased to 36% vs 73% respectively at 0.6 MPa (Fig. 14B). These results are consistent with those reported previously (49). At 0.3 MPa the tail flick rate by Piezo1-transfected mice was more than double that of the control mice, and we chose this condition to treat free-moving, plasmid-transfected mice. We quantified the ultrasound-induced head movements per stimulus when the mice were stationary. The Piezo1-transfected free-moving mice exhibited a significantly higher head movement rate than the control mice (51% vs 31%) upon ultrasound (Fig. 14C). Additionally, ultrasound stimulation in the M1 region urged Piezo1 transfected mice to run around with no such effects on control mice. We also examined neural excitation using c-Fos expression as an indicator. Neural activity triggered by ultrasound in M1 was significantly higher in Piezo1-transfected mice, with 13.4% c-Fos-positive cells, compared to only 5.6% in control mice (Fig. 14D). In this way, upregulating Piezo1 in mouse brains enabled us to increase neuronal sensitivity to the excitatory effects of ultrasound stimulation.

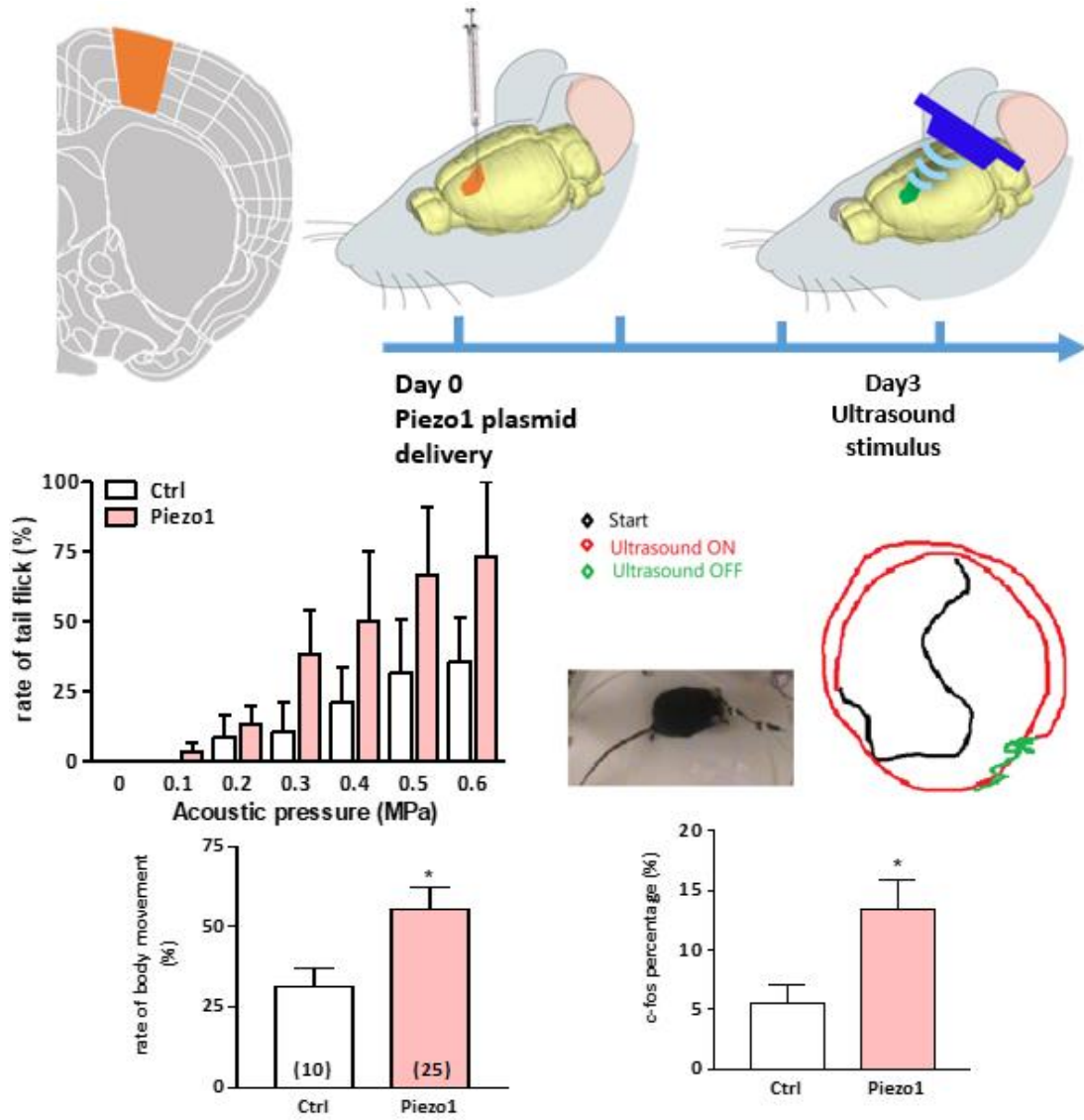


Figure 14 Selective brain stimulation via activation of Piezo1 *in vivo*. *Top: The *in vivo* experimental scheme for this study. Mouse brains were made to overexpress Piezo1 by injecting plasmid locally into the M1 region. 3 days later mice were treated with ultrasound, in either an anesthetized or free-moving state; Bottom: Piezo1 was successfully expressed in M1 of mouse brains, 3 days after plasmid injection. (B) A higher rate of tail flicks is induced by ultrasound stimulation (0.1 - 0.6 MPa) in Piezo1-transfected mice than that of control mice under anesthesia. No significance found by a*

*two-tailed unpaired t-test, n = 3. (C) Ultrasound (0.3 MPa) induces a higher rate of head movement in Piezo1-transfected mice than in control mice when moving freely, n was labelled in the columns, *P < 0.05, two-tailed unpaired t-test. (D) c-Fos expression after ultrasound stimulation is significantly higher in Piezo1-transfected mice than in control mice. *P < 0.05, two-tailed unpaired t-test, n = 3.*

Taken together, the present study elucidates the feasibility of using Piezo1 as an effective mediator of neural activity and signaling when treated with ultrasound. By manipulating Piezo1 expression in the 293T cells, CLU199 cells, and neurons, we demonstrate a new approach for selective, non-invasive brain stimulation. The various consequent effects of this strategy, regulating genes with functions from transcription control to neurotransmitter production, cast ultrasound as a modality with wide-ranging effects that could be applied therapeutically to a variety of different conditions. We believe that such an approach can be utilized for probing brain functions and treating disorders, which could be identified through more in-depth research about the treatment's effect on behavior.

We found that primary neurons express Piezo1, which is known to play an important role in neural development and differentiation (176). This endogenous expression is a complicating factor in this study, as it could have reduced the precision with which neurons were targeted. This may be remedied to an extent by utilizing methods that upregulate Piezo1 to an even greater degree in vivo, such as viral infection. This can be expected to reduce the ultrasound dose required to activate the desired cells, thereby leaving others mostly unaffected and increasing the specificity of the intervention. On the other hand, while alternatives do exist, given that Piezo1 is one of the most sensitive

mechanosensitive channels, choosing alternatives would likely involve a trade-off in the sensitivity of the cells to ultrasound. Thus, future research should aim to identify ultrasound mediators or methods that sacrifice neither cell-type/circuit-element specificity nor sensitivity to ultrasound. This might involve inducing the expression of exogenous or artificially engineered proteins, or an approach that uses targeted microbubbles to achieve this end.

In this study, we demonstrated that ultrasound can activate Piezo1. Martin and his colleagues also demonstrated that higher frequency ultrasound at 43 MHz can activate Piezo1 by microstreaming induced by radiation force, while Pan *et al.* showed that ultrasound at 2 MHz can activate Piezo1 in the presence of microbubbles. Either case is not closely relevant in *in vivo* neural stimulation. Our studies fulfilled the frequency space at the *in vivo* condition. However, in our study, we cannot confirm which biophysical mechanism involved for open Piezo1, which needs to be addressed in near future. It is suggested that radiation force or particle displacement could play important roles in initiating neural activation with evidence from retina stimulation by higher frequency ultrasound (104). But whether it is true still needs to be tested.

Piezo1 plays key roles in physiological and developmental stages that involve mechanosensitivity, including touch, breathing, vascular development and more. It has an unusual dome shape causing deformation of synthetic membrane vesicles. The curvature of the arms could induce deformation of the cell membrane which sense the changes in membrane tension and on channel opening. As shown in Fig. 13, simulation results demonstrate that ultrasound can induce membrane curvature in a frequency dependent

manner. It is interesting to test whether ultrasound can induce membrane curvature which open the Piezo1.

Besides Piezo1, which increases neural activity, mechanosensitive potassium or chloride channels may also serve as potential mediators with inhibitory effects, making it possible to reduce neural activity as well. Moreover, the ultrasonic paradigm may be expanded to trigger mechanosensitive ion channels endogenously expressed in various tissues, such as the peripheral or enteric nervous system, which could have therapeutic implications. Such non-invasive control of neurons in deep tissue, whether in the brain or elsewhere, whose inaccessibility currently poses substantial challenges to biomedicine could be a way to address diseases or neurological conditions of many varieties in the future.

3. Materials and Methods:

1. Cell culture

293T cells were purchased from ATCC. The embryonic mouse hippocampal cell line mHippoE-18 (referred to in the text as “CLU199”) was purchased from Cedarlane Laboratories. 293T and CLU199 cells were maintained in Dulbecco’s Modified Eagle Medium (DMEM) (high glucose and no sodium pyruvate), supplemented with 10% fetal bovine serum, 100 units/mL penicillin and 100 µg/mL streptomycin (all from Gibco), inside a humidified incubator 37°C with 5% CO₂. For experiments requiring transfected cells, cells were seeded in 35 mm dishes or collagen-I-coated (Corning) glass coverslips (5 µg/cm²), at 1.5 x 10⁶ cells per dish, allowed to grow overnight, and treated with ultrasound the next day.

2. Primary cortical neuron harvest

Primary cortical neurons from embryonic mice brains were harvested as described previously (1) with slight modifications. Briefly, pregnant mice were sacrificed at E16.5-E17, and brains from the embryonic mice were collected. They were then dissected under a microscope to separate the cortex from the other brain mass. Cortical cells were dispersed and seeded into culture dishes or collagen-coated glass coverslips (4 µg/cm²). At DIV 10, the cells were used for further experiments.

3. Plasmid transfection and siRNA reverse-transfection

pcDNA3.1 plasmids, both the control plasmid and the one containing Piezo1-EGFP, were provided by Dr. Ardem Patapoutian (Scripps Institute). Transfections on 293T cells were performed using 1 µL of Lipofectamine™ LTX Reagent with PLUS™ Reagent

(Invitrogen) with 500 ng of plasmid DNA in Opti-MEM (Gibco) per 35 mm dish or 6-well plate. The media was changed to DMEM + FBS after 24 hours. Transfected cells were used for imaging and ultrasound stimulation 48 hours after transfection. Primary cortical neurons were transfected on DIV 7 following the same protocol as for 293T cells. Transfected primary neurons were used for imaging and ultrasound stimulation 72 hours after transfection.

SMARTpool ON-TARGETplus Piezo1 siRNA (L-061455-00-0005) and ON-TARGETplus Non-Targeting Pool (D-001810-10) siRNA were obtained from Dharmacon. Transfection complexes were prepared by incubating siRNA with Lipofectamine RNAiMAX (Invitrogen) in Opti-MEM for 5 minutes at room temperature. 300 μ l of complexes added per 35 mm dish or collagen-coated coverslips (5 μ g/cm²). 1.5 x 10⁶ cells were added per dish in fully-supplemented DMEM such that the final siRNA concentration was 125 nM. Cells were incubated for 48 hours post-transfection, and then used for further experiments.

4. Calcium imaging

Cells were loaded with the fluorescent calcium indicator Cal590 (AAT Bioquest), according to the manufacturer's instructions. A customized calcium imaging and ultrasound stimulation system (Fig. S1) was utilized for the study. The calcium imaging system consisted of a modified upright epifluorescence microscope. The excitation light was generated by a dual-color LED, filtered by excitation filters and delivered to the sample for illuminating the calcium sensor. The fluorescence signals from the cells were collected by a water immersion objective (UMPlanFLN, Olympus), filtered by a filter wheel with green (525 nm) or red (633 nm) channels and captured by a sCMOS camera

(ORCA- Flash4.0 LT Plus C114400-42U30, Hamamatsu). To minimize phototoxic effects, the LEDs were triggered at 1 Hz and synchronized with sCMOS time-lapse imaging. The ultrasound stimulation system consisted of a commercial transducer (I7-0012-P-SU, Olympus), two function generators, and a power amplifier (Electronics and Innovation, A075) to produce 200 tone burst pulses at a center frequency of 500 kHz and a repetition frequency of 1 kHz with a duty cycle of 40%. The output intensity was limited to 0.1 - 0.6 MPa. These parameters are similar to which has been reported to effectively evoke behavior responses (3). To deliver ultrasound, a triangle waveguide was attached to the ultrasound transducer and placed under the culture dish at a 45-degree angle to the horizontal axis. The other site of the waveguide was mounted with an acoustic absorber to minimize acoustic reverberation. During calcium imaging, the cells were placed in a buffer solution with 130 mM NaCl, 2 mM MgCl₂, 4.5 mM KCl, 10 mM Glucose, 20 mM HEPES, and 2 mM CaCl₂, pH 7.4.

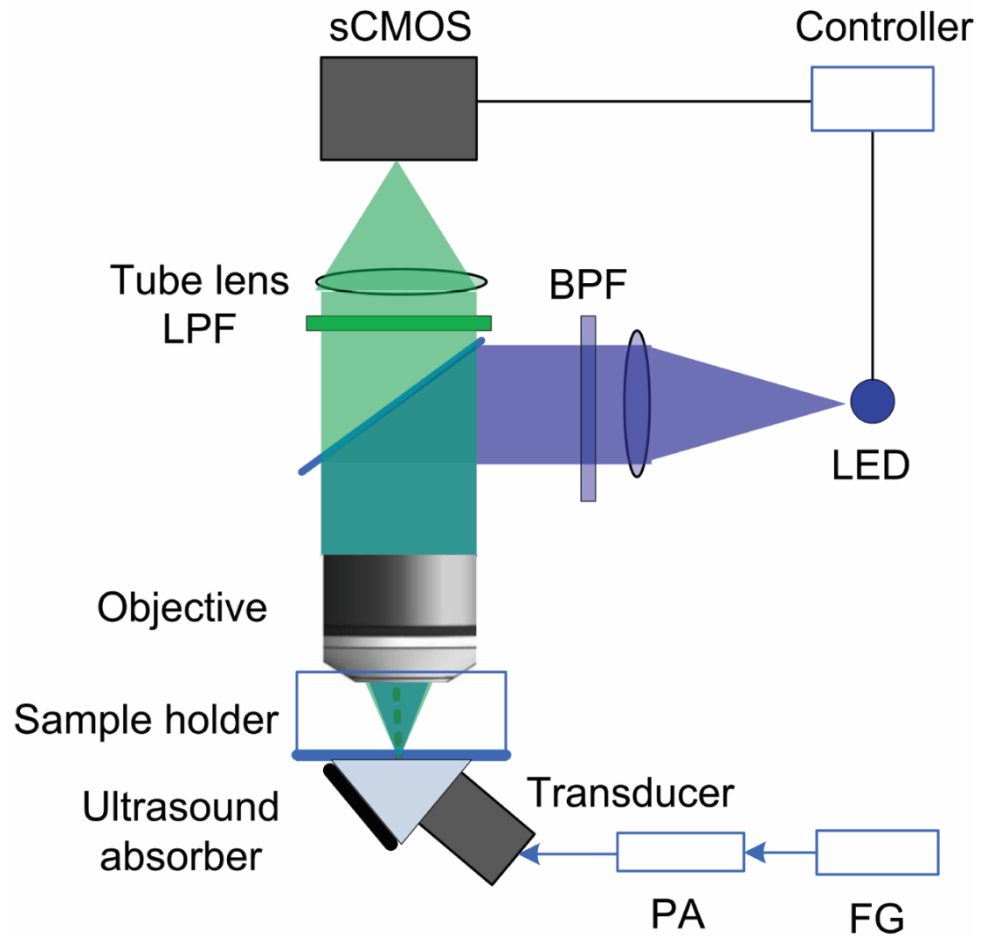


Figure 15 In vitro experimental system. *This setup combines a calcium imaging system and an ultrasound stimulation system.*

5. Ultrasound treatment of cells

CLU199 cells or primary cortical neurons at DIV 10 were treated with ultrasound at acoustic pressures of 0.1, 0.3 or 0.5 MPa for 20 minutes with 20s interval inside a humidified incubator, 37°C, 5% CO₂. The ultrasonic stimulation system and treatment parameters are the same as those described in section 4. Yoda1 (Tocris Bioscience) was used as a Piezo1 agonist with a concentration of 1 μM, while GsMTx-4 (Abcam) was used as a Piezo1

blocker at a concentration of 10 μ M. Yoda1 was added to culture media, followed by a 20-minute incubation or immediate ultrasound treatment. GsMTx-4 was added to culture media, allowed for 30 minutes incubation, and followed by a further 20-minute incubation or ultrasound treatment.

6. Western blotting

Cells were lysed with RIPA buffer (EMD Millipore), supplemented with 1X Halt™ Protease and Phosphatase Inhibitor Cocktail (Thermo Fisher Scientific) on ice, centrifuged to clear the lysate, and protein concentrations measured using the Bio-Rad protein assay. 30 or 50 μ g total protein per well was loaded on 10% SDS-PAGE gels, electrophoresed, and transferred to methanol-activated PVDF membranes. Membranes were blocked with 3% BSA in Tris-buffered-saline + 0.05% Tween-20 (TBST). Membranes were incubated in primary antibody diluted in 5% BSA in TBST overnight, washed with TBST and incubated in secondary antibody solutions, diluted in blocking buffer, for 1 hour at room temperature. Membranes were then washed, signals developed with SuperSignal™ West Pico (cat. no. 34078) or Pierce ECL (cat. no. 32106) chemiluminescent substrates according to the manufacturer's instructions, and imaged using the Bio-Rad ChemiDoc MP system.

Primary antibodies used were phospho-CREB (cat. no. 9198), CREB (cat. no. 9197), phospho-CaMKII (cat. no. 12716) and CaMKII-pan (cat. no. 4436) all from Cell Signaling Technology and diluted at 1:500 and β -actin (A1978, Sigma-Aldrich) at 1:2,000 was the loading control. Secondary antibodies used were goat-anti-rabbit IgG (H+L)

HRP (cat. no. 31460) and goat-anti-mouse IgG (H+L) HRP (cat. no. 31430) from Thermo Fisher Scientific, diluted at 1: 5,000 in blocking buffer.

Protein levels were quantified through image densitometry using ImageJ. Protein levels were expressed as a fold change compared to the untreated control, an average \pm SEM of at least three independent experiments, except in Fig. 2E. Statistical significance was calculated using a two-tailed unpaired student's *t*-test and *P* values below 0.05 were considered significant.

7. RNA extraction and reverse-transcription

Cells were lysed with RNAiso Plus (Takara) and RNA was extracted from these lysates using RNA Direct-zol columns (Zymo Research) according to the manufacturer's instructions, including a DNase incubation step to eliminate genomic DNA from the final product. RNA was quantified using a NanoVue spectrophotometer (GE Healthcare Life Sciences), and 1 μ g of total RNA was reverse-transcribed using the Transcriptor First Strand cDNA Synthesis Kit (Roche).

8. Semi-quantitative PCR and real-time qPCR

1 μ l cDNA from CLU199 cells was mixed with 2X PCR Premix *Ex* Taq (Takara) (final concentration 1X), forward and reverse primers (mouse *Piezo1* and β -actin, final concentration 200 nM) and H₂O to a final reaction volume of 20 μ l. PCR was performed on a Bio-Rad DNA Engine thermal cycler, for 25 cycles, T_a 56°C. PCR product was loaded on a 2% agarose gel, electrophoresed, visualized in an AlphaImager HP (ProteinSimple) UV Transilluminator. The resulting bands were quantified using image densitometry in ImageJ.

For real-time qPCR, 1 μ l cDNA from plasmid-transfected 293T or siRNA-transfected CLU199 cells was mixed with appropriate forward and reverse primers (final concentration 250 nM), 2X SYBR Green Premix *Ex Taq* (Takara) and H₂O to a final volume of 10 μ l. PCR was performed on Applied Biosystem 7500 Fast Real-Time PCR system (Thermo Fisher Scientific). Results are expressed as a fold change compared to the appropriate control, mean \pm SD of 3 independent experiments. Primer sequences were as follow:

Mouse β -actin: F - AGG GTG TGA TGG TGG GAA TG, R - TGG CGT GAG GGA GAG CAT AG, 402 bp; human β -actin: F - GTG GGG CGC CCC AGG CAC CA, R - CTC CTT AAT GTC ACG CAC GAT TTC, 539 bp; mouse Piezo1: F - GCA GTG GCA GTG AGG AGA TT, R – GAT ATG CAG GCG CCT ATC CA, 143 bp ; human Piezo1: F – ATCGCCATCATCTGGTTCCC, R – TGGTGAACAGCGGCTCATAG, 124 bp; mouse GAPDH: F - AAC GAC CCC TTC ATT GAC, R - TCC ACG ACA TAC TCA GCA C, 190 bp.

9. qPCR array

CLU199 cells seeded in 35 mm dishes were treated with ultrasound, Yoda1 or GsMTx-4 as appropriate. Total RNA was collected as described in section 7, and the concentration measured on NanoDrop™ One (Thermo Fisher Scientific). Samples with 260/280 > 1.8 and 260/230 > 2.0 were run on a 1% agarose gel containing bleach to check for RNA integrity (2). Samples with good integrity were reverse-transcribed using the RT² First Strand Kit (Qiagen), using 1 μ g total RNA, according to the manufacturer's instructions. RT product was diluted as described in the manufacturer's protocol, and mixed with RT² SYBR® Green qPCR Mastermix (Qiagen). This solution was then loaded into appropriate

wells of the RT² Profiler™ PCR Array Mouse cAMP / Calcium Signaling PathwayFinder (cat. no. PAMM-066Z), centrifuged and cycled according to the manufacturer's instructions on the QuantStudio™ 7 Flex Real-Time PCR System (Life Technologies). Ct values were calculated using the Quantstudio™ software, exported into a spreadsheet and uploaded to SABiosciences' online array data analysis software (accessible at: <http://pcrdataanalysis.sabiosciences.com/pcr/arrayanalysis.php>). Results were normalized to three housekeeping genes (Gapdh, Gusb and Hsp90ab1). Resulting clustergrams and a spreadsheet containing the analyzed results were obtained from this software. The number of genes that were upregulated (fold change > 1.00) or downregulated (fold change < 0.50) compared to the untreated control were calculated, and the list of genes whose expression was altered by ultrasound treatment by more than 2 times was collected. The results were categorized according to the nature of the gene's regulation and the function of the encoded protein, according to information provided in the PCR array's product literature (4) and in a paper, that also used this array (5).

10. Immunocytochemical fluorescent staining

CLU199 cells and primary neurons at DIV 10, including treated with (+) or without (-) ultrasound, were fixed using 4% paraformaldehyde + PBS and permeabilized using 0.1% Triton X-100 + PBS. Cells were blocked using 3% normal goat serum + 3% BSA in PBST, and incubated overnight in primary antibodies diluted in 5% BSA + 0.05% sodium azide. Secondary antibody incubation was performed the next day, diluted in 3% BSA in PBST for one hour at room temperature. Cells were washed, coverslips dried, and mounted on glass slides using small drops of Prolong Diamond Antifade Mountant with DAPI (Life Technologies), and allowed to cure in the dark at room temperature overnight. All wash

steps were performed using PBS. Coverslip edges were then sealed using transparent nail enamel, and imaged using a confocal laser scanning microscope (TCS SP8, Leica). The number of c-Fos⁺ cells were determined by counting the number of DAPI and c-Fos signals co-located with DAPI from 10 FOVs photographed per condition. Results were expressed as a percentage of c-Fos versus DAPI signals, and were subjected to a one-way ANOVA followed by a *post-hoc* Tukey test. *P* values below 0.05 were considered significant.

Primary antibodies, used at a dilution of 1:200, were phospho-CREB, phospho-CaMKII and c-Fos (cat. no. 2250) all from Cell Signaling Technology, Piezo1 (15939-1-AP, Proteintech Group), and MAP2 (MAB3417, EMD-Millipore). Secondary antibodies, used at a dilution of 1:1,000, were goat anti-rabbit IgG (H+L), Alexa Fluor 488 (A-11008) and goat anti-mouse IgG (H+L), Alexa Fluor 555 (A-21422) from Invitrogen.

11. Animal care

Male, 8-week old, C57BL/6J mice, were used for ultrasound stimulation with 6 in an anesthetized group and 6 in a free-moving group. Mice were housed under standard housing condition with food and water available ad libitum. Animal use and care were performed following the guideline of the Department of Health - Animals (Control of Experiments) of the Hong Kong S.A.R. government.

12. Plasmid injection and ultrasound transducer mounting

Mice were anaesthetized by intraperitoneal injection of Ketamine and Xylazine (100mg/kg and 10mg/kg respectively) followed by removing the skin above M1 area. Using the stereotaxic apparatus, a hole was drilled to allow pipette injection (AP=1.34, ML=1.50, DV=0.75). 1 μ g plasmid mixed with *in vivo*-jetPEI® (Polyplus Transfection) was injected at a rate of 0.5 μ l/min, and followed by a 10-minute pause. The pipette was then retracted slowly, including a 5-minute pause at the halfway point. To stimulate anesthetized mice, a transducer (I7-0012-P-SU, Olympus) was placed above the mouse head and directed to M1 region coupled by ultrasound gel. To stimulate free-moving mice, a holder for a customized wearable ultrasound transducer was mounted to the mouse brain (Movies S1, S2, and S3). After 3 days recovery, an ultrasound transducer at a center frequency of 775 kHz was clicked to the pre-mounted holder and locked tightly with preloaded ultrasound gel for stimulation.

13. Ultrasound stimulation and behavior recording

Anesthetized mice, were given 10-15 min to reach to an appropriate anesthesia plane. The mice were treated with 500 kHz ultrasound of 200 tone burst pulses and a repetition

frequency of 1 kHz with 40% duty cycle and 0.1 - 0.6 MPa acoustic pressure. The number of tail flicks versus the number of ultrasound stimuli were recorded. The results were analyzed with an unpaired two-tailed *t-test*, and *P*-values below 0.05 were considered significant.

For the free-moving experiment, mice were given 4 minutes to calm down and their motor responses following ultrasound stimulus at 0.3 MPa were recorded with a camera. Ultrasound stimuli were performed in batches of 10 each, each referred to as 1 “trial” in the text, and mice were allowed one minute of rest between trials. The number of head swings following every ultrasound stimulus was counted per trial. The number of head movements versus the number of ultrasound stimuli per trial were then analyzed with a two-tailed unpaired *t-test*, and *P* values below 0.05 were considered significant.

14. Immunohistochemical fluorescent staining

Mice were sacrificed 90 minutes after ultrasound treatment and perfused with PBS, followed by 4% paraformaldehyde (PFA) (cat. no. P1110, Solarbio) in PBS. After dissection, brains were *post-fixed* overnight in 4% PFA and then dehydrated in 15%, 20% and 30% sucrose diluted in PBS for the following 3 days. Starting from the injection plane, 60 continuous coronal brain slices at a thickness of 30 μm were collected. Slices were blocked using 1% normal goat serum + 5% BSA + PBS, and incubated overnight in primary antibody solution diluted in 5% BSA + 0.05% sodium azide. Slices were then washed, and incubated with secondary antibodies diluted in PBS for 1 hour at room temperature. Slices were then washed, coverslips dried, and mounted on glass slides using small drops of Prolong Diamond Antifade Mountant with DAPI, and allowed to cure in the dark at room temperature overnight. Coverslip edges were sealed using transparent

nail enamel, and imaged using a confocal laser scanning microscope (TCS SP8, Leica). 3 ROIs were chosen from a slice and the number of cells showing blue (DAPI) and red (c-Fos) signals were counted using ImageJ, and the number of c-Fos signals were expressed as a percentage of the number of DAPI signals. The number of c-Fos positive cell vs DAPI positive cell were analysis by unpaired two-tailed *t*-test and *P* values lower than 0.05 were considered significant.

Primary antibodies used were c-Fos (2250, CST, dilution 1:50), Piezo1 (15939-1-AP, Proteintech Group, dilution 1:50), and MAP2 (PA1-16751, Invitrogen, dilution 1:100). Secondary antibodies, used at a dilution of 1:500, were goat anti-rabbit IgG (H+L), Alexa Fluor 488 (A-11008, Invitrogen) and goat anti-mouse IgY (H+L), Alexa Fluor 633 (A-21103, Invitrogen).

Chapter 3: Toolkit for non-invasive brain stimulation by ultrasound

Sonogenetics enabled by MscL

Ultrasound can activate mechanosensitive ion channels which is a foundation to achieve selective brain stimulation facilitating understanding brain functions and treating brain disorders. Here we demonstrate a selective neural excitation strategy via activation of mechanosensitive ion channels MscL by non-invasive ultrasound. Our results showed that MscL, when triggered by ultrasound, was activated to induce reversible neural activity as measured by calcium imaging and patch clamping techniques in vitro and ex vivo. Ultrasonic stimulation in the primary motor cortex (M1) of mouse brains induced activity of neurons expressing MscL, resulting in elevated c-fos expression correlated to increased movement in both anesthetized and free-moving mice. Thus, we demonstrate a novel tool for targeting ultrasound into intact brain structures non-invasively, allowing selective neuronal control.

1. Introduction

Controlling local or global neural activity and signaling by physical intervention is a powerful way to gain causal insight into brain functions¹ and treat brain disorders (Fig. 16). To achieve this, diverse modalities have been developed in the past few decades, including deep brain stimulation (DBS), transcranial direct current stimulation (tDCS), transcranial magnetic stimulation (TMS), transcranial ultrasound brain stimulation⁸, chemogenetics and optogenetics (13, 35, 177). This has resulted in the rapid accumulation of knowledge about brain functions as well as treatment strategies for brain diseases(13, 35). These findings have also, however, highlighted the need for stimulation techniques that possess cell-type or circuit-element specificity, high spatiotemporal resolution, brain-wide accessibility for local or global stimulation, and non-invasiveness for repeated implementation, all of which are crucial for fundamental research and clinical translation (35, 177). These requirements being currently unmet, there is a strong impetus for new research techniques to be developed that can fulfill these goals.

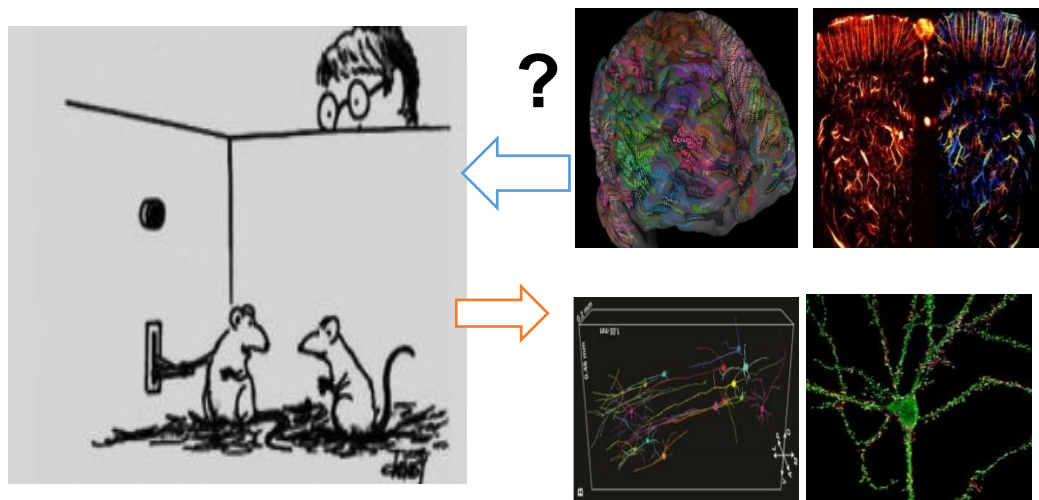


Figure 16 Strategies for probing brain function. *To dissect the neural circuits, it is required established a behavior model and then detect the structural, functional changes*

correlated to the behavior. However, to get causal information, it still needs an external stimulation modality to excite or inhibit neural activity. This stimulation modality can also translate as a treatment technique.

Ultrasound-based brain stimulation is a promising candidate because it can potentially access deep brain structures non-invasively through the intact skull and be steered to millimeter-sized dynamic focal spots in deep brain regions (178). However, the treatment is currently not able to target a desired population of neurons by cell-type, which could result in the dilution of its effects, or even side-effects, depending on the application. Selectivity for cell-types could be achieved through a strategy that confers ultrasonic sensitivity to targeted neurons, analogous to the optogenetic approach, could grant precise control of mammalian neurons and animal behavior upon ultrasonic stimulation. Such a key could lie with “mechanosensitive” ion channels, a crucial component of the cellular force-sensing machinery. The opening of these ion channels is controlled by diverse mechanical stimuli such as touch, hearing, crowding, stretch and cell volume, which can convert physical force into cellular signaling. Cellular mechanosensation through ion channels could thus be a mechanism utilized for ultrasonic stimulation of neurons.

There are multiple known mechanisms through which ultrasound exerts effects on cells and progressing towards clinical application would require understanding and controlling them. At high acoustic intensities, ultrasound exerts its therapeutic influence primarily through thermal or cavitation effects, but such intensities have been found inappropriate for projecting ultrasound safely through the cranium. Since lower intensities will be needed for brain stimulation, these mechanisms are unlikely to play major roles in the process. Ultrasound has been shown to can generate nano-newton level radiation force and micrometer displacement in soft tissues (56), which could lead to the opening of

mechanosensitive ion channels. Low-intensity ultrasound has been shown to activate non-endogenous mechanosensitive ion channels in various cell-based systems, in a *C. elegans* model and in primary neurons. However, the role of mechanosensitive ion channel activation by ultrasound *in vivo* remains to be demonstrated. Therefore, it is compelling to examine whether low-intensity ultrasound alone can directly act on such channels under physiological conditions and induce activity and signaling in targeted neurons in mammalian brains *in vivo*.

In the present study, we demonstrate a non-invasive and selective ultrasound brain stimulation method through manipulating the activity of a mechanosensitive ion channel, MscL-G22S, both *in vitro* and *in vivo*, illustrated schematically in Fig. 17A. The MscL-G22S channel is a mutant version of the well-established bacterial mechanosensitive channel with a lower threshold for gating which has been shown to respond to ultrasound. We used this channel to sensitize 293T cells and primary neurons to ultrasound and found that ultrasound could consistently induce Ca²⁺ influx into cells at significantly lower intensities in cells expressing MscL-G22S. We also stimulated mouse brains with ultrasound and found that mice expressing MscL-G22S in their M1 areas showed significantly higher activation and motor responses at low intensities than those without. We thus show for the first time a feasible method to selectively sensitize neurons *in vivo* to low-intensity ultrasound by inducing the expression of a mechanosensitive ion channel.

We first confirmed that heterologously-expressed MscL-G22S could sensitize cells to ultrasound in our system. We first tested this in 293T cells, known to have minimal endogenous expression of mechanosensitive ion channels^{25,26}, and transfected a plasmid encoding a MscL-G22S-EGFP fusion protein (designed by Cox et al.²⁷). The expression

of MscL-G22S in 293T cells was verified by qPCR and fluorescence imaging compared to a mock transfection control (Fig. 17B). To measure any inward current upon ultrasound stimulation, we used a patch clamp setup combined with an ultrasound stimulation system (as in Fig. 17C). We treated cells with 0.5-1 MHz ultrasound of 200 cycles, at 1 kHz pulse repetition frequency (PRF) with 200 tone bursts at from 0.025 – 0.15 MPa. Ultrasound at 0.05 MPa induced significantly higher inward current in the cells expressing MscL-G22S compared to the control, which showed a minimal response (Fig. 17D). A ratiometric fluorescent calcium indicator (Fura-2) was used to observe and measure the movement of calcium ions (Ca^{2+}) into the cells. Cells expressing MscL-G22S were found to show significantly higher Ca^{2+} influx in response to ultrasound than the control, and the response also varied depending on the ultrasound intensity (Figure 17E and F). In addition, the ratiometric Ca^{2+} dye used enabled us to ascertain that the increase in fluorescence seen was not an artifact of the ultrasound setup. We thus found that ultrasound stimulation could activate MscL-G22S when expressed heterologously in 293T cells.

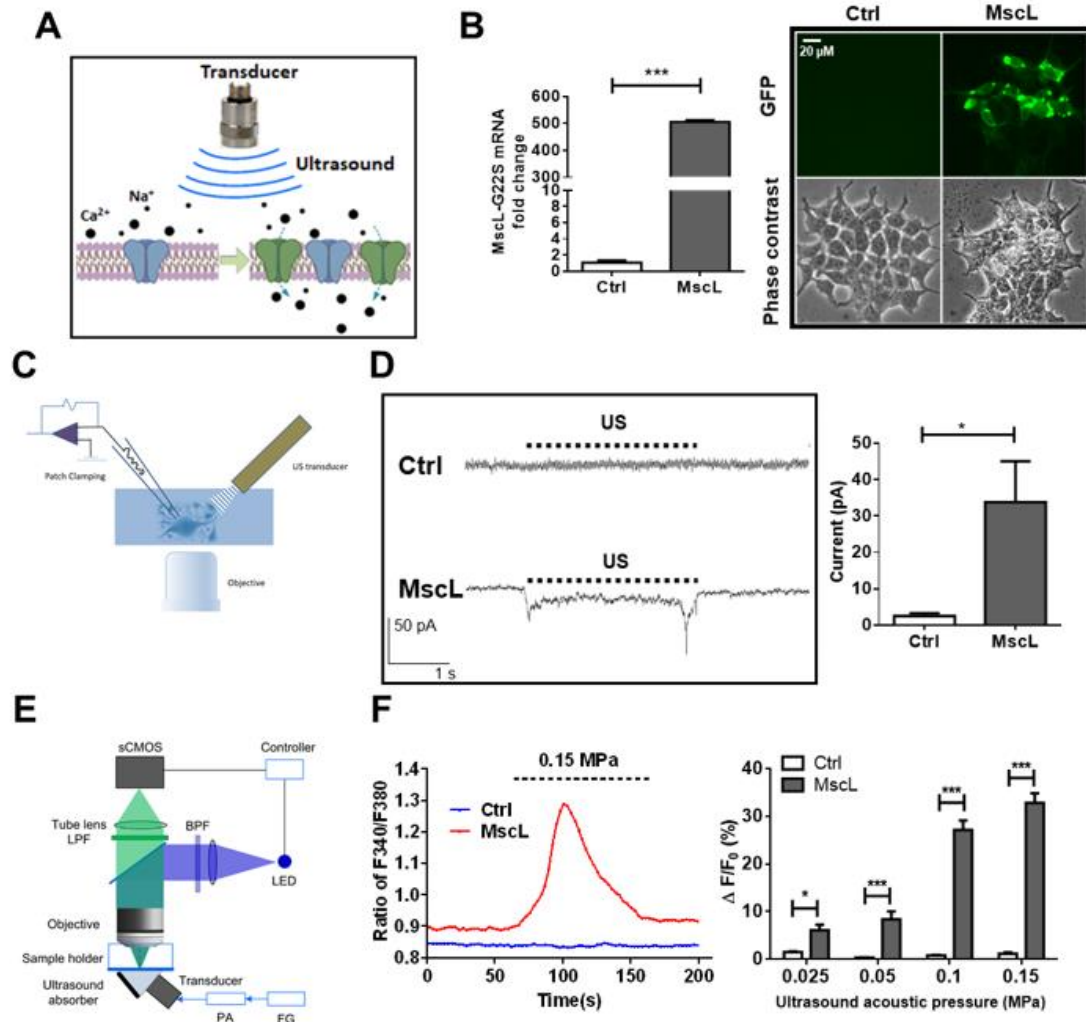


Figure 17 Ultrasound induces intracellular calcium influx by MscL activation in 293T cells. (A). Schematic representation of our experimental plan. Briefly, this involves sensitizing cells to ultrasound by heterologously expressing a mechanosensitive ion channel, MscL-G22S, in their cell membranes. Thereafter, these channels will react to ultrasound stimulation by opening, and allow the entry of cations such as Ca^{2+} . (B) The expression of MscL-G22S in transfected cells was assessed by qRT-PCR and microscopy, in comparison with a mock-transfection control. Left: The bar chart of qPCR results represents mean \pm SEM of three independent experiments, $n = 3$, *** $P < 0.001$. Right:

*Representative images of GFP fluorescence and phase contrast are shown. (C) An illustration of our patch clamp recording setup. The ultrasound stimulation system is composed of a needle transducer incorporated into a patch clamping system. (D) Left: Current clamp recording of inward-flowing current in cells stimulated by 0.05 MPa ultrasound (US). Right: *t* voltage clamp experiments, $n = 4$ * $P < 0.05$, unpaired two-tailed *t*-test. (E) A schematic illustration of the combined ultrasound stimulation and calcium imaging system used. (F) Left: A representative time-course of ratiometric Ca^{2+} imaging comparing ultrasound stimulation of Control and MscL-transfected cells at 0.15 MPa. Right: The bar chart shows the mean \pm SEM of 3 independent Ca^{2+} imaging experiments. $n = 9$, * $P < 0.05$, *** $P < 0.001$, two-tailed unpaired *t*-test with Holm-Sidak correction.*

We next tested the effects of ultrasound on primary cortical neurons harvested from embryonic mouse brains (E16) to test the feasibility of selectively stimulating live neurons with ultrasound. To induce MscL-G22S expression in neurons, we used AAV-based viruses with a human synapsin (hSyn) promoter, which preferentially infects neurons over other cell types. Primary neurons at day in vitro (DIV) 7 were transduced with rAAV/9-hSyn-MscL-G22S-EYFP-pA or rAAV/9-hSyn-EYFP-pA viruses. At DIV 12 these neurons were found to show EYFP fluorescence co-located with the expression of the neuron marker MAP2 (Fig. 18A), thus confirming the neuron specificity of the viruses. Neurons treated with the MscL-containing virus showed increased firing of action potentials and greater spike amplitude in response to 0.05 MPa ultrasound, compared to the control (Fig. 18).

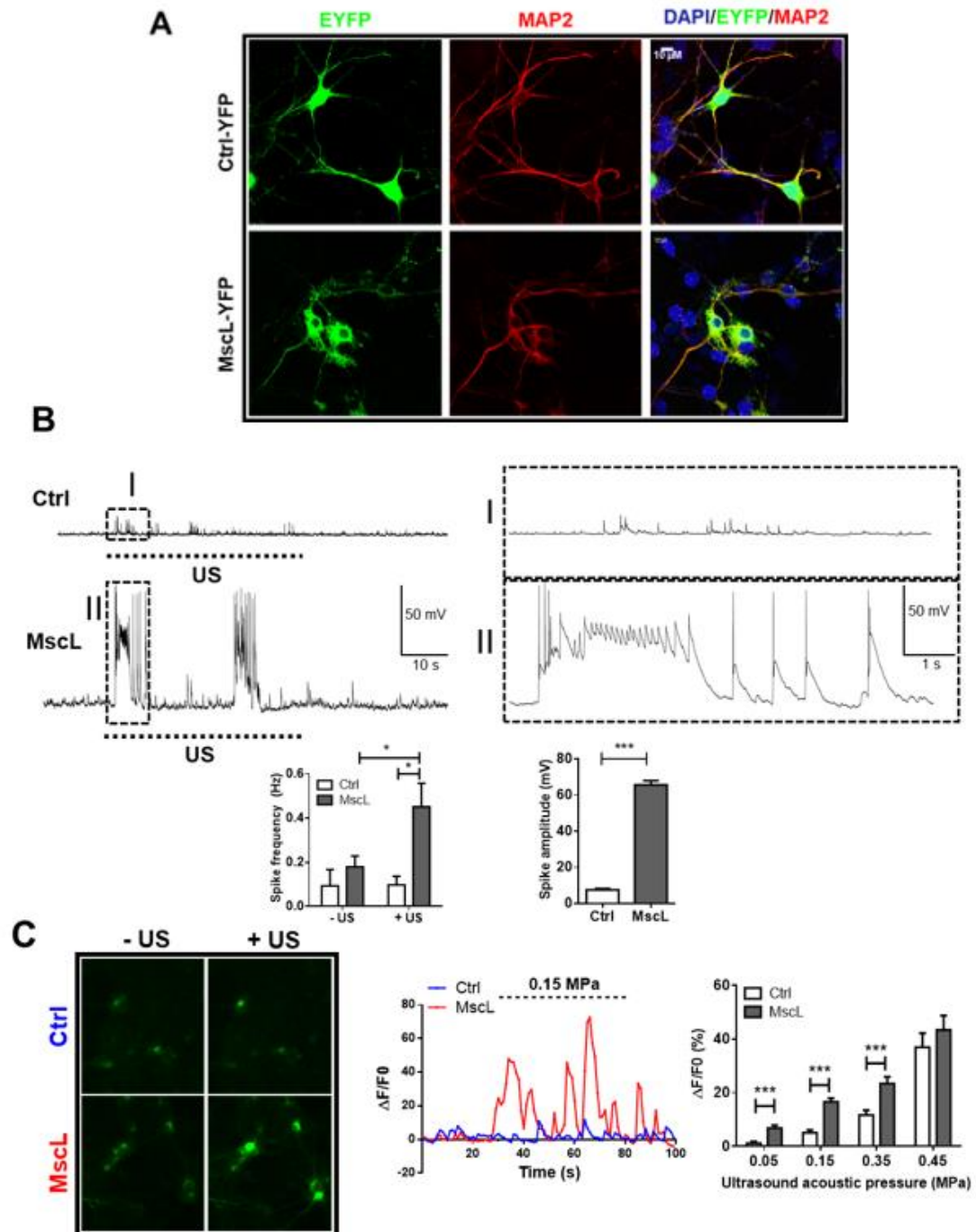


Figure 18 Ultrasound regulates the neural activity of calcium signaling and electrophysiology. (A) Representative immunocytochemical staining of primary neurons transduced with *rAAV/9-hSyn-EYFP-pA* and *rAAV/9-hSyn-MscL-G22S-EYFP-pA*

viruses at DIV 12. Cells were imaged for MAP2 (red) staining and EYFP fluorescence (green) to confirm the virus' ability to preferentially transduce neurons. (B) (Upper) Voltage clamp recordings of virus-transduced primary neurons treated stimulated with 0.05 MPa ultrasound. (Lower) Bar charts show the mean \pm SEM spike frequencies and amplitudes of 3 independent experiments. * $P < 0.05$. *** $P < 0.001$, unpaired two-tailed t -tests. (C) (Left) Representative Ca^{2+} imaging result of primary neurons transduced with rAAV/9-hSyn-GCaMP6S-pA and rAAV/9-hSyn-MscL-G22S-GCaMP6S-pA viruses and stimulated with 0.15 MPa ultrasound at DIV 12. (Middle) Representative time-course of Ca^{2+} imaging of transduced neurons stimulated with ultrasound. (Right) Bar charts represent mean \pm SEM of neurons stimulated with ultrasound at varying intensities from 3 independent experiments. $N = 6$, *** $P < 0.001$, unpaired 2-tailed t -tests with Holm-Sidak correction.

Alternatively, neurons at DIV 7 were treated with either rAAV/9-hSyn-MscL-G22S::GCaMP6S or rAAV/9-hSyn::GCaMP6S, where GCaMP6S is a fluorescent calcium indicator protein, and calcium imaging was performed at DIV 12. Neurons expressing MscL-G22S accumulated significantly more intracellular Ca^{2+} in response to ultrasound compared to the control (Fig. 18C). The Ca^{2+} influx responses showed some degree of dose-dependence, with increasing acoustic pressure inducing greater Ca^{2+} influx. We thus see that introducing MscL-G22S into primary neurons could successfully sensitize them to ultrasound, an effect reflected in the significantly lowered intensities at which neurons were able to respond to ultrasound. At 0.05 MPa neurons expression MscL-G22S showed significant Ca^{2+} influx as well as fired action potentials, whereas the control showed little to no change. The control cells showed significantly lower Ca^{2+}

influx than the MscL-G22S-expressing cells, up to 0.45 MPa, at which intensity the endogenously-expressed mechanosensitive channels appeared to be activated. Both groups of cells showed no difference in resting membrane potential, which we measured as an indication of cell health (Fig. 19). We hence concluded that MscL-G22S could successfully sensitize neurons to and mediate the effects of ultrasound, when expressed in primary neurons.

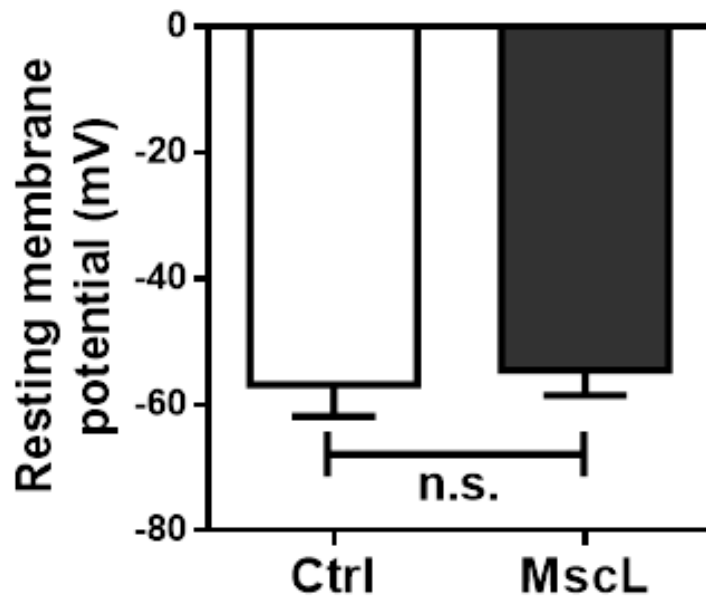


Figure 19 Resting membrane potentials of transduced primary neurons. Resting membrane potentials of primary neurons transduced with Ctrl-EYFP or MscL-EYFP viruses. Bar chart represents mean \pm SEM of at least 3 independent experiments, n for Ctrl = 4, n for MscL = 6. Differences are non-significant according to an unpaired 2-tailed t -test.

Finally, to test the ultimate feasibility of our setup, we sensitized neurons *in vivo* by injecting the control and MscL-G22S viruses into the primary motor cortices of mice. Eight-week-old mice were injected with viruses, and five weeks later they were subjected to ultrasound stimulation for 40 minutes under anesthesia (illustrated in Fig. 20A) using a mounted transducer setup. We tested the neuronal activation in our mice subjects by staining for the important activation marker c-Fos which is known to respond to calcium influx^{29,30}. Mice injected with the control and MscL-G22S viruses were treated with 0.3 MPa ultrasound, and the regions of viral expression as judged by EYFP expression were stained for c-Fos expression. The M1 regions of mice untreated with ultrasound were also stained in the same manner. We found ultrasound treatment induced significantly higher expression of c-Fos in both virus groups, but the magnitude of the effects was much higher in the MscL-G22S group. Ultrasound stimulation increased the c-Fos levels in the control mice to 1.96 times the untreated condition, but it increased c-Fos in the MscL-G22S group 20.8 times compared to the untreated condition (Fig. 20B). A similar comparison of mice with sham injections showed no significant difference in c-Fos expression between the M1 areas of mice treated or untreated with ultrasound (Figure 21) and the treated mice showed no obvious health effects as judged by body weight. We thus see that the application of ultrasound to mouse brains can induce neuronal activity, but the induced MscL expression made this effect many times stronger. Furthermore, the spatial extent of neural activation was largely co-located with MscL expression in the M1 area. Therefore, MscL-G22S could successfully mediate and increase neural activation in mice brains by ultrasound stimulation.

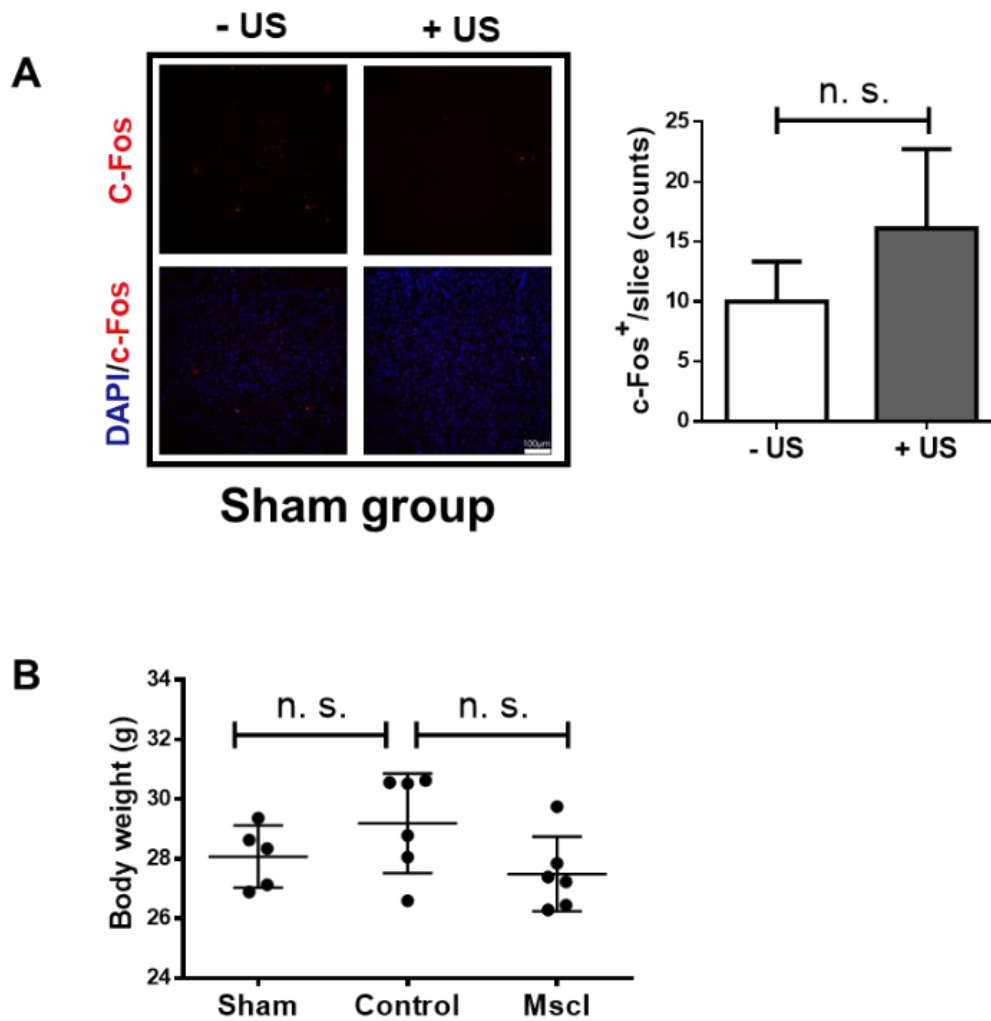


Figure 20 Additional data from mice. A. (Left) Representative images of MI areas of mouse brains in the sham group, with and without ultrasound, stained for c-Fos. (Right) Bar charts represent mean \pm SEM, $n = 3$. Differences are non-significant according to an unpaired 2-tailed t -test. B. Body weight measurements of mice with sham transduction, and transduced with the Ctrl-EYFP and MscL-EYFP viruses. Scatter plot shows body weights of different mice and mean \pm SD are shown. Differences are non-significant according to one-way ANOVA with post-hoc Tukey test.

We also studied whether the MscL-G22S mediated neural activation in the brain could evoke behavior changes using an assay to measure the number of motor responses upon ultrasound stimuli. Mice injected with viruses were anesthetized slightly and exposed to ultrasound in the range of 0.3 - 0.6 MPa. Motor responses were recorded and quantified as success rate with the number of body movements per ultrasound stimulus (illustrated in Fig. 21C). Motor responses induced by ultrasound stimulation were found to increase in the MscL-G22S transfected mice compared to the control mice up to a point. At 0.3 MPa, the success rate of body movements upon ultrasound stimulation were 7.8% for the control and 57.7% for the MscL-G22S mice, and this pattern increased to 23.3% and 77.3% respectively at 0.5 MPa, and these differences were significant (Fig. 21D). However, at 0.6 MPa the success rate of body movement increased to 62.3% and 65.0% for the control and MscL-G22S mice respectively (Fig. 21D). This pattern is like that seen in primary neurons and could also be explained by the activation of endogenous mechanosensation in the mice brains. However, at lower intensities the motor responses to ultrasound are minimal in the control group, while being significantly higher in the MscL-G22S group. Thus, our behavior assay also demonstrated that MscL-G22S can significantly sensitize neurons to ultrasound stimulation at lower intensities, and that our approach is functional at the behavioral level.

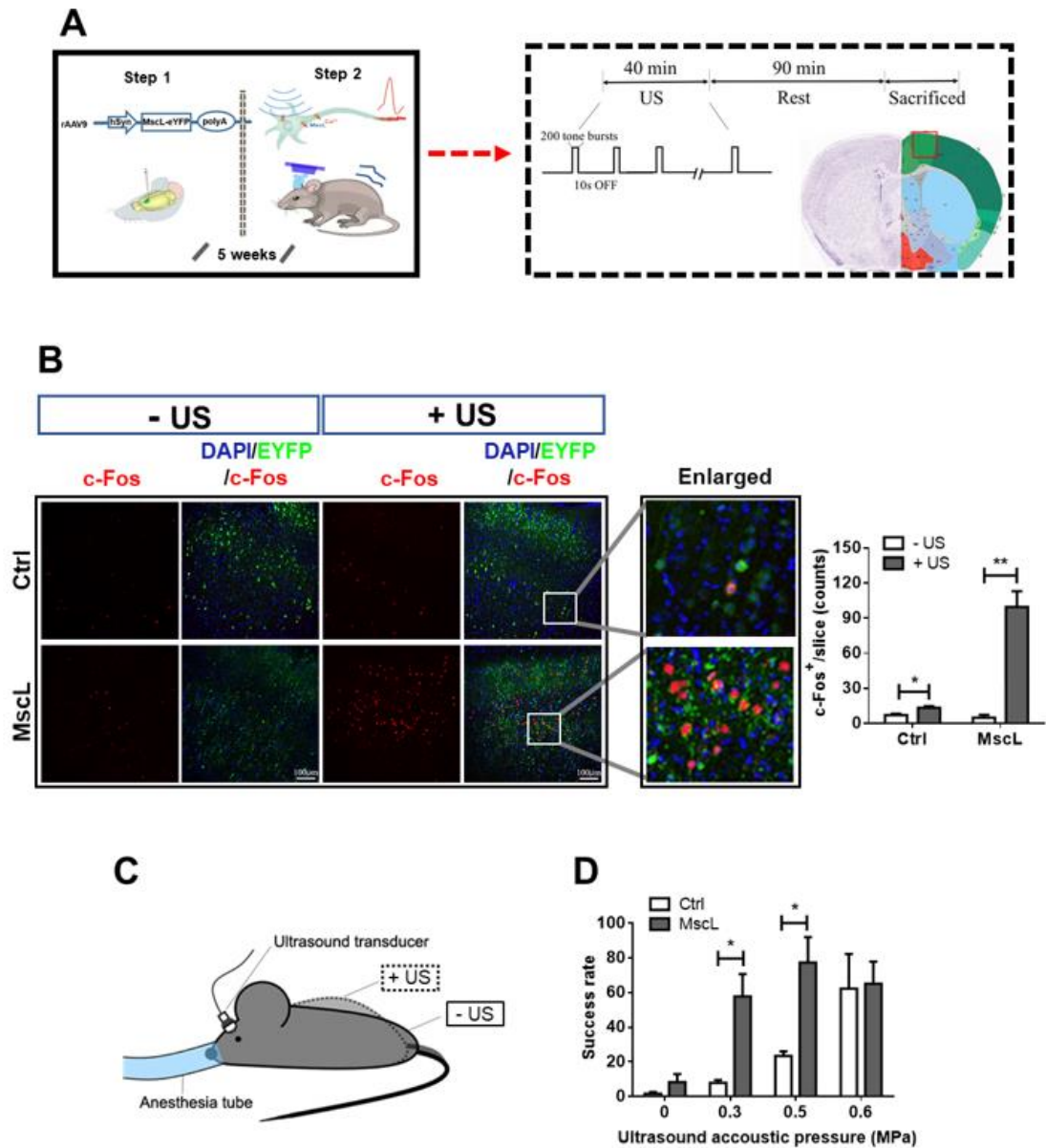


Figure 21 Ultrasound induces *c-fos* expression in MscL expressing neurons. (A) Schematic illustration of our *in vivo* neuron sensitization and ultrasound stimulation plan. Mice at 8 weeks were injected with viruses in their M1 regions and were treated with ultrasound 5 weeks later. The mice were tested for motor responses to ultrasound and their M1 regions stained for *c-Fos* expression. (B) (Left) Representative images of transduced M1 regions stained for *c-Fos* and EYFP expression, with or without 0.3 MPa

*ultrasound. Bars represent 100 μ m. (Right) Bar charts represent mean \pm SEM of c-Fos+ cells per stained slice. n for Ctrl groups = 3 and n for MscL groups = 6. * $P > 0.05$, ** $P > 0.01$, unpaired 2-tailed t-test with Holm-Sidak correction. (C) Schematic illustration of the motor response assay used. The mice were stimulated with ultrasound and various intensities, and the movement considered a 'response' is shown here. The ratio of responses per ultrasound stimulus was recorded as a 'success rate'. (D) Success rates of motor response per ultrasound stimulus at varying ultrasound intensities. Results are mean \pm SEM, n = 3, * $P > 0.05$, unpaired 2-tailed t-test with Holm-Sidak correction.*

Taken together, the present study elucidates the feasibility of using MscL as an effective mediator of neural activity and signaling when treated with ultrasound. By manipulating MscL expression in the desired neurons, we demonstrate a new approach for selective, non-invasive brain stimulation. The various consequent effects of this strategy, regulating genes with functions from transcription control to neurotransmitter production, cast ultrasound as a modality with wide-ranging effects that could be applied therapeutically to a variety of different conditions. We believe that such an approach can be utilized for probing brain functions and treating disorders, which could be identified through more in-depth research about the treatment's effect on behavior.

In all, our results constitute a proof-of-concept that mechanosensitive ion channel-mediated ultrasound stimulation can work specifically at lower frequency and low intensities. We were able to induce neuron-specific activity in both primary neurons as well as in the M1 regions of mice, using ultrasound applied non-invasively. Our approach also showed significant sensitization of neurons to ultrasound, with lower intensities being

enough to activate neurons in MscL-expressing cells. The non-invasiveness of this approach makes it promising for eventual clinical translation, while the cell-type selectivity could facilitate the elucidation and management of neural circuits involved in specific behaviors or disorders. Such a combination of these two features would be immensely helpful to target areas in the deep brain in conditions where treatments require non-invasiveness and repeatability e.g. targeting the substantia nigra in Parkinson's disease. Furthermore, the spatial specificity of neural activation targeted by MscL-G22S can be further increased by using focused ultrasound, which is compatible with other imaging modalities such as MRI and optical imaging, to achieve dynamic and precise focus in desired brain regions. This could enable a new way to understand brain functions, targeting precise areas of the brain and observing the outcomes of their stimulation.

Our results also brought out an interesting aspect of stimulating neurons with ultrasound, which is that neurons express some level of mechanosensitive ion channels endogenously. Both in vivo and in vitro, we found that increasing the ultrasound intensity also resulted in stimulation of the control group of cells. We consistently found that expression of MscL-G22S significantly reduced the intensity of ultrasound needed to stimulate neuronal activity and motor responses, while higher intensities were able to stimulate the control groups as well. These results highlight the importance of understanding the inherent mechanosensitive properties of the brain and neurons, which are now widely understood to have some ability to sense physical forces (179). At the lower limit of ultrasound intensities, we applied, we found that MscL-G22S-expressing cells were able to respond to ultrasound with minimal response in the control group. c-Fos activation of neurons was also limited to the area of EYFP expression (i.e. the area

successfully transduced by the viruses). Our approach thus was able to successfully sensitize cells to ultrasound, and ultrasound stimulation was limited to the desired area of influence. Hence, keeping the ultrasound intensity low could be a way of limiting the ultrasound effects to only the desired cell-types and the desired area. Such specificity is crucial in the eventual development of ultrasound-based treatments and could be useful in minimizing side-effects.

We did not observe obvious side effects of MscL-G22S expression as indicated by behavior, mice body weight, resting membrane potential, etc., but further and more pointed experiments are needed to test the possible artifacts of such a treatment. The G22S mutant of MscL is reported not to be spontaneously active(180), which could plausibly explain the lack of these indicators; nevertheless, it remains crucial to reduce the possibility of adverse effects as much as possible. MscL is a non-selective ion channel and has a large pore-size (over 30Å, according to Cruickshank and colleagues (180)) it conducts ions other than Ca²⁺ and even small proteins, which could complicate the profile of activation effects, and it will require specific experiments to tease out the effects of individual factors from the others.

The performance of this approach can be further improved by utilizing other ultrasonic sensitive ion channels or engineering novel MscL mutants. On the other hand, mechanosensitive potassium or chloride channels may also serve as potential mediators with inhibitory effects, making it possible to reduce neural activity as well (181, 182). Moreover, the ultrasonic paradigm may be expanded to trigger mechanosensitive ion channels endogenously expressed in various tissues, such as the peripheral or enteric nervous system, which could have therapeutic implications. Such non-invasive control of

neurons in deep tissue, whether in the brain or elsewhere, whose inaccessibility currently poses substantial challenges to biomedicine could be a way to address diseases and neurological conditions of many varieties in the future.

While the experiments detailed in the present study involve a minimally-invasive procedure to induce the expression of MscL-G22S, the availability of newer methods could potentially eliminate this need. Recently, the novel rAAV/PHP.eB (183) which can infect neurons in the brain through a simple tail-vein injection³⁴ showed potentially noninvasive gene delivery to specific neurons. With further development such technology could reduce the severity of the invasion even further, thus making it easier to implement a system like ours.

2. Materials and Methods:

15. Cell culture

293T cells were purchased from ATCC and were maintained in Dulbecco's Modified Eagle Medium (DMEM) (high glucose and no sodium pyruvate), supplemented with 10% fetal bovine serum, 100 units/mL penicillin and 100 µg/mL streptomycin (all from Gibco), inside a humidified incubator 37°C with 5% CO₂.

16. Plasmid transfection

293T cells were seeded into 35 mm culture dishes at 1 x 10⁶ cells per dish. The next day, the cells were transfected using the Lipofectamine 3000 kit (Invitrogen). 2.5 µg plasmid (replaced with water for the mock condition), 5 µl of P3000 and 5 µl of Lipofectamine 3000 were complexated according to the manufacturer's instructions, and

added to the cells. 24 hours later, the transfected cells were trypsinised and reseeded, partially into glass-bottomed confocal dishes (SPL Life Sciences) at 1/8 cell density, and partially back into the original dish. Live cells were photographed using a Nikon Eclipse TS100-F microscope 24 hours later, and were then used for further experiments.

17. Primary cortical neuron harvest

Primary cultures of the cortices of mouse embryos at embryonic day 16 were obtained as previously described³⁵. Briefly, cortices were dissected in ice-cold Neurobasal medium (Gibco) and incubated in 0.25% trypsin-EDTA (Gibco) for 15 minutes. The cells were then centrifuged and washed in Neurobasal medium containing 10% FBS, 0.25% L-Glutamine and 1% Penicillin-Streptomycin (all from Gibco) and centrifuged again. The cells were resuspended in medium and gently mechanically triturated with a pipette, and then allowed to stand for 15 minutes. The resultant supernatant was discarded, and the cells were resuspended in the abovementioned medium further supplemented with 2% B27 serum-free supplement (Gibco). The cells were plated at 5×10^5 cells in 35 mm dishes containing PLL-coated coverslips, or at 1×10^5 cells into confocal dishes. After 24 hours, the medium was changed to Neurobasal + 2% B27 + 0.25% L-Glutamine + 1% Penicillin-Streptomycin. The medium was half-changed every 72 hours.

18. Viral transduction

Viruses were packaged by BrainVTA (Wuhan) Co. Ltd. (China), and all viral aliquots were placed at -80°C prior to use. We used a rAAV-9 vector, with a human

synapsin (hSyn) promoter, which enabled the viruses to preferentially transduce neurons. The MscL-G22S sequence was fused with either the fluorescent reporter EYFP or the Ca²⁺ sensor protein GCaMP6S, and a polyA tag at the end of the sequence. In addition to the MscL-containing viruses, we also used vector controls. The viruses used in this study were rAAV/9-hSyn-EYFP-pA, rAAV/9-hSyn-MscL-G22S-EYFP-pA, rAAV/9-hSyn-MscL-G22S-GCaMP6S-pA and rAAV/9-hSyn-GCaMP6S-pA.

Primary neurons were transduced with at DIV 7 using viruses diluted 1/10 in PBS at RT. For every 5 x 10⁵ primary neurons seeded, 10⁹ genome copies (GC) of the CTRL virus and 10¹⁰ GC of the MscL-G22S virus were added directly into the cell medium. The plates were gently shaken and placed in the incubator. Cells were allowed to incubate for between 4-5 days while being monitored for fluorescence and cell condition, after which they were used for further experiments.

19. Patch clamping

Patch clamp recording for transduced primary neurons was done on DIV 12, and 48 hours post-transfection with 293T cells. Only cells with visible fluorescence were selected for patch clamping. Borosilicate glass-made patch pipettes (Vitrex, Modulohm A/S, Herlev, Denmark), were pulled with a micropipette puller (P-97, Sutter Instrument Co., USA) to a resistance of 5–7M Ω after being filled with pipette solution. Voltage clamp and current clamp was used for recording current in 293T cells and membrane potential in primary neurons respectively. Digidata 1440B (Axon instruments) and amplifier (Axopatch-700A, Axon Instruments, USA) were applied for data recording with pClamp Version 9 software. The data were analyzed with Clampfit 10.0. Cells were bathed in the following solution: 130 mM NaCl, 5 mM KCl, 1 mM MgCl₂, 2.5 mM CaCl₂, 20 mM HEPES (pH 7.4). Pipettes were filled with the following solution: 138 mM KCl, 10 mM NaCl, 1 mM MgCl₂, 10 mM Glucose and 10 mM HEPES, with D-mannitol compensated for osm 290 (pH7.2).

20. Calcium imaging

Cells loaded with the fluorescent calcium indicator Fura-2 (F1200, Invitrogen) according to the manufacturer's instructions, or primary neurons at DIV 11-12 expressing GCaMP6S, were used. A customized calcium imaging and ultrasound stimulation system (illustrated in Figure 1D) was utilized. The system consisted of a modified upright epifluorescence microscope. The excitation light was generated by switchable LED light source (pE-340fura, CoolLED system), filtered by excitation filters and delivered to the

sample for illuminating the calcium sensor. The fluorescence signals from the cells were collected by a water immersion objective (UMPlanFLN, Olympus), filtered by a filter wheel with green (525 nm) or red (633 nm) channels and captured by a sCMOS camera (ORCA- Flash4.0 LT Plus C114400-42U30, Hamamatsu). To minimize phototoxic effects, the LEDs were triggered at 1 Hz and synchronized with sCMOS time-lapse imaging. a triangle waveguide was attached to the ultrasound transducer and placed under the culture dish at a 45-degree angle to the horizontal axis. For Fura-2 imaging, dual excitation 340nm/380nm lights were inter-switched at 1 Hz, the calcium signaling were measured as the ratio of the signals at 340 nm and 380 nm. The other site of the waveguide was mounted with an acoustic absorber to minimize acoustic reverberation. During calcium imaging, the cells were placed in a buffer solution with 130 mM NaCl, 2 mM MgCl₂, 4.5 mM KCl, 10 mM Glucose, 20 mM HEPES, and 2 mM CaCl₂, pH 7.4.

21. RNA extraction and reverse-transcription

RNA was collected from cells using the GeneJET RNA Purification Kit (Thermo Scientific) according to the manufacturer's instructions, and RNA concentrations were measured using a NanoDrop One (Thermo Scientific). 1 µg RNA was reverse-transcribed using the iScript™ gDNA Clear cDNA Synthesis Kit (Bio-Rad), according to the manufacturer's instructions (including a gDNA digestion step), using a C1000 Touch thermal cycler (Bio-Rad).

22. Real-time qPCR

1 μ l cDNA from plasmid-transfected 293T or virus-transduced primary neurons at DIV 12 was mixed with appropriate forward and reverse primers (final concentration 250 nM), 2X SYBR Green Premix Ex Taq (Takara) and H₂O to a final volume of 10 μ l. PCR was performed on Applied Biosystem 7500 Fast Real-Time PCR system (Thermo Fisher Scientific). Results are expressed as a fold change compared to the appropriate control, mean \pm SD of 3 independent experiments. Primer sequences were as follow:

Mouse β -actin: F - AGG GTG TGA TGG TGG GAA TG, R - TGG CGT GAG GGA GAG CAT AG, 402 bp; human β -actin: F - GTG GGG CGC CCC AGG CAC CA, R - CTC CTT AAT GTC ACG CAC GAT TTC, 539 bp; MscL-G22S: F – GTCTCTTCACTGGTTGCCGA, R – TGCATCACAACAGCAGGGAT, 125 bp.

23. Immunocytochemical fluorescent staining

Primary neurons transduced with viruses were fixed at DIV 12 using 4% paraformaldehyde + PBS and permeabilized using 0.1% Triton X-100 + PBS. Cells were blocked using 5% normal goat serum in TBST and incubated overnight in primary antibodies diluted in 5% BSA + TBST. Secondary antibody incubation was performed the next day, diluted in 3% BSA in PBST for one hour at room temperature. Cells were washed, coverslips dried, and mounted on glass slides using small drops of Prolong Glass Antifade Mountant with NucBlue (Life Technologies) and allowed to cure overnight at room temperature. All steps from the secondary antibody incubation onwards were performed in the dark. Coverslip edges were then sealed using transparent nail enamel

and imaged using a confocal laser scanning microscope (TCS SP8, Leica), at the University Research Facility in Life Sciences (ULS), The Hong Kong Polytechnic University.

MAP2 primary antibody (PA1-10005, Invitrogen) and goat anti-chicken IgY (H+L) Alexa Fluor 633 (A-21103, Invitrogen) were used at a dilution of 1:1000.

24. Animal care

Male, 8-week old, C57BL/6J mice, were used for ultrasound stimulation. Mice were housed under standard housing condition with food and water available ad libitum. Animal use and care were performed following the guideline of the Department of Health - Animals (Control of Experiments) of the Hong Kong S.A.R. government.

25. Stereotaxic injection

C57BL/6 mice were anesthetized with Ketamine and Xylazine (100mg/kg and 10mg/kg respectively) followed by removing the skin above M1 area. Using the stereotaxic apparatus, a hole was drilled to allow pipette injection. The coordinates used for the primary motor cortex injection were AP 0.25 mm, ML-1.50mm, DV 1.00 mm. This injection side received 1ul of rAAV/9-hSyn-MscL-G22S-EYFP-pA or rAAV/9-hSyn-EYFP-pA virus ($2-3 \times 10^{12}$ GC/ml) viral particles with 0.1 μ l/min injection rate, followed by a ten-minute pause. The pipette was then retracted slowly, including a five-minute pause at the halfway point. The puncture site was then disinfected and sutured, and the mice were returned to their housing areas.

26. Ultrasound stimuli in primary motor cortex

Five weeks post-injection, the mice were anesthetized by intraperitoneal injection of ketamine (100mg/kg) and xylazine (10mg/kg). Body weights were measured, the mice's heads were shaved and ultrasound gel was applied to the head to promote acoustic coupling. The transducer was placed on top of the M1 area (right forebrain). Mice were stimulated with ultrasound (Fig. 20) (500 kHz ultrasound of 200 tone burst pulses and a repetition frequency of 1 kHz with 40% duty cycle and 0.3 MPa) for 40 minutes with a 10 second stimulation interval. After stimulation, the mice were returned to their original cage.

27. Immunohistochemical fluorescent staining

90 minutes after ultrasound treatment, mice were perfused with PBS, followed by 4% paraformaldehyde (PFA) (cat. no. P1110, Solarbio) in PBS. After dissection, brains were post-fixed overnight in 4% PFA. Starting from the injection plane, coronal brain slices at a thickness of 40 μ m were collected. Slices were blocked using and incubated overnight in primary antibody solution diluted in 1% normal goat serum + 5% BSA + PBS + 0.3% Triton. Slices were then washed with PBS, incubated with secondary antibodies diluted in PBS for two hours at room temperature. Slices were then washed, coverslips dried, and mounted on glass slides using small drops of Prolong Diamond Antifade Mountant with DAPI. Imaged using a confocal laser scanning microscope (TCS SP8, Leica). Primary antibodies used were c-Fos (2250, CST, dilution 1:500). Secondary antibodies, used at a dilution of 1:1000, were goat anti-rabbit IgG (H+L), Alexa Fluor 555

(A214428, Life Technologies corporation). 3 ROIs were chosen from a slice and the number of cells showing blue (DAPI) and red (c-Fos) signals were counted using ImageJ, and the number of c-Fos signals per slice was calculated. These results were statistically analyzed by an unpaired *t*-test with a Holm-Sidak correction, and *P* values below 0.05 were considered significant.

28. Assessment of ultrasound stimulation-evoked motor response

Four weeks after viral injection, mice were anesthetized with isoflurane mixed with oxygen for two minutes in an isoflurane cage. Following the initial induction of anesthesia, the animals were positioned in a stereotaxic apparatus and an anesthesia tube connected to the nose (Figure 3C). The mice were given a low concentration of isoflurane (1.5/4 isoflurane /oxygen) through the tube for two minutes. The ultrasound transducer was directed to the M1 region coupled by ultrasound gel. Mice were under slight anesthesia throughout the process of recording, with a slight reduction of the concentration of the anesthetic plane (0.5/ 4 isoflurane/ oxygen). The ultrasound stimulation period was recorded using a video camera. The mice were repeatedly stimulated by ultrasound 10 times at acoustic pressures of 0.3, 0.5, 0.6 MPa respectively with 1 second interval. The mice were allowed to rest for 1 minute after each round of ultrasound stimulation. Motor responses were quantified as a success rate of body movement (muscle contraction) per ultrasound stimulus. The results were analyzed using an unpaired *t*-test with a Holm-Sidak correction, and *P* values below 0.05 were considered

significant.

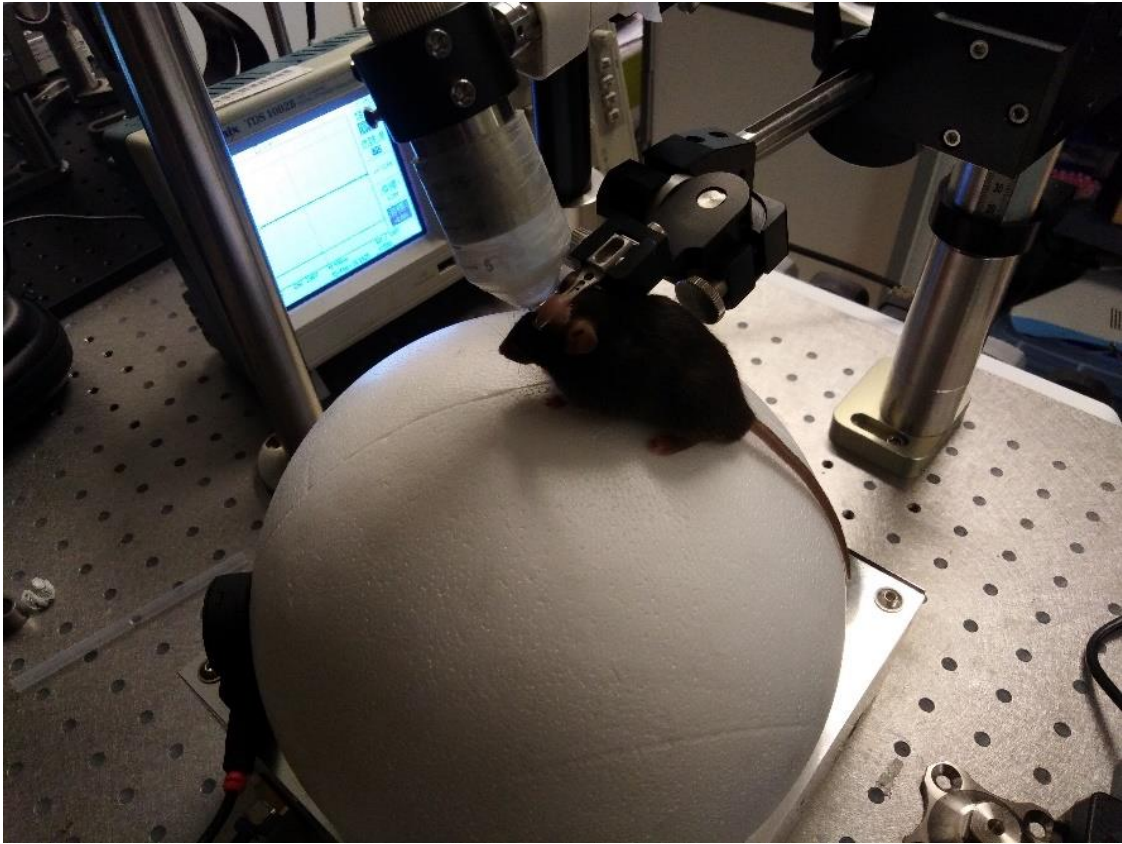


Figure 22 Ultrasound stimulation of anesthetized mice

Chapter 4: Toolkit for non-invasive brain stimulation by ultrasound

Biogenetic acoustic actuator for mediating neuronal activity

Physical tools for modulating cellular behavior are promising for both fundamental and clinical applications. In previous sessions, we addressed these issues by showing ultrasonic neuromodulation with genetic targeting to the specific neurons allowing us to control neural activity by using non-invasive ultrasound. However, the requirement of using genetic modifications would be a safety concern in certain conditions. In addition, the expression of ion channels in CNS by rAAV virus needs time to allow the expression. Here explored an alternative strategy which are genetic free for targeting cellular surface receptors cellular by ultrasound. We revealed that the presence nano- gas vesicles can mediate well-controllable neural stimulation. To evaluate how gas vesicles, mediate neural activity by ultrasound, we utilized calcium imaging on different cell lines and with different solutions. We show that these neuronal activations are through activating mechanosensitive ion channels and release the intracellular calcium store.

1. Introduction

The use of new tools to non-invasively manipulate the brain will continue to advance our understanding of how the human brain gives rise to thought and action (184-186). Recently, ultrasonic brain stimulation, as one of the most promising techniques, has gain significant attention since it can be non-invasively delivered to deep brain tissue through the skull (186-189). The study of ultrasound stimulation on human brain has shown clinical effectiveness, without damaging brain tissues (187, 190). In the previous sessions, we showed that ultrasound is not only a promising method for stimulating specific brain region with high spatial resolution, but also a non-invasive modality with cell type selectivity. However, despite these exciting developments, the major challenge lies in the genetic modifications to the specific neurons which would face some challenge in some conditions for example neural developmental questions and difficult to translate to clinical use.

The key to achieve selective stimulation requires confining the ultrasonic stimulation to specific neurons, as the ultrasound intensity cannot be localized in an area as small as an individual cell. Selectively enhancing neuronal sensitivity to ultrasound stimulation is the key issue to achieve precise neuron stimulation. Inspired by optogenetics(191), sonogenetics were developed, in which mechano-sensitive ion proteins were engineered to overexpress in chosen neurons. We will further develop this method to be a widely used tool.

Alternatively, nano-medicine based approaches for enhancing neuron sensitivity are gaining momentum for selective stimulation (192-197). The fundamental principles

for these approaches are using targeted nanoparticles to convert external field (light, electromagnetic, or ultrasound) into localized bio-effect to trigger the chosen neuronal activity. Based on this, we hypothesize that the inscription of ultrasonic sensitivity to specific neurons may be achieved by targeted nanoparticles, which can intensify and localize the ultrasound field. Outstanding examples are nano-particles assisted photothermal neural stimulation (194), magnetothermal stimulation (198), mechanogenetics (102), and upconversion nanoparticle enabled NIR optogenetics(199, 200). From these pioneer studies, the possible candidates could be the ultrasound contrast agent (201, 202).

Bubbles with large differences in the acoustic properties of the surrounding medium and the gas core are highly responsive to ultrasound (202). Recently, microbubbles have been utilized to stimulate immune cells through activating Piezo1 (102). It has also been utilized to stimulate neurons in *C. elegans* to initiate neural activates and behavior change (203). However, traditional micron-sized bubbles are constrained in blood vessels and they are extremely unstable (204, 205). The microbubbles-based stimulation could also be disruptive as the oscillating are in micron size level (206, 207). Microbubble mediated ultrasonic bio-effects have been widely explored and been utilized to open cell membranes and blood brain barrier (208-213). Currently, stable biogenic nano-sized bubbles have been extracted from cyanobacteria and demonstrated significant contrast enhancement showing great potential for molecular imaging (124, 214, 215). In our lab, it is also showed good permeability to targeted tissues due to is nano-size (216). Hence, the nano-bubble could be an excellent candidate nanoparticle to enable selective stimulation of neurons by ultrasound.

2. Results and discussion

To advance ultrasonic brain stimulation, specifically to manipulate chosen neurons with high selectivity, we inscribed ultrasonic sensitivity to neurons by the nano-bubbles. Biogenic nano-bubbles will be prepared as previously described (217), which have been successfully achieved as shown in Fig. 23. Oscillating NGVs will insert mechanical perturbations on the cell membranes and induce ion influx to give rise to cellular activities. As shown in our results, the simple mix of NGVs and primary cultured neurons expressing GCaMP6s can be visualized directly under a fluorescent microscope. After ultrasound stimulation, the intensity of GCaMP6s were increased significantly. In addition, the temporal resolution of the stimulation was also characterized by the fluorescence imaging. Upon ultrasound stimulation, the GCaMP6s fluorescence will be lighten up immediately. These effects are repeatable with good synchronization with ultrasound onset time manner. These results demonstrated that NGVs can mediate ultrasound stimulation on neurons with high temporal resolution.

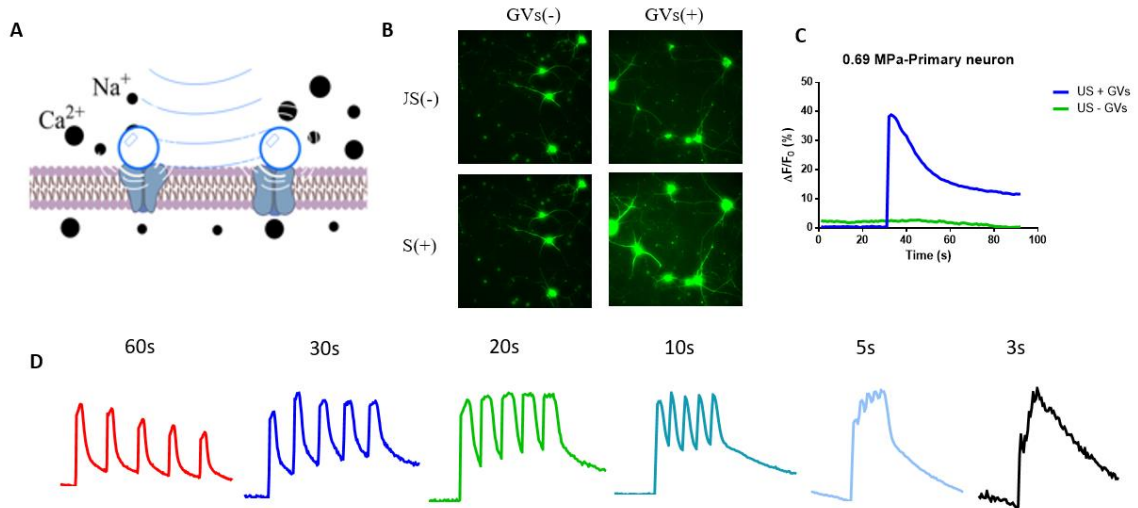


Figure 23 GVs mediated ultrasound neural stimulation (A) scheme of nano-bubbles mediated neuron stimulation by interacting with membrane surface proteins upon ultrasound illuminating; (B) calcium imaging of neurons with and without GVs before and ultrasound stimulation. There is no difference between GCaMP6s fluorescence imaging with and without GVs before ultrasound stimulation while GVs group shows significant higher GCaMP6s fluorescence after ultrasound stimulation; (C) temporal profile of ultrasound induced calcium change with and without GV. Upon ultrasound stimulation, there is a fast activation of GCaMP6s at 30; (D) time-resolved stimulation induced calcium responses. Neurons were stimulated with different interval time, and induced precise calcium responses from 60s, 30s, 20s, 10s, 5s, to 3s. The subsecond stimulation were characterized with a fast dopamine sensor as indicated in other sessions.

To investigate the mechanisms underlying, we utilized a neural cell line CLU199 which are homogeneous expressing various neural markers. As shown in (Fig. 24 (A) and (B)) in the presence of GVs, ultrasound stimulation can induce a dramatic calcium response in CLU199s. The fluorescence change of calcium sensitive dye Fluo4 were summarized in Fig. 24 (C). It is clearly showed that ultrasound can also mediate calcium signaling in CLU199. In addition, to facilitate the further experiments, we characterize the dose dependence of calcium responses on GVs concentration. As shown in Fig. 24 (D), without GVs, there are rare fluorescence changes while in the presence of GVs, there were clear fluorescence changes depending on the concentration. We chose a 0.4 nM for further experiments to eliminate the possible toxic effects while remaining a good phenotype.

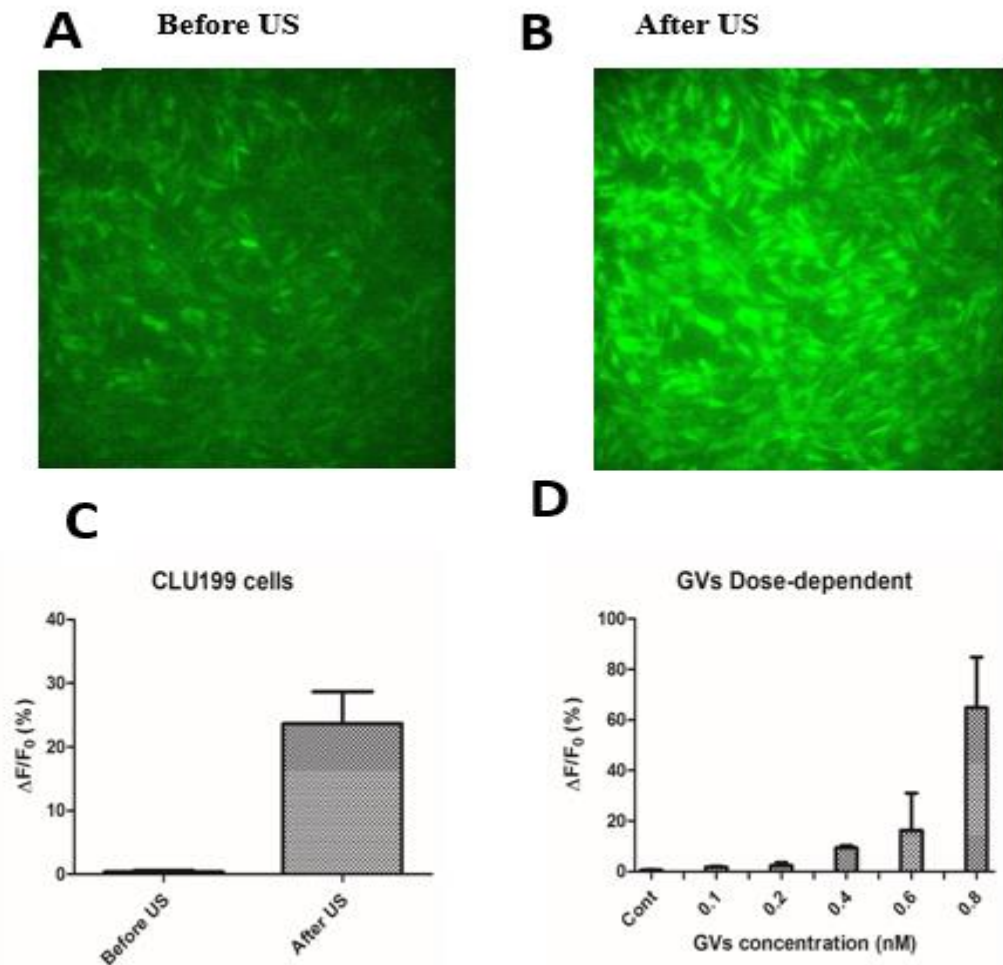


Figure 24 Characterization of ultrasound effects on CLU199 neural cell line. *Calcium imaging of CLU199 before (A); and after (B) ultrasound stimulation; (C) the statistics of fluorescence differences before and after ultrasound stimulation; (D) The dependence of calcium responses as a function of the concentration of GVs;*

As oscillating NGVs could induce mechanical perturbations to the cells nearby, we hypothesize that ultrasound can activate mechanosensitive ion channels facilitating the calcium influx pathways. To validate, we first utilized a wide spectrum calcium channel blocker Ruthenium Red (RR) to test whether there is any mechanosensitive ion channel

mediated calcium influx. In addition to CLU199, CHO cells with minimal expression of Piezo1 were also included in this experiments as a compare. As shown in Fig. 25 (A) and (B), the fluorescence changes of Fluo4 for CLU199 is much higher than CHO cells in normal artificial cerebral fluids. The difference suggest that the effects is not caused by the membrane disruption. We then subject the cells in the calcium free artificial cerebral fluids and observed a significant reduced fluorescence but there is still fluorescence changes after calcium ion replacement in the extracellular solution suggesting there are also intracellular release. To further confirm, we release the calcium instore prior to ultrasound stimulation by incubator TG. After TG treatment, the calcium responses also reduced significantly. TG treated groups are representing calcium influx and calcium free condition suggests intracellular release. There sum-up value (dashed line) are similar to the normal artificial cerebral fluids condition. These results suggest that intracellular Ca^{2+} elevation may be induced by two different pathways: (i) through calcium influx; (ii) through the calcium release from the intracellular calcium restore.

The molecular expression of mechanosensitive membrane ion channels, such as Piezo1 were described in previous sessions. we added 100 μ M RR to the Ca^{2+} solution to evaluate the effect of mechanosensitive ion channels on GVs-US elicited Ca^{2+} response. Under the same US parameters, where there was no detectable membrane poration, the Ca^{2+} response was reduced significantly. This result suggests that the opening of mechanosensitive ion channels allowing extracellular calcium influx is the dominated pathway. Based on these results we proposed a working mechanism for the neural activation mediated by NGVs. The transient Ca^{2+} signal inside the cytosol may spread out via the CICR mechanism through ER that has been well established in the biology

literature. Therefore, we used 7.5 μM thapsigargin (Thaps) to discharge intracellular Ca^{2+} stores before the GVs-US treatment by inhibiting ER Ca^{2+} -ATPases, which, in turn, will reduce the Ca^{2+} release from the ER during GVs-US treatment. The Ca^{2+} response was found to be suppressed in Ca^{2+} free solution, compared with the regular Ca^{2+} solution. Overall, Thaps, RR, and Ca^{2+} free media were found to affect the Ca^{2+} response.

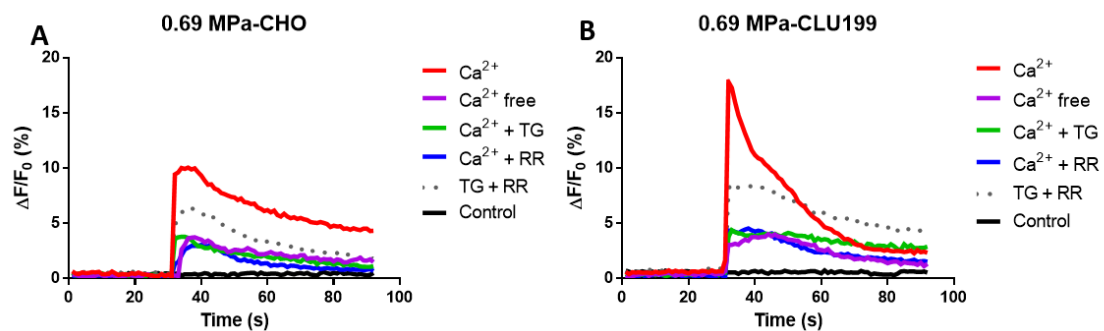


Figure 25 intracellular release and calcium influx induced by ultrasound in: A) CHO cells and B) CLU199 cells. The most significant responses were observed in the normal condition with calcium ions that are like physiological conditions. Movement of calcium ions in extracellular solution reduced the effects dramatically, indicating there were intracellular calcium release as confirmed by using TG to chelate the intracellular calcium store. On the other hand, blockage of mechanosensitive ion channels by RR also reduced the calcium responses. In these conditions, the calcium responses are significantly different with the control group which without any GVs. Comparing the CHO and CLU199 Cells, it is found that the CLU199 has much larger responses as there are more mechanosensitive ion channels expression.

We tested the NGV mediated ultrasound stimulation on different cell including MCF7, 293T, their dynamics are compared in Fig. 26. It is shown that both these cells are responses to the stimulation although the aptitude is different each to each. It requires further experiments to clarify the exact mechanism. On the other hand, these results

suggested NGV mediated ultrasound stimulation is a robust tool for probing the mechanosensitivity of cells noninvasively. Compare with the existed method like AFM, patterned substrates, and cavitation-based strategies, it has higher spatiotemporal resolution and it do not damage the cells showing a very good repeatability in the same experiments.

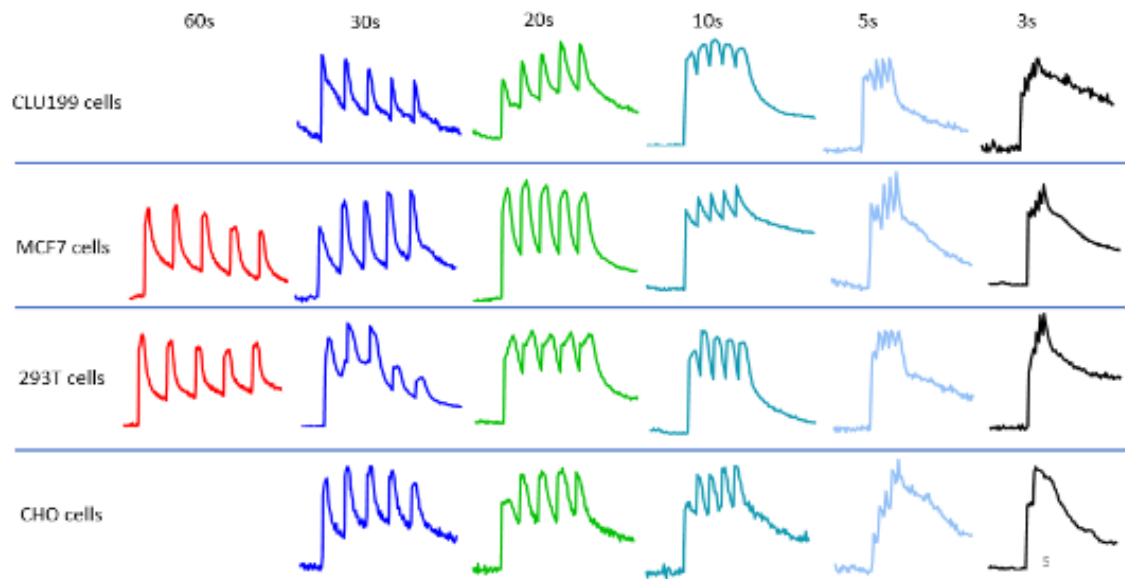


Figure 26 Temporal calcium responses upon ultrasound stimulation for different cell types. Different cell lines are utilized in this case studies. The amplitude of the responses was normalized. The calcium response shows great synchronizations with ultrasound stimulation.

The data presented are based on free NGVs that are not targeted to a specific cell compartment and marker. In some cases, it is still not achieved in our final goal. There are various functional groups on the NGVs surface which are easy to be functionalized with antibodies, ligand et.al. The targeting properties are important to the selectivity of ultrasound stimulation. Therefore, the bio-effects of oscillating nano-bubbles on neurons need to be determined to understand the mechanism and to precisely control the

stimulation results. On the other hand, the binding process could alternate the acoustic properties of NGVs, which requires further characterization. Then, the functionalized nano-bubbles will be delivered via a theta capillary tube pulled to approximately 20 μm tip diameter on a Flaming/Brown pipette puller. One side of the theta capillary will be filled with the nano-bubble solution while the other half will be filled with bath solution for washing. Each side of the tube will be connected to independently-controlled pressurized air. After binding antibodies, functionalized nano-bubbles will be incubated with neurons. During different incubation time, the neurons will be continuously washed with PBS solution at every 30 min. The binding efficiency and the distribution of nano-bubbles with subcellular resolution will be examined by confocal fluorescence microscope and the phase contrast mode. The concentration of nano-bubbles and incubation time will be optimized to ensure sufficient binding.

In addition, to understand how oscillating nano-bubbles interact with neurons, physical effects of oscillating nano-bubbles need to be examined. With well characterized properties of the functionalized nano-bubbles achieved, the nano-bubbles will expand and contract under ultrasound sonication and generate acoustic radiation force and microstreaming around the bubbles. The flow velocity near the oscillating nano-bubbles attached to a neuron will be traced by using micro-particle image velocimetry (mPIV), with 0.5 μm diameter polystyrene particles. The resulting shear stress on the cell will also be calculated. In the presence of polystyrene, different pressure and frequencies (typically 0.5, 1, 2, 4, 10, and 20 MHz) of ultrasound will be irradiated to nano-bubble targeted and non-targeted neurons. A region of interest near an oscillating bubble will be recorded continuously with microscope. After obtaining the displacement of the polystyrene

particles, the streaming velocity will be determined. The shear stress exerted by microstreaming of the medium will be calculated using $\tau = \mu \cdot d\mu/dy$, where μ is the medium viscosity, $d\mu$ is the flow velocity difference between the bubble equator plane and the cell membrane, and dy is the same as the bubble radius.

After successfully loading the nano-bubbles on neurons and with well characterized properties, selective ultrasound stimulation to neurons targeted to different mechano-sensitive proteins and the underlying mechanism can be investigated. A system to deliver ultrasound stimulation and record corresponding physiological effects will be instrumented. In this system, the ultrasound intensity, frequency, and pulse duration and duty cycle will be adjustable. The electrophysiology and intracellular ion influx in response to ultrasound will be studied.

The physiological changes of nano-bubble targeted neurons in response to ultrasound stimulation will be studied using a customized system. The system will be composed of stimulation components, including an ultrasound transducer, a function generator and a power amplifier to produce ultrasonic waves with different acoustic parameters. In addition, ultrasound absorption material will be arranged at the opposite side of the culture dish to avoid multiple reflections. The ultrasonic wave distribution with the petri dish setup will be mapped with a hydrophone. The stimulation components will be incorporated with a patch-clamp system under voltage-clamp to monitor the action potential triggered by ultrasound. When the giga-seal is achieved, a whole-cell patch clamp configuration will be reached by applying a pulse of negative pressure inside the pipette. The expected series resistance at that point will be constrained to less than three

times of the initial pipette resistance before touching the neuron. The amplifier mode will be changed to current clamp and the cell sensitivity to ultrasound will be tested with 1 millisecond current injection pulses of increasing amplitudes. The output membrane voltage will be filtered at 5 kHz and digitized at 20 kHz.

Membrane poration has been previously shown to play an important role in the initiation of intracellular Ca^{2+} response produced by cavitation bubbles, yet a detailed understanding of the process is limited. We therefore carried out a systematic analysis of the PI uptake for individual cells treated with GVs-US. In general, the intensity of the Ca^{2+} response showed a clear US intensity independency without PI uptake, suggesting that the effects are unlikely induced by ultrasound poration.

Previous studies have showed that ultrasound as a mechanical pressure wave can exert mechanical stimulus to activate mechanosensitive ion channels to give rise to the neural activity in the presence of microbubbles at low frequency or at higher frequency in *C. elegans*. However, these conditions are not clinically relevant as microbubbles cannot penetration through the blood vessels and are extremely unstable while high frequency ultrasound cannot penetrate through the skull in rodent. Furthermore, the physical mechanism of ultrasound acting on biological samples are varied depending on the frequency and parameters used, thus the conclusions may not be able to transfer to low frequency ultrasound condition. Our results have fulfilled the need of using particles to go beyond the blood vessels to activate neurons *in vivo*.

On the other hand, there are other possible mechanism in addition to radiation force hypothesis. However, there are other possible mechanisms, we utilized an unbiased strategy to assay the possible bioeffects. It is shown that while neurons in the head and body can be activated by ultrasound, the profound effects on neurons observed in the gut (data not shown). Most of the worms with neurons activated in the gut will exhibit reversal responses (19 out of 20 trials), while the worms without neural activation has less reversal responses (10 out of 14 trials). The relevant neuron in the head and tail would respond to ultrasound stimulation and their mechanosensitive protein would be activated. There are about 65.51% shock worm responded to ultrasound stimulation with calcium responses in the gut. As there are mechanosensing neurons in the gut, which agree well with the hypothesis that ultrasound can activate the mechanosensing neurons. This fact can lead to novel application of ultrasound stimulation on the neural activity in human gut-brain axial.

The development of light responsive proteins and nano-particles such as fluorescent proteins and photosensitive ion channels (ChR2) and varied nanoparticles enables molecular and functional imaging and modulation, facilitating in situ causal investigation of specific biological questions with high spatiotemporal resolution. Recent years it witnesses rapid advances in nearly all the biological systems from *in vitro* to *in vivo*. The very example is the application of neuronal activity imaging by fluorescent proteins and optogenetics to dissecting complex neural circuits for understanding and treating brain functions. However, due to limited penetration depth of light, it is challenge to access to deep tissue *in vivo*.

Recent years, great efforts have been made to extend the imaging and stimulation depth by adopting different modalities such as ultrasound and magnetic energy. Ultrasound as one of the most promising strategies is known to be able to access to deep tissue *in vivo* for imaging and stimulation of excitable cells. However, as the wavelength of ultrasonic wave is longer than biological specific proteins, its contrast and stimulation lack molecular specificity and cellular selectivity. To date, microbubbles oscillating under ultrasound field can generate strong ultrasound contrast which has been utilized to as ultrasound contrast agent for ultrasonic function imaging. On the other hand, it has also been explored to exert forces to activate mechanosensitive ion channels for controlling cellular activity by generating radiation force and acoustic streaming driven by ultrasound. However, these microbubbles are not stable, and it is unable to penetrate through the blood vessel as it is in micrometer diameter.

Gas vesicle (GV), a naturally formed nano size protein shell with gas and water inside are promising to address all these concerns. It produces satisfied ultrasound and magnetic contrasts in response to ultrasound field, which is promising reporters for specific genes, molecules and cellular activities. It has several advantages comparing to traditional ultrasound contrast agent, GVs generated from Ana and stable despite their nanometre size. Besides, clinical imaging of the blood pool and related physiology and have recently been proposed as potential cell-internalized labels. GVs have unique acoustic properties and it can oscillate and generates mechanical perturbation in responsive ultrasound stimulation. It is possible to generate mechanical stimuli to cells nearby. It is rational to test whether GVs can mediated cellular activities driven by ultrasound.

3. Materials and methods

1. Cell culture

293T cells were purchased from ATCC. The embryonic mouse hippocampal cell line mHippoE-18 (referred to in the text as “CLU199”) was purchased from Cedarlane Laboratories. 293T and CLU199 cells were maintained in Dulbecco’s Modified Eagle Medium (DMEM) (high glucose and no sodium pyruvate), supplemented with 10% fetal bovine serum, 100 units/mL penicillin and 100 µg/mL streptomycin (all from Gibco), inside a humidified incubator 37°C with 5% CO₂. For experiments requiring transfected cells, cells were seeded in 35 mm dishes or collagen-I-coated (Corning) glass coverslips (5 µg/cm²), at 1.5 x 10⁶ cells per dish, allowed to grow overnight, and treated with ultrasound the next day.

2. Chemicals and consumables

Glucose, NaCl, HEPES, MgCl₂, CaCl₂, PLL, DMSO and are purchased from Sigma-Aldrich (St. Louis, MO, USA). Dulbecco’s Modified Eagle Medium (DMEM), Fetal bovine serum (FBS), trypsin-EDTA solution and Penicillin-streptomycin solution were purchased from Gibco (Life Technologies, Carlsbad, CA, USA). Hoechst33342, Propidium Iodide (PI), 3-(4,5-dimethylthiazol-2-diphenyl-tetrazolium) bromide (MTT) and Fluo-4 AM were purchased from Invitrogen (Carlsbad, CA, USA). The distilled water was generated by the MilliQ Plus System (Millipore Corporation, Bedford, USA).

3. Gas vesicle preparation

Anabaena flos-aquae was cultured in sterile BG-11 medium at 25 °C under fluorescence lighting with 14 hours/10 hours light/dark cycle. GVs were isolated by hypertonic lysis to

release GVs with quickly adding sucrose solution to a final concentration of 25%. GVs were isolated by centrifugation at 400 x g for 3 hours after hypertonic lysis. To purify the GVs solution, it was washed by the same centrifugation process 3 times and stored in PBS at 4 °C. GVs solution concentration was measured by optical density at 500 nm (OD500) by UV-Visible spectrophotometer.

4. Ultrasound stimulation setup and characterization

Transducer (from Oplympus) with a center frequency of 1.0 MHz was employed in this study. Function generator and power amplifier are responsible for generating ultrasonic pulse. For the ultrasound stimulation procedure, a planar transducer with a diameter of 1.0 cm was fixed so that the transducer was facing downward. Cells were grown on glass cover slips that overcome ultrasonic standing wave. Coverslip is held 1.0 cm away from transducer coupled by plastic wrap encase degas deionized water at 25 °C. Acoustic intensity and field were characterized by hydrophone.

5. Cell Culture and Handling.

CLU199 cells were routinely maintained in DMEM culture medium, CHO cells were maintained in F12k culture medium supplemented with 10% FBS in a cell culture incubator at 37 °C with 5% CO₂. Cells were trypsinized and resuspended into prewarmed (37 °C) culture medium before being injected into the coverslips. The introduced cells were incubated in the coverslips at 37 °C for 24 h to allow adhesion onto the PLL-coated coverslips. Thereafter, the culture medium was replaced with Fluo-4 AM working solution [5 μM in Ca²⁺ solution (pH 7.4)], and the cells were incubated at 37 °C in the dark for 30 min. Subsequently, Ca²⁺ solution was used to flush out unloaded Fluo-4 AM

solution before ultrasound stimulation. In mechanistic studies, several different media were used. For example, in order to remove extracellular Ca²⁺, the coverslip was covered with Ca²⁺ free solution with 0.5 mM EGTA to ensure that residual Ca²⁺ was completely chelated. To monitor concurrent cell membrane sonoporation during Ca²⁺ response measurement, the coverslip was perfused with PI solution (100 µg/mL in Ca²⁺ solution). The molecular expression of mechanosensitive membrane ion channels, such as PIEZO 1 has been reported in CLU199 cells whose function can be blocked by Ruthenium Red (RR). Therefore, we added RR solution (100 µM RR in Ca²⁺ solution) into the culture medium to evaluate the effect of mechanosensitive ion channels on GVs-US elicited Ca²⁺ response.

6. GVs mediated US stimulation and Optical Imaging.

As shown schematically in Fig. 1b, the coverslip with Fluo-4AM-loaded cells was fixed on an inverted microscope. We drop GVs onto the cover slip and then cells were exposed to ultrasound. A camera was used to record the intracellular Fluo-4 images with defined time intervals from a function generator at excitation wavelengths of 488 nm for Fluo-4 AM. A BF image was taken to register the morphology of the cell immediately before and after the GVs mediated US stimulation. We used software to communicate and coordinate the operation sequence between the microscope and monochromator.

7. Effect of GVs mediated US stimulation-Induced Cell Death

The MTT assay was used to evaluate cytotoxicity 1, 2, 4 and 8 hrs after GVs mediated US stimulation in the treated CLU199 and CHO cells. Briefly, the GVs were added to the microwell plates under ultrasound with a series of acoustic pressure (0–0.71 MPa)

stimulation, in which the CLU199 and CHO cells were seeded a density of 1×10^4 cells/well and then incubated for 24 h. Subsequently, 200 μ L of 0.5 mg/mL MTT solution was added into each well and incubated for another 4 h, and finally 100 μ L of DMSO was added and incubated for another 15 min. The absorbance of the solutions was measured at 570 nm on a microplate spectrophotometer (Bio Tek Instrument Inc., USA).

8. Sonoporation detection

Infrared temperature sensor can be employed to detect temperature change during US stimulation. Cavitation events were measured by passive cavitation detection method in solution with and without GVs. Scattered ultrasonic signal from examples was received by transducer and the corresponding power spectra are shown in S4. PI is a 668.4 Da marker molecule often used for sonoporation studies because its fluorescence spectrum is shifted and significantly enhanced when it enters the cell and binds with intracellular nucleic acids. In this study, microscope was employed to detect PI fluorescence change during US stimulation.

Chapter 5: Conclusion and outlook

Ultrasound brain stimulation is a promising technology for clinical and basic neuroscience. In summary, the mechanism of ultrasound neuron stimulation remains elusive as the ultrasonic bio-effects are diverse. Various possible mechanisms of ultrasound brain stimulation have been proposed and discussed intensively. It is shown that ultrasound can activate mechanosensitive ion channels, Piezo1 and MscL-G22s. Based on this foundation, I have developed a non-invasive brain stimulation toolkit by which can target specific neurons expressing exogenous mechanosensitive ion channels followed by ultrasound stimulation. Thus, ultrasound-based tool is added to the selective brain stimulation list. The advantages of ultrasound-based toolkit are that ultrasound is non-invasive which has great potential for future application both in clinical

and fundamental research. An alternative strategy to achieve selective neural stimulation has also been proposed as shown in Fig. 27. Which will be further developed.

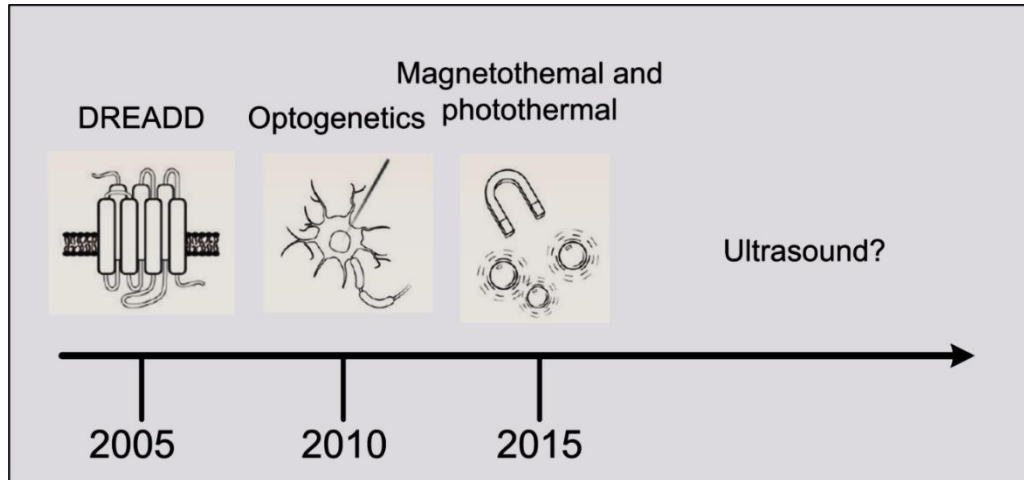


Figure 27 Ultrasound is a non-invasive and selective brain stimulation modality. There are various selective neuromodulation technologies from DREAD, optogenetics, to other analogical modalities. However, there isn't any method that can targeted neural stimulation non-invasively. Now, we add ultrasound stimulation to this list.

The selectivity of ultrasound brain stimulation Ultrasound brains stimulation is a promising technology for clinical and basic neuroscience. In summary, the mechanism of ultrasound neurons stimulation remains elusive as the ultrasonic bio-effects are diverse. Various possible mechanisms of ultrasound brain stimulation have been proposed and discussed intensively. It is showed that ultrasound can activate mechanosensitive ion channels, Piezo1 and MscL-G22s. Based on this foundation, I have developed a non-

invasive brain stimulation toolkit by which can targeting specific neurons expressing exogenous mechanosensitive (Fig. 28).

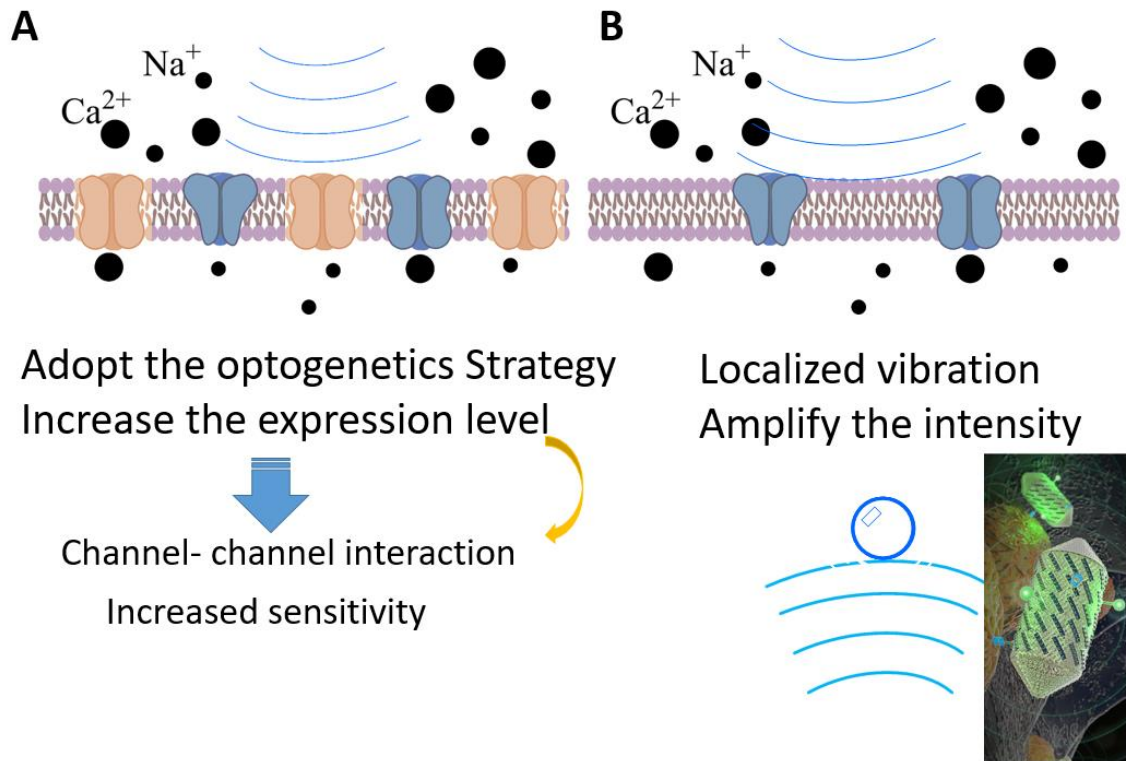


Figure 28 *summary of the different strategies include in this thesis; A) sonogenetics enabled by MscL-G22s; B) acoustic mechanogenetics mediated by biogenic gas vesicles. The first strategy is a genetics-based technology which requires genetic modifications in CNS. This procedure could raise the safety concern. The second strategy with NGV mediated*

In the first session, it is shown that primary neurons express Piezo1, which is known to play an important role in neural development and differentiation (168-178). In addition, this endogenous expression is a complicating factor in this study, as it could have reduced the precision with which neurons were targeted. This may be remedied to an extent by utilizing methods that upregulate Piezo1 to an even greater degree in vivo,

such as viral infection. This can be expected to reduce the ultrasound dose required to activate the desired cells, thereby leaving others mostly unaffected and increasing the specificity of the intervention. On the other hand, while alternatives do exist, given that Piezo1 is one of the most sensitive mechanosensitive channels, choosing alternatives would likely involve a trade-off in the sensitivity of the cells to ultrasound. Thus, future research should aim to identify ultrasound mediators or methods that sacrifice neither cell-type/circuit-element specificity nor sensitivity to ultrasound. This might involve inducing the expression of exogenous or artificially engineered proteins, or an approach that uses targeted microbubbles to achieve this end.

Besides Piezo1, which increases neural activity, mechanosensitive potassium or chloride channels may also serve as potential mediators with inhibitory effects, making it possible to reduce neural activity as well. Moreover, the ultrasonic paradigm may be expanded to trigger mechanosensitive ion channels endogenously expressed in various tissues, such as the peripheral or enteric nervous system, which could have therapeutic implications. Such non-invasive control of neurons in deep tissue, whether in the brain or elsewhere, whose inaccessibility currently poses substantial challenges to biomedicine could be a way to address diseases or neurological conditions of many varieties in the future.

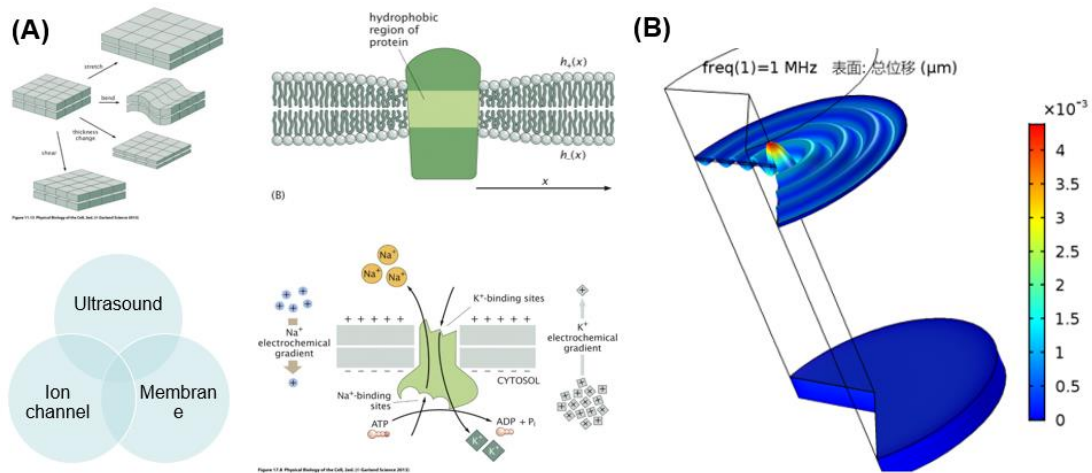


Figure 29 the road to biophysical mechanisms. A) Cell membranes are lipid bilayer which can be stretched, bended under different conditions. There were varied ion channels embedded in cell membranes. Upon ion channels opening, the cell membrane will be polarized or depolarized to give rise to neural activates. The wavelength of ultrasound at mm range are much longer than the size of an ion channel protein. Thus, the biophysical mechanism is underlying the interaction among ultrasound, cell membranes, and ion channels: B) Membrane dynamics under ultrasound stimulation

Although the ultrasonic responsive proteins and selective brain stimulation strategies have been developed. However, the detailed biophysical mechanisms of how ultrasound interacts with proteins are still unclear. The key point is that there is significant mismatch with ultrasound wavelength in millimeter range and the scale of a protein in nanometer range. One possibility is that the ultrasound can interact with cell membrane and the resulting mechanical impact gating the mechanosensitive ion channel subsequently. As shown in Fig. 29 (A), it is emergent to understand how ultrasound, cell membrane and ion channels interact with each other and results in action potentials. As shown in Fig. 29 (B), the finite element simulation demonstrated that ultrasound can

induce cell membrane oscillations with 20 nm amplitude. The oscillations agree well with the particle displacement hypothesis. Interestingly, the displacement is at the range of piezo1 shape which has been resolved recently.

1. Applications

With these toolkits in hand, one of the future applications is to apply the tools to addressing clinical challenges. Recent years, tremendous efforts have been conducting to develop new technologies such as interporal interfered electrical stimulation, optogenetic, transcranial magnetic stimulation, and ultrasound brain stimulation etc. to understand and treat brain diseases (35). Among which, ultrasound brain stimulation is considered as one of the most promising technology for clinical translation since ultrasound can be focused into a millimeter spot through the skull non-invasively (49). It has been demonstrated to be able to stimulate prefrontal cortex improving task in human without causing any biased effects. It is also shown that ultrasound can be used to stimulate visual cortex in monkeys (218-220). Ultrasound stimulation shows good spatiotemporal resolution and neurons can be activated or suppressed depending on different ultrasound parameters and stimulation locations. People have also tried to use ultrasound to treat brain diseases, like epilepsy, as well as other mental diseases like depression etc. Recently, it is also found that incorporated with circulating microbubbles, ultrasound can treat Alzheimer's disease (60). In this regard, ultrasound brain stimulation could be a good alternative strategy to existing electrical based stimulation (e.g. DBS) for treating Parkinson's disease.

Meanwhile, recent years witnessed significant advances in understanding the mechanism of treating PD by physical interventions with the development of optogenetics with neuronal type selectivity and high spatiotemporal resolution. Optogenetics gained a lot of attention as it shed light in many neural circuit fundamentals of the DBS treatment of Parkinson's disease. Especially, in contrast to clinical practice and animal experiments by DBS demonstrating that the subthalamic nucleus plays a major role in the regulation of autonomous basal ganglia (221), selective stimulation of the subthalamic nucleus by optogenetics does not improve mobility deficits in Parkinson's mice model, but is stimulated by M1 brain regions projections of nerve fiber bundles projecting into the subthalamic nucleus can play a similar role as DBS (222, 223). This indicates that the projection from M1 to the subthalamic nucleus plays an important role in autonomous motor control and Parkinson's disease emphasizing the importance of cellular selectivity of the stimulation technology. More and more evidence showed that brain stimulation with cellular selectivity have superior effects on the treatment of neural degeneration disease as it can target to specific neurons in animal models.

However, due to the limited penetration of light in the skull and brain tissue, it requires using fibers to deliver light into deep brain regions, making it invasive and a limited illumination area. Different strategies are explored to extent the penetration of light to achieve goal by developing red photo-responsive proteins and up-conversion nanoparticles to convert near infrared light, which is less scattering, into blue light to activate the ion channels. But they are still invasive or lacks satisfied penetration depth. In our lab, we are exploring another strategy for accessing deep brain structure with alternative energy to activate neurons. Specifically, we are conducting fundamental

investigation on ultrasound-based brain stimulation and developing a novel non-invasive and selective brain stimulation technology with great translational potential for treating brain disease. Our preliminary data showed that ultrasound can open mechanosensitive ion channels, which can be utilized to achieve cellular selectivity.

In addition, the timing of the release of dopaminergic neurons is important in the input of striatum-integrated motor cortical neural networks (224-226). New discoveries showed that dopamine plays important role in initiating movement other than sustaining an ongoing movement (227). This led us to realize that there may be important temporal and spatial couplings in the microcircuits that are clustered together, reflecting the need for temporal resolution of stimulation and treatment. This is aligned with the accumulated evidences showing that close-loop brain stimulation technology is superior to open-loop method for treating PD (228). In this aspect, our finding showed that stimulation on hypothalamic nucleus can induce theta band oscillations in cortical area, which can be utilized as a hallmark of effectiveness of treating PD in real time. These studies also highlight the requirement of incorporating electrophysiological monitoring during the treatment as a dosimetry monitoring guidance for precise treatment. In principle, ultrasound can be incorporated with other modalities as functional guidance and adaptive adjustment during the treatment for precise and targeted treatment.

Taking together, ultrasound brain stimulation holds great potential to break the fundamental challenges for treating PD as it is a non-invasive and compactable strategy with neuronal selectivity for targeting neural circuits of PD. To this end, future project addresses the major clinical issues and technical bottlenecks in Parkinson's disease treatment is emergent. Based on our previous studies I believe there are several future

directions can be done: 1) Develop a spatiotemporal precise ultrasound brain stimulation system; 2) Characterize the effects of the ultrasound-based methods for treating PD models; 3) Develop an electrophysiology guided and adaptive close-loop methods for treating PD (Fig. 30); 4) validate the effects of the proposed methods for treating PD in preclinical.

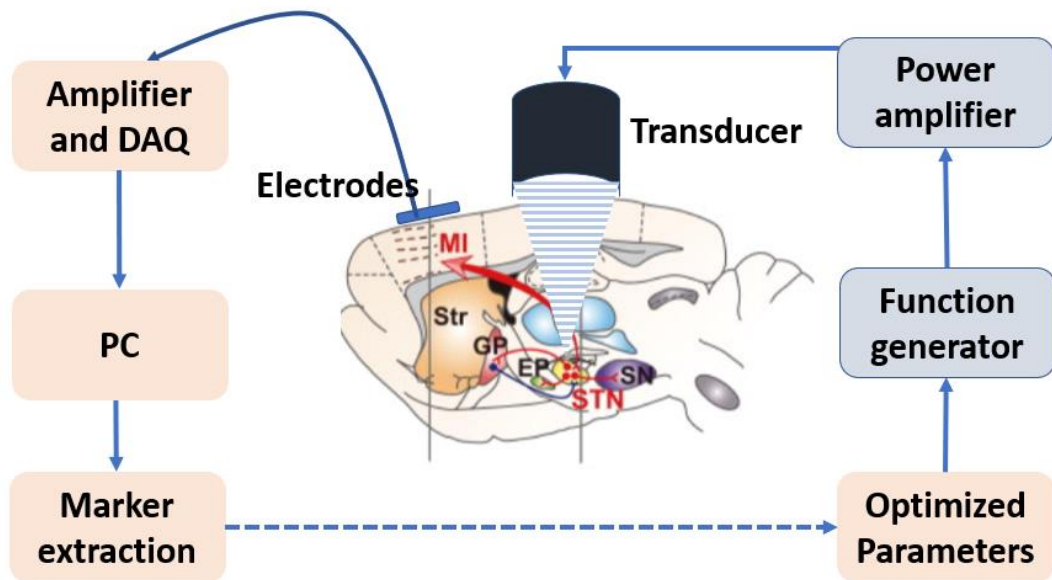


Figure 30 one of the possible future development of ultrasound based closed loop stimulation system for targeting Dopaminergic neurons.

2. Challenges

For the MscL based ultrasonic brain stimulation toolkit, it is possible to make it a pure non-invasive brain stimulation strategy by three different strategies: a) using different serum type of the virus, as reported by a research group in Caltech, rAAV/PhP.eb

can go across the BBB and infect neurons effectively, making possible to eliminate the viral infection in the brain; b) transiently open BBB by using microbubble facilitated ultrasound pulsation; c) using Cre dependent MscL transgenic mice which can be a great mice model for investigate nice questions. In addition, the clinical translation still need to be evaluated by three aspects: the ultrasound energy delivery, the viral carrier such as rAAV/PhP.eb, and the effects of expression of MscL. Ultrasound has been utilized an imaging modality for a long history and recently some clinical trials have been carried out demonstrating the safety for treating AD in human patient. rAAV virus also been widely studied for gene therapy, showing great potential for translating. The key challenge is the safety issue of MscL. It is a large pore opening ion channels. The possible toxic effects need to be carefully examined. Preliminary data showed that Fig. 27, the expression of MscL with 6 weeks dose not influence the body weight of the mice with the viral infection and MscL expression giving a rough test of the biosafety of MscL expression. But future work needs to be carried out to conclude this issue (Fig. 31).

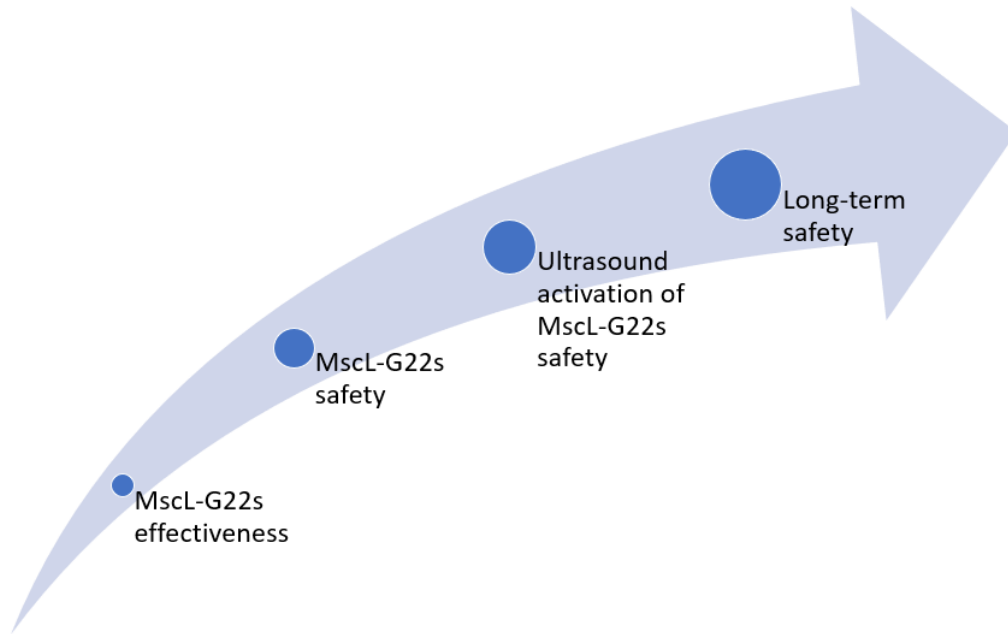


Figure 31 Road map to clinical translation

Another major challenge is to develop novel ultrasound beam control method to achieve better spatial control. However, the ultrasound focusing is diffraction limited which results in millimeter range focusing to achieve transcranial neural stimulation. The acoustic properties of human skull are heterogeneity to achieve well controlled acoustic focusing, it not only needs pre-knowledge about the structure of the skull and brain structure but also needs to map the acoustic properties simultaneously or using complicated real time feed-back strategy. Moreover, in millimeter range area, there could be many neurons inside, firing with different temporal patterns even within the same neural type. This problem seems to be unsolvable for ultrasound-based brain stimulation. One possible way is to increase the frequency of ultrasound by sacrificing penetration depth. As shown in Fig. 32, with a 100 MHz transducer, it can achieve 15 micrometer focal spot facilitating single neuron stimulation in cell cultures. It doesn't require exogenous introducing of any particles and proteins and purely compatible with optical

imaging systems, making it a good tool for studying neural functions in small animals such as zebrafish, Drosophila, and C elegans. On the other hand, to achieve better resolution, a possible way is to utilize the non-linear effects. In the previous sessions, we demonstrate the ultrasound stimulation with the help of GVs, which has unique non-linear ultrasound properties which with worth of investigate in the future.

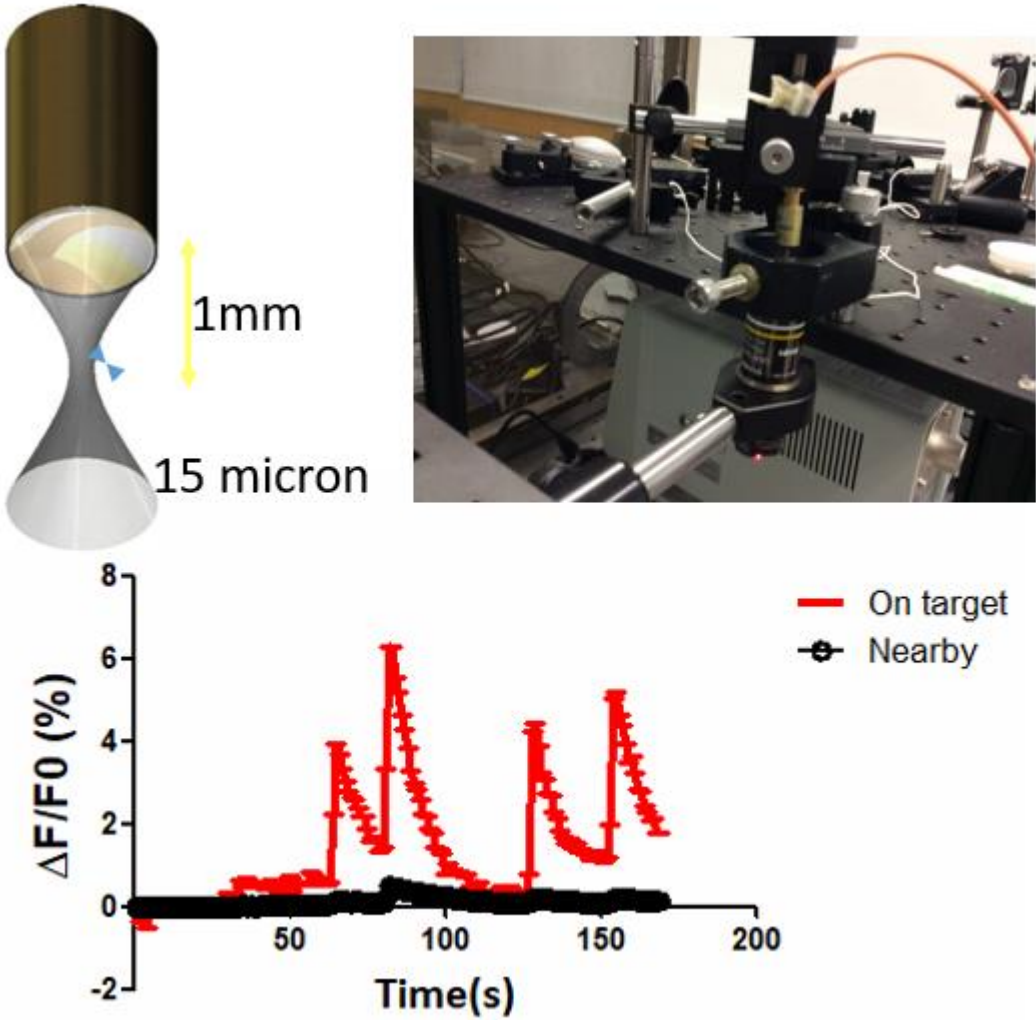


Figure 32 Single neuron activation by high frequency ultrasound

3. Philosophy

Life is like an ocean. There are always waves pushing you up and then knocking you down. These waves, however, are surprisingly amazing, without which life could be boring. There are mechanical waves producing sound and electromagnetic waves colouring our world. Fortunately, enough, I have been dealing with light waves and acoustic waves, which probably the sources make our universe fascinating in the past few years not only in the laboratory but also in daily life.

With a certain amount of physics knowledge accumulated during my undergraduate studies, I know that the wave- particle duality is probably the basic nature of our universe in fact. With long period of thinking in sleepless night, I am convinced at least by myself that what I am doing is all about the wave. There are three reasons as following: First, waves are everywhere in different forms surrounding us. It is so common that making it less interesting in our daily life. One may be familiar with water waves, sound waves, electromagnetic wave like light and heat, and others which you may not be familiar with such as brain electrical waves, gravitation waves. They are amazingly and useful for biological systems. One of the magic waves is music, a typical form of modulated sound wave. It can be produced by human and some birds, which can express and interference with our complex feelings in our mind. It is just in a simple way by modulating the sound wave amplitude and frequency. We said interference, interestingly, which can be engineered with the wave-front shaping techniques to generate designed interference pattern, for controlling the propagation of the wave to access specific locations in specific space and time. It has been one of the hottest topics in ultrasound and optical imaging. Second, assume that one factors of our university can be describe by a typical function,

one could be appreciated that this function describing our universe can be written as a Fourier transform of various wave functions which include different frequency. These two reasons grant my thought that waves are very important and should be well studied if our aim is to understand our world.

On the other hand, humans are always learning skills from our nature to develop tools to make new discoveries. As we, if correctly, our universe made of waves and affecting our environment and behaviours, people should be able to use ways to invent waves to manipulate things need to be control. Imaging that there are soils, including small golds, kicking by water waves on the beach, randomly. How we can selectively brush the soils out and leave the gold on the beach to make us rich? This kind of techniques are relied on our understanding of how water wave interacts with soils and gold differently which seems a blue-sky curiosity which we can never imaging that could yields money.

There are three key aspects needed to be considered when we are talking about a wave: its generation, the propagation and its interaction with others which could be waves, objects, and particles etc. Three things should be considered very carefully when we are talking about waves: The amplitude, frequency, and the phase. So far, we are talking about waves like a physicist. How about when we are speaking to a biologist? Can waves access to genes, proteins, cellular structures, to influence cells, even entire biological systems and at last human mind? The answer seems a yes. By using fluorescence proteins and photosensitive ion channels, one can visualize and control the cellular process by using light which is electromagnetic wave. There are lots of other examples of how we can use light to control electrical waves as well as chemical waves in biological systems.

What is the different among electromagnetic wave, acoustic wave, gravitational waves, and other waves if any? The most significant two parameters are frequency and phase which represent the unique nature of a wave. The frequency is a determinate of wavelength of a wave which can then influence the probability of its interaction with other objects. Only a wave whose wavelength is close to the object acting on could interact with it. However, if you are thinking of a sand on the beach which are washed by water waves, you will find that they can be pushed backward to the beach. The sand is much smaller than the water wave. When I was trying to understand the mechanism of ultrasound-cell interaction, I will always think of this situation. On the other hand, the phase is also a magic parameter. In quantum mechanics, a particle or a wave can be described by a function with amplitude and imaginary phase. It gives us a way to manipulate the wave propagation by engineering the phase, as aforementioned.

It is hard to tell all the nice things of a wave in a short sentence. In the previous sessions, a mechanical wave and its nice applications have been demonstrated.

References

1. Greely HT, Grady C, Ramos KM, Chiong W, Eberwine J, Farahany NA, et al. Neuroethics Guiding Principles for the NIH BRAIN Initiative. *J Neurosci*. 2018;38(50):10586-8.
2. The impact of the NIH BRAIN Initiative. *Nat Methods*. 2018;15(11):839.
3. Koroshetz W, Gordon J, Adams A, Beckel-Mitchener A, Churchill J, Farber G, et al. The State of the NIH BRAIN Initiative. *J Neurosci*. 2018;38(29):6427-38.
4. Mott MC, Gordon JA, Koroshetz WJ. The NIH BRAIN Initiative: Advancing neurotechnologies, integrating disciplines. *PLoS Biol*. 2018;16(11):e3000066.
5. Alivisatos AP, Chun M, Church GM, Greenspan RJ, Roukes ML, Yuste R. The brain activity map project and the challenge of functional connectomics. *Neuron*. 2012;74(6):970-4.
6. Alivisatos AP, Andrews AM, Boyden ES, Chun M, Church GM, Deisseroth K, et al. Nanotools for neuroscience and brain activity mapping. *ACS Nano*. 2013;7(3):1850-66.
7. Zhang F, Aravanis AM, Adamantidis A, de Lecea L, Deisseroth K. Circuit-breakers: optical technologies for probing neural signals and systems. *Nature Reviews Neuroscience*. 2007;8(8):577-81.
8. Zhang F. Circuit-Breakers: Optical Technologies for Probing Neural Signals and Systems. *J Physiol Sci*. 2009;59:37-.
9. Luan S, Williams I, Nikolic K, Constandinou TG. Neuromodulation: present and emerging methods. *Front Neuroeng*. 2014;7:27.
10. Temel Y, Jahanshahi A. Neuroscience. Treating brain disorders with neuromodulation. *Science*. 2015;347(6229):1418-9.
11. Bernstein JG, Garrity PA, Boyden ES. Optogenetics and thermogenetics: technologies for controlling the activity of targeted cells within intact neural circuits. *Current Opinion in Neurobiology*. 2012;22(1):61-71.
12. Hauser M. Optogenetics: the age of light. *Nat Methods*. 2014;11(10):1012-4.
13. Adamantidis A, Arber S, Bains JS, Bamberg E, Bonci A, Buzsaki G, et al. Optogenetics: 10 years after ChR2 in neurons-views from the community. *Nature Neuroscience*. 2015;18(9):1202-12.

14. Adamantidis A, Arber S, Bains JS, Bamberg E, Bonci A, Buzsaki G, et al. Optogenetics: 10 years after ChR2 in neurons--views from the community. *Nat Neurosci.* 2015;18(9):1202-12.
15. Chen YJ, Xiong M, Zhang SC. Illuminating Parkinson's therapy with optogenetics. *Nature Biotechnology.* 2015;33(2):149-50.
16. Deisseroth K. Optogenetics: 10 years of microbial opsins in neuroscience. *Nature Neuroscience.* 2015;18(9):1213-25.
17. Deisseroth K. Optogenetics: 10 years of microbial opsins in neuroscience. *Nat Neurosci.* 2015;18(9):1213-25.
18. Govorunova EG, Sineshchekov OA, Janz R, Liu X, Spudich JL. NEUROSCIENCE. Natural light-gated anion channels: A family of microbial rhodopsins for advanced optogenetics. *Science.* 2015;349(6248):647-50.
19. Hososhima S, Yuasa H, Ishizuka T, Hoque MR, Yamashita T, Yamanaka A, et al. Near-infrared (NIR) up-conversion optogenetics. *Sci Rep.* 2015;5:16533.
20. Steinbeck JA, Choi SJ, Mrejeru A, Ganat Y, Deisseroth K, Sulzer D, et al. Optogenetics enables functional analysis of human embryonic stem cell-derived grafts in a Parkinson's disease model. *Nature Biotechnology.* 2015;33(2):204-9.
21. Peralvarez-Marin A, Garriga P. Optogenetics Comes of Age: Novel Inhibitory Light-Gated Anionic Channels Allow Efficient Silencing of Neural Function. *Chembiochem.* 2016;17(3):204-6.
22. Delbeke J, Hoffman L, Mols K, Braeken D, Prodanov D. And Then There Was Light: Perspectives of Optogenetics for Deep Brain Stimulation and Neuromodulation. *Front Neurosci.* 2017;11:663.
23. Hernandez LF, Castela I, Ruiz-DeDiego I, Obeso JA, Moratalla R. Striatal Activation by Optogenetics Induces Dyskinesias in the 6-Hydroxydopamine Rat Model of Parkinson Disease. *Movement Disord.* 2017;32(4):530-7.
24. Wang ST, Kugelman T, Buch A, Herman M, Han Y, Karakatsani ME, et al. Non-invasive, Focused Ultrasound-Facilitated Gene Delivery for Optogenetics. *Sci Rep-Uk.* 2017;7.
25. Wallace SL, Kelley RS, Mehta S, Descalzi G, Fantl JA, Ascher-Walsh C. Transdermal light neuromodulation: Optogenetics in the murine urinary tract. *Neurourol Urodyn.* 2018;37(4):1281-5.

26. Chung S, Weber F, Zhong P, Tan CL, Nguyen TN, Beier KT, et al. Identification of preoptic sleep neurons using retrograde labelling and gene profiling. *Nature*. 2017;545(7655):477-+.
27. Weber F, Dan Y. Circuit-based interrogation of sleep control. *Nature*. 2016;538(7623):51-9.
28. Kay M, Wagner S. Analysis of social behavior deficits in a rat model of autism spectrum disorders. *J Mol Neurosci*. 2014;53:S67-S8.
29. Smeesters D, Wheeler SC, Kay AC. Indirect Prime-to-Behavior Effects: The Role of Perceptions of the Self, Others, and Situations in Connecting Primed Constructs to Social Behavior. *Adv Exp Soc Psychol*. 2010;42:259-317.
30. Tonegawa S, Pignatelli M, Roy DS, Ryan TJ. Memory engram storage and retrieval. *Current Opinion in Neurobiology*. 2015;35:101-9.
31. Liu X, Ramirez S, Pang PT, Puryear CB, Govindarajan A, Deisseroth K, et al. Optogenetic stimulation of a hippocampal engram activates fear memory recall. *Nature*. 2012;484(7394):381-U415.
32. Tonegawa S. Mammalian Learning and Memory Studied by Gene Targeting. *DNA: The Double Helix*. 1995;758:213-7.
33. Hsu WY, Ku Y, Zanto TP, Gazzaley A. Effects of noninvasive brain stimulation on cognitive function in healthy aging and Alzheimer's disease: a systematic review and meta-analysis. *Neurobiol Aging*. 2015;36(8):2348-59.
34. Lee J, Jin Y, Oh S, Lim T, Yoon B. Noninvasive brain stimulation over dorsolateral prefrontal cortex for pain perception and executive function in aging. *Arch Gerontol Geriatr*. 2018.
35. Polania R, Nitsche MA, Ruff CC. Studying and modifying brain function with non-invasive brain stimulation. *Nat Neurosci*. 2018;21(2):174-87.
36. Chen S, Weitemier AZ, Zeng X, He L, Wang X, Tao Y, et al. Near-infrared deep brain stimulation via upconversion nanoparticle-mediated optogenetics. *Science*. 2018;359(6376):679-84.
37. Shoham S. Optogenetics meets optical wavefront shaping. *Nat Methods*. 2010;7(10):798-9.

38. Grossman N, Bono D, Dedic N, Kodandaramaiah SB, Rudenko A, Suk HJ, et al. Noninvasive Deep Brain Stimulation via Temporally Interfering Electric Fields. *Cell*. 2017;169(6):1029-41 e16.
39. Ye X, Liu H, Qiao Y, Chen X. Enhancement of surface plasmon polariton excitation via feedback-based wavefront shaping. *Opt Lett*. 2018;43(24):6021-4.
40. Jang M, Horie Y, Shibukawa A, Brake J, Liu Y, Kamali SM, et al. Wavefront shaping with disorder-engineered metasurfaces. *Nat Photonics*. 2018;12:84-90.
41. Yoon J, Lee K, Park J, Park Y. Measuring optical transmission matrices by wavefront shaping. *Opt Express*. 2015;23(8):10158-67.
42. Behrens S, Daffertshofer M, Spiegel D, Hennerici M. Low-frequency ultrasound enhances thrombolysis through the skull. *Stroke*. 1998;29(1):331-.
43. Behrens S, Daffertshofer M, Spiegel D, Hennerici M. Low-frequency, low-intensity ultrasound accelerates thrombolysis through the skull. *Ultrasound Med Biol*. 1999;25(2):269-73.
44. Clement GT, White J, Hynynen K. Investigation of a large-area phased array for focused ultrasound surgery through the skull. *Physics in Medicine and Biology*. 2000;45(4):1071-83.
45. Clement GT, Hynynen K. A non-invasive method for focusing ultrasound through the human skull. *Physics in Medicine and Biology*. 2002;47(8):1219-36.
46. Clement GT, White PJ, Hynynen K. Enhanced ultrasound transmission through the human skull using shear mode conversion. *Journal of the Acoustical Society of America*. 2004;115(3):1356-64.
47. Tyler WJ, Tufail Y, Finsterwald M, Tauchmann ML, Olson EJ, Majestic C. Remote excitation of neuronal circuits using low-intensity, low-frequency ultrasound. *PLoS One*. 2008;3(10):e3511.
48. Tufail Y, Matyushov A, Baldwin N, Tauchmann ML, Georges J, Yoshihiro A, et al. Transcranial pulsed ultrasound stimulates intact brain circuits. *Neuron*. 2010;66(5):681-94.
49. Tufail Y, Yoshihiro A, Pati S, Li MM, Tyler WJ. Ultrasonic neuromodulation by brain stimulation with transcranial ultrasound. *Nat Protoc*. 2011;6(9):1453-70.

50. Tyler WJ. Noninvasive neuromodulation with ultrasound? A continuum mechanics hypothesis. *Neuroscientist*. 2011;17(1):25-36.
51. Liu Y, Song Y, Qin SC. Preliminary study of diagnostic ultrasound associated with microbubbles to open the rat blood brain barrier through the skull. *Brain Injury*. 2012;26(4-5):402-3.
52. Deffieux T, Younan Y, Wattiez N, Tanter M, Pouget P, Aubry JF. Low-intensity focused ultrasound modulates monkey visuomotor behavior. *Curr Biol*. 2013;23(23):2430-3.
53. Legon W, Sato TF, Opitz A, Mueller J, Barbour A, Williams A, et al. Transcranial focused ultrasound modulates the activity of primary somatosensory cortex in humans. *Nat Neurosci*. 2014;17(2):322-9.
54. Panczykowski DM, Monaco EA, Friedlander RM. Transcranial Focused Ultrasound Modulates the Activity of Primary Somatosensory Cortex in Humans. *Neurosurgery*. 2014;74(6):N8-N.
55. Kubanek J, Shi J, Marsh J, Chen D, Deng C, Cui J. Ultrasound modulates ion channel currents. *Sci Rep*. 2016;6:24170.
56. Kubanek J, Shukla P, Das A, Baccus SA, Goodman MB. Ultrasound Elicits Behavioral Responses through Mechanical Effects on Neurons and Ion Channels in a Simple Nervous System. *Journal of Neuroscience*. 2018;38(12):3081-91.
57. Ye PP, Brown JR, Pauly KB. Frequency Dependence of Ultrasound Neurostimulation in the Mouse Brain. *Ultrasound Med Biol*. 2016;42(7):1512-30.
58. Leinenga G, Langton C, Nisbet R, Gotz J. Ultrasound treatment of neurological diseases - current and emerging applications. *Nature Reviews Neurology*. 2016;12(3):161-74.
59. King RL, Brown JR, Newsome WT, Pauly KB. Effective parameters for ultrasound-induced in vivo neurostimulation. *Ultrasound Med Biol*. 2013;39(2):312-31.
60. Leinenga G, Gotz J. Scanning ultrasound removes amyloid-beta and restores memory in an Alzheimer's disease mouse model. *Sci Transl Med*. 2015;7(278):278ra33.
61. Lee W, Lee SD, Park MY, Foley L, Purcell-Estabrook E, Kim H, et al. Image-Guided Focused Ultrasound-Mediated Regional Brain Stimulation in Sheep. *Ultrasound Med Biol*. 2016;42(2):459-70.

62. Hadjisavvas V, Mylonas N, Ioannides K, Damianou C. An MR-compatible phantom for evaluating the propagation of high intensity focused ultrasound through the skull. *Aip Conf Proc.* 2012;1481:119-24.
63. Park TY, Pahk KJ, Kim H. A novel numerical approach to stimulation of a specific brain region using transcranial focused ultrasound. *Conf Proc IEEE Eng Med Biol Soc.* 2018;2018:3697-700.
64. Seok C, Ali Z, Yamaner FY, Sahin M, Oralkan O. Towards an Untethered Ultrasound Beamforming System for Brain Stimulation in Behaving Animals. *Conf Proc IEEE Eng Med Biol Soc.* 2018;2018:1596-9.
65. Wang TR, Dallapiazza RF, Moosa S, Huss D, Shah BB, Elias WJ. Thalamic Deep Brain Stimulation Salvages Failed Focused Ultrasound Thalamotomy for Essential Tremor: A Case Report. *Stereotact Funct Neurosurg.* 2018;96(1):60-4.
66. Su WS, Wu CH, Chen SF, Yang FY. Transcranial ultrasound stimulation promotes brain-derived neurotrophic factor and reduces apoptosis in a mouse model of traumatic brain injury. *Brain Stimul.* 2017;10(6):1032-41.
67. Guo T, Li H, Lv Y, Lu H, Niu J, Sun J, et al. Pulsed Transcranial Ultrasound Stimulation Immediately After The Ischemic Brain Injury is Neuroprotective. *IEEE Trans Biomed Eng.* 2015;62(10):2352-7.
68. Kim H, Chiu A, Lee SD, Fischer K, Yoo SS. Focused ultrasound-mediated non-invasive brain stimulation: examination of sonication parameters. *Brain Stimul.* 2014;7(5):748-56.
69. Han S, Kim M, Kim H, Shin H, Youn I. Ketamine Inhibits Ultrasound Stimulation-Induced Neuromodulation by Blocking Cortical Neuron Activity. *Ultrasound Med Biol.* 2018;44(3):635-46.
70. Airan RD, Butts Pauly K. Hearing out Ultrasound Neuromodulation. *Neuron.* 2018;98(5):875-7.
71. Guo H, Hamilton M, 2nd, Offutt SJ, Gloeckner CD, Li T, Kim Y, et al. Ultrasound Produces Extensive Brain Activation via a Cochlear Pathway. *Neuron.* 2018;98(5):1020-30 e4.
72. Zhou Y, Han X, Jing X, Chen Y. Construction of Silica-Based Micro/Nanoplatfoms for Ultrasound Theranostic Biomedicine. *Adv Healthc Mater.* 2017;6(18).

73. Jenssen C, Gilja OH, Serra AL, Piscaglia F, Dietrich CF, Rudd L, et al. European Federation of Societies for Ultrasound in Medicine and Biology (EFSUMB) Policy Document Development Strategy - Clinical Practice Guidelines, Position Statements and Technological Reviews. *Ultrasound Int Open*. 2019;5(1):E2-E10.
74. Ferraioli G, Wong VW, Castera L, Berzigotti A, Sporea I, Dietrich CF, et al. Liver Ultrasound Elastography: An Update to the World Federation for Ultrasound in Medicine and Biology Guidelines and Recommendations. *Ultrasound Med Biol*. 2018;44(12):2419-40.
75. Dietrich CF, Horn R, Morf S, Chiorean L, Dong Y, Cui XW, et al. Ultrasound-guided central vascular interventions, comments on the European Federation of Societies for Ultrasound in Medicine and Biology guidelines on interventional ultrasound. *J Thorac Dis*. 2016;8(9):E851-E68.
76. Tourette C, Tron E, Mallet S, Levy-Mozziconacci A, Bonnefont JP, D'Ercole C, et al. Three-dimensional ultrasound prenatal diagnosis of congenital ichthyosis: contribution of molecular biology. *Prenat Diagn*. 2012;32(5):498-500.
77. Delorme S, Krix M. Contrast-enhanced ultrasound for examining tumor biology. *Cancer Imaging*. 2006;6:148-52.
78. Nicolaides AN. Epidemiology, ultrasound and molecular biology in atherosclerosis--can we bridge the gaps? *Curr Med Res Opin*. 2000;16 Suppl 1:s2.
79. Kinlay S. What has intravascular ultrasound taught us about plaque biology? *Curr Atheroscler Rep*. 2001;3(3):260-6.
80. Miller AD, Chama A, Louw TM, Subramanian A, Viljoen HJ. Frequency sensitive mechanism in low-intensity ultrasound enhanced bioeffects. *PLoS One*. 2017;12(8):e0181717.
81. Goertz DE. An overview of the influence of therapeutic ultrasound exposures on the vasculature: high intensity ultrasound and microbubble-mediated bioeffects. *Int J Hyperthermia*. 2015;31(2):134-44.
82. Al-Mahrouki AA, Karshafian R, Giles A, Czarnota GJ. Bioeffects of ultrasound-stimulated microbubbles on endothelial cells: gene expression changes associated with radiation enhancement in vitro. *Ultrasound Med Biol*. 2012;38(11):1958-69.

83. Wahab RA, Choi M, Liu Y, Krauthamer V, Zderic V, Myers MR. Mechanical bioeffects of pulsed high intensity focused ultrasound on a simple neural model. *Med Phys*. 2012;39(7):4274-83.
84. Hassan MA, Campbell P, Kondo T. The role of Ca(2+) in ultrasound-elicited bioeffects: progress, perspectives and prospects. *Drug Discov Today*. 2010;15(21-22):892-906.
85. ter Haar G. Ultrasound bioeffects and safety. *Proc Inst Mech Eng H*. 2010;224(2):363-73.
86. Miller DL, Averkiou MA, Brayman AA, Everbach EC, Holland CK, Wible JH, Jr., et al. Bioeffects considerations for diagnostic ultrasound contrast agents. *J Ultrasound Med*. 2008;27(4):611-32; quiz 33-6.
87. Dalecki D. Mechanical bioeffects of ultrasound. *Annu Rev Biomed Eng*. 2004;6:229-48.
88. Suhr D, Brummer F, Irmer U, Wurster C, Eisenmenger W, Hulser DF. Bioeffects of diagnostic ultrasound in vitro. *Ultrasonics*. 1996;34(2-5):559-61.
89. Sapozhnikov OA, Tsysar SA, Khokhlova VA, Kreider W. Acoustic holography as a metrological tool for characterizing medical ultrasound sources and fields. *J Acoust Soc Am*. 2015;138(3):1515-32.
90. Chardon G, Daudet L, Peillot A, Ollivier F, Bertin N, Gribonval R. Near-field acoustic holography using sparse regularization and compressive sampling principles. *J Acoust Soc Am*. 2012;132(3):1521-34.
91. Jacobsen F, Moreno-Pescador G, Fernandez-Grande E, Hald J. Near field acoustic holography with microphones on a rigid sphere (L). *J Acoust Soc Am*. 2011;129(6):3461-4.
92. Zhang YB, Jacobsen F, Bi CX, Chen XZ. Near field acoustic holography based on the equivalent source method and pressure-velocity transducers. *J Acoust Soc Am*. 2009;126(3):1257-63.
93. Melde K, Mark AG, Qiu T, Fischer P. Holograms for acoustics. *Nature*. 2016;537(7621):518-22.
94. Menz MD, Ye P, Firouzi K, Pauly KB, Khuri-Yakub BT, Baccus SA. Physical mechanisms of ultrasonic neurostimulation of the retina. *bioRxiv*. 2017:231449.
95. Kubanek J, Shukla P, Das A, Baccus SA, Goodman MB. Ultrasound elicits behavioral responses through mechanical effects on neurons and ion channels in a simple nervous system. *Journal of Neuroscience*. 2018:1458-17.

96. Basu D, Haswell ES. Plant mechanosensitive ion channels: an ocean of possibilities. *Current opinion in plant biology*. 2017;40:43-8.
97. Gao Q, Cooper PR, Walmsley AD, Scheven BA. Role of Piezo Channels in Ultrasound-stimulated Dental Stem Cells. *Journal of endodontics*. 2017;43(7):1130-6.
98. Liu W-W, Li P-C. Ultrasound Modulates Piezo1-Mediated Mechanotransduction in Neuro2A Cells. *Biophysical Journal*. 2018;114(3):113a.
99. Ye J, Tang S, Meng L, Li X, Wen X, Chen S, et al. Ultrasonic Control of Neural Activity through Activation of the Mechanosensitive Channel MscL. *Nano letters*. 2018.
100. Darrow DP. Focused Ultrasound for Neuromodulation. *Neurotherapeutics*. 2018:1-12.
101. Li F, Yang C, Yuan F, Liao D, Li T, Guilak F, et al. Dynamics and mechanisms of intracellular calcium waves elicited by tandem bubble-induced jetting flow. *Proceedings of the National Academy of Sciences*. 2018;115(3):E353-E62.
102. Pan Y, Yoon S, Sun J, Huang Z, Lee C, Allen M, et al. Mechanogenetics for the remote and noninvasive control of cancer immunotherapy. *Proceedings of the National Academy of Sciences*. 2018:201714900.
103. Ibsen S, Tong A, Schutt C, Esener S, Chalasani SH. Sonogenetics is a non-invasive approach to activating neurons in *Caenorhabditis elegans*. *Nature communications*. 2015;6:8264.
104. Prieto ML, Firouzi K, Khuri-Yakub BT, Maduke M. Activation of Piezo1 but Not Nav1.2 Channels by Ultrasound at 43 MHz. *Ultrasound in medicine & biology*. 2018;44(6):1217-32.
105. Zhou W, Wang J, Wang K, Huang B, Niu L, Li F, et al. Ultrasound neuro-modulation chip: activation of sensory neurons in *Caenorhabditis elegans* by surface acoustic waves. *Lab on a Chip*. 2017;17(10):1725-31.
106. MECHANOBIOLOGY SO. Forces in cell biology. *Nature Cell Biology*. 2017;19(6):579.
107. Tyler WJ. The mechanobiology of brain function. *Nature Reviews Neuroscience*. 2012;13(12):867.
108. Ibsen S, Tong A, Schutt C, Esener S, Chalasani SH. Sonogenetics is a non-invasive approach to activating neurons in *Caenorhabditis elegans*. *Nature Communications*. 2015;6.

109. Shapiro MG, Homma K, Villarreal S, Richter C-P, Bezanilla F. Infrared light excites cells by changing their electrical capacitance. *Nature communications*. 2012;3:736.
110. Prieto ML, Oralkan Ö, Khuri-Yakub BT, Maduke MC. Dynamic response of model lipid membranes to ultrasonic radiation force. *PLoS One*. 2013;8(10):e77115.
111. Krasovitski B, Frenkel V, Shoham S, Kimmel E. Intramembrane cavitation as a unifying mechanism for ultrasound-induced bioeffects. *Proceedings of the National Academy of Sciences*. 2011:201015771.
112. Plaksin M, Shoham S, Kimmel E. Intramembrane cavitation as a predictive bio-piezoelectric mechanism for ultrasonic brain stimulation. *Physical review X*. 2014;4(1):011004.
113. Hines JH, Ravanelli AM, Schwindt R, Scott EK, Appel B. Neuronal activity biases axon selection for myelination in vivo. *Nature neuroscience*. 2015;18(5):683.
114. Brady ST, Morfini GA. Regulation of motor proteins, axonal transport deficits and adult-onset neurodegenerative diseases. *Neurobiol Dis*. 2017;105:273-82.
115. Millecamps S, Julien JP. Axonal transport deficits and neurodegenerative diseases. *Nat Rev Neurosci*. 2013;14(3):161-76.
116. Mammoto T, Mammoto A, Ingber DE. Mechanobiology and developmental control. *Annu Rev Cell Dev Biol*. 2013;29:27-61.
117. Reilly GC, Engler AJ. Intrinsic extracellular matrix properties regulate stem cell differentiation. *J Biomech*. 2010;43(1):55-62.
118. Noriega S, Hasanova G, Subramanian A. The effect of ultrasound stimulation on the cytoskeletal organization of chondrocytes seeded in three-dimensional matrices. *Cells Tissues Organs*. 2013;197(1):14-26.
119. Cox CD, Bae C, Ziegler L, Hartley S, Nikolova-Krstevski V, Rohde PR, et al. Removal of the mechanoprotective influence of the cytoskeleton reveals PIEZO1 is gated by bilayer tension. *Nat Commun*. 2016;7:10366.
120. Ray PD, Huang BW, Tsuji Y. Reactive oxygen species (ROS) homeostasis and redox regulation in cellular signaling. *Cell Signal*. 2012;24(5):981-90.
121. Duco W, Grosso V, Zaccari D, Soltermann AT. Generation of ROS mediated by mechanical waves (ultrasound) and its possible applications. *Methods*. 2016;109:141-8.

122. Pan X, Bai L, Wang H, Wu Q, Wang H, Liu S, et al. Metal-Organic-Framework-Derived Carbon Nanostructure Augmented Sonodynamic Cancer Therapy. *Adv Mater.* 2018;30(23):e1800180.
123. Song L, Huang Y, Hou X, Yang Y, Kala S, Qiu Z, et al. PINK1/Parkin-Mediated Mitophagy Promotes Resistance to Sonodynamic Therapy. *Cell Physiol Biochem.* 2018;49(5):1825-39.
124. Bourdeau RW, Lee-Gosselin A, Lakshmanan A, Farhadi A, Kumar SR, Nety SP, et al. Acoustic reporter genes for noninvasive imaging of microorganisms in mammalian hosts. *Nature.* 2018;553(7686):86-90.
125. Postema M, Bouakaz A. Acoustic bubbles in therapy: Recent advances with medical microbubbles, clouds, and harmonic antibubbles Preface. *Appl Acoust.* 2018;140:150-2.
126. Healey AJ, Sontum PC, Kvale S, Eriksen M, Bendiksen R, Tornes A, et al. Acoustic Cluster Therapy: In Vitro and Ex Vivo Measurement of Activated Bubble Size Distribution and Temporal Dynamics. *Ultrasound Med Biol.* 2016;42(5):1145-66.
127. Zhang SY, Shang SQ, Han YQ, Gu CM, Wu S, Liu SH, et al. Ex Vivo and In Vivo Monitoring and Characterization of Thermal Lesions by High-Intensity Focused Ultrasound and Microwave Ablation Using Ultrasonic Nakagami Imaging. *Ieee T Med Imaging.* 2018;37(7):1701-10.
128. Chen R, Romero G, Christiansen MG, Mohr A, Anikeeva P. Wireless magnetothermal deep brain stimulation. *Science.* 2015;347(6229):1477-80.
129. Plaksin M, Kimmel E, Shoham S. Cell-Type-Selective Effects of Intramembrane Cavitation as a Unifying Theoretical Framework for Ultrasonic Neuromodulation. *Eneuro.* 2016;3(3).
130. Gomez JL, Bonaventura J, Lesniak W, Mathews WB, Sysa-Shah P, Rodriguez LA, et al. Chemogenetics revealed: DREADD occupancy and activation via converted clozapine. *Science.* 2017;357(6350):503-+.
131. Szablowski JO, Lee-Gosselin A, Lue B, Malounda D, Shapiro MG. Acoustically targeted chemogenetics for the non-invasive control of neural circuits. *Nat Biomed Eng.* 2018;2(7):475-84.

132. Lipsman N, Meng Y, Bethune AJ, Huang YX, Lam B, Masellis M, et al. Blood-brain barrier opening in Alzheimer's disease using MR-guided focused ultrasound. *Nature Communications*. 2018;9.
133. Burgess A, Dubey S, Yeung S, Hough O, Eterman N, Aubert I, et al. Alzheimer Disease in a Mouse Model: MR Imaging-guided Focused Ultrasound Targeted to the Hippocampus Opens the Blood-Brain Barrier and Improves Pathologic Abnormalities and Behavior. *Radiology*. 2014;273(3):736-45.
134. Trivedi N, Stabley DR, Cain B, Howell D, Laumonnerie C, Ramahi JS, et al. Drebrin-mediated microtubule-actomyosin coupling steers cerebellar granule neuron nucleokinesis and migration pathway selection. *Nat Commun*. 2017;8:14484.
135. Musiek FE. Probing brain function with acoustic stimuli. *ASHA*. 1989;31(8):100-6, 55.
136. Poldrack RA, Farah MJ. Progress and challenges in probing the human brain. *Nature*. 2015;526(7573):371-9.
137. Lerner TN, Ye L, Deisseroth K. Communication in Neural Circuits: Tools, Opportunities, and Challenges. *Cell*. 2016;164(6):1136-50.
138. Schinder AF, Lanuza GM. Whispering neurons fuel cortical highways. *Science*. 2018;360(6386):265-6.
139. Sick TJ, Perez-Pinzon MA. Optical methods for probing mitochondrial function in brain slices. *Methods*. 1999;18(2):104-8.
140. Rashid AJ, Yan C, Mercaldo V, Hsiang HL, Park S, Cole CJ, et al. Competition between engrams influences fear memory formation and recall. *Science*. 2016;353(6297):383-7.
141. Roy DS, Arons A, Mitchell TI, Pignatelli M, Ryan TJ, Tonegawa S. Memory retrieval by activating engram cells in mouse models of early Alzheimer's disease. *Nature*. 2016;531(7595):508-12.
142. Hashikawa K, Hashikawa Y, Falkner A, Lin D. The neural circuits of mating and fighting in male mice. *Curr Opin Neurobiol*. 2016;38:27-37.
143. Anderson DJ. Circuit modules linking internal states and social behaviour in flies and mice. *Nat Rev Neurosci*. 2016;17(11):692-704.
144. Steinberg EE, Christoffel DJ, Deisseroth K, Malenka RC. Illuminating circuitry relevant to psychiatric disorders with optogenetics. *Curr Opin Neurobiol*. 2015;30:9-16.
145. Gao K. Expanding the optogenetics toolkit. *Nat Methods*. 2018;15(12):1003.

146. Brown J, Behnam R, Coddington L, Tervo DGR, Martin K, Proskurin M, et al. Expanding the Optogenetics Toolkit by Topological Inversion of Rhodopsins. *Cell*. 2018;175(4):1131-40 e11.
147. Berndt A, Deisseroth K. OPTOGENETICS. Expanding the optogenetics toolkit. *Science*. 2015;349(6248):590-1.
148. Kim HK, Alexander AL, Soltesz I. Optogenetics: Lighting a Path from the Laboratory to the Clinic. *Optogenetics: A Roadmap*: Springer; 2018. p. 277-300.
149. Terraneo A, Leggio L, Saladini M, Ermani M, Bonci A, Gallimberti L. Transcranial magnetic stimulation of dorsolateral prefrontal cortex reduces cocaine use: a pilot study. *Eur Neuropsychopharm*. 2016;26(1):37-44.
150. Bikson M, Grossman P, Thomas C, Zannou AL, Jiang J, Adnan T, et al. Safety of transcranial direct current stimulation: evidence based update 2016. *Brain Stimul*. 2016;9(5):641-61.
151. Vitek S, Vortman K. Asymmetric ultrasound phased-array transducer for dynamic beam steering to ablate tissues in MRI. *Google Patents*; 2015.
152. Deffieux T, Wattiez N, Tanter M, Pouget P, Aubry J-F, Younan Y. Low intensity focused ultrasound modulates monkey visuomotor behavior. *Journal of Therapeutic Ultrasound*. 2015;3(S1):O25.
153. Moore ME, Loft JM, Clegern WC, Wisor JP. Manipulating neuronal activity in the mouse brain with ultrasound: A comparison with optogenetic activation of the cerebral cortex. *Neuroscience letters*. 2015;604:183-7.
154. Kim H, Park MY, Lee SD, Lee W, Chiu A, Yoo S-S. Suppression of EEG visual-evoked potentials in rats via neuromodulatory focused ultrasound. *Neuroreport*. 2015;26(4):211.
155. Hakimova H, Kim S, Chu K, Lee SK, Jeong B, Jeon D. Ultrasound stimulation inhibits recurrent seizures and improves behavioral outcome in an experimental model of mesial temporal lobe epilepsy. *Epilepsy & Behavior*. 2015;49:26-32.
156. Ranade SS, Syeda R, Patapoutian A. Mechanically activated ion channels. *Neuron*. 2015;87(6):1162-79.
157. Brohawn SG. How ion channels sense mechanical force: insights from mechanosensitive K2P channels TRAAK, TREK1, and TREK2. *Annals of the New York Academy of Sciences*. 2015;1352(1):20-32.

158. Schüler A, Schmitz G, Reft A, Özbek S, Thurm U, Bornberg-Bauer E. The rise and fall of TRP-N, an ancient family of mechanogated ion channels, in metazoa. *Genome biology and evolution*. 2015;7(6):1713-27.
159. Chesler AT, Szczot M. Piezo Ion Channels: Portraits of a pressure sensor. *eLife*. 2018;7:e34396.
160. Coste B, Mathur J, Schmidt M, Earley TJ, Ranade S, Petrus MJ, et al. Piezo1 and Piezo2 are essential components of distinct mechanically activated cation channels. *Science*. 2010;330(6000):55-60.
161. Lewis AH, Cui AF, McDonald MF, Grandl J. Transduction of repetitive mechanical stimuli by Piezo1 and Piezo2 ion channels. *Cell reports*. 2017;19(12):2572-85.
162. Liang X, Howard J. Structural Biology: Piezo Senses Tension through Curvature. *Current Biology*. 2018;28(8):R357-R9.
163. Syeda R, Florendo MN, Cox CD, Kefauver JM, Santos JS, Martinac B, et al. Piezo1 Channels Are Inherently Mechanosensitive. *Cell Rep*. 2016;17(7):1739-46.
164. Tufail Y, Yoshihiro A, Pati S, Li MM, Tyler WJ. Ultrasonic neuromodulation by brain stimulation with transcranial ultrasound. *nature protocols*. 2011;6(9):1453.
165. Lacroix JJ, Botello-Smith WM, Luo Y. Probing the gating mechanism of the mechanosensitive channel Piezo1 with the small molecule Yoda1. *Nature communications*. 2018;9(1):2029.
166. Lacroix JJ, Botello-Smith WM, Luo Y. Probing the gating mechanism of the mechanosensitive channel Piezo1 with the small molecule Yoda1. *Nat Commun*. 2018;9(1):2029.
167. Evans EL, Cuthbertson K, Endesh N, Rode B, Blythe NM, Hyman AJ, et al. Yoda1 analogue (Dooku1) which antagonizes Yoda1-evoked activation of Piezo1 and aortic relaxation. *Br J Pharmacol*. 2018;175(10):1744-59.
168. Dela Paz NG, Frangos JA. Yoda1-induced phosphorylation of Akt and ERK1/2 does not require Piezo1 activation. *Biochem Biophys Res Commun*. 2018;497(1):220-5.
169. Vandorpe DH, Xu C, Shmukler BE, Otterbein LE, Trudel M, Sachs F, et al. Hypoxia activates a Ca²⁺-permeable cation conductance sensitive to carbon monoxide and to GsMTx-4 in human and mouse sickle erythrocytes. *PLoS One*. 2010;5(1):e8732.

170. Bowman CL, Gottlieb PA, Suchyna TM, Murphy YK, Sachs F. Mechanosensitive ion channels and the peptide inhibitor GsMTx-4: history, properties, mechanisms and pharmacology. *Toxicon*. 2007;49(2):249-70.
171. Jung HJ, Kim PI, Lee SK, Lee CW, Eu YJ, Lee DG, et al. Lipid membrane interaction and antimicrobial activity of GsMTx-4, an inhibitor of mechanosensitive channel. *Biochem Biophys Res Commun*. 2006;340(2):633-8.
172. Sheng M, Greenberg ME. The regulation and function of c-fos and other immediate early genes in the nervous system. *Neuron*. 1990;4(4):477-85.
173. McHugh BJ, Buttery R, Lad Y, Banks S, Haslett C, Sethi T. Integrin activation by Fam38A uses a novel mechanism of R-Ras targeting to the endoplasmic reticulum. *J Cell Sci*. 2010;123(Pt 1):51-61.
174. Yamauchi T. Neuronal Ca²⁺/calmodulin-dependent protein kinase II--discovery, progress in a quarter of a century, and perspective: implication for learning and memory. *Biol Pharm Bull*. 2005;28(8):1342-54.
175. Hardingham GE, Arnold FJ, Bading H. Nuclear calcium signaling controls CREB-mediated gene expression triggered by synaptic activity. *Nat Neurosci*. 2001;4(3):261-7.
176. Koser DE, Thompson AJ, Foster SK, Dwivedy A, Pillai EK, Sheridan GK, et al. Mechanosensing is critical for axon growth in the developing brain. *Nature neuroscience*. 2016;19(12):1592.
177. Chen R, Romero G, Christiansen MG, Mohr A, Anikeeva P. Wireless magnetothermal deep brain stimulation. *Science*. 2015;347(6229):1477-80.
178. Bystritsky A, Korb AS, Douglas PK, Cohen MS, Melega WP, Mulgaonkar AP, et al. A review of low-intensity focused ultrasound pulsation. *Brain Stimul*. 2011;4(3):125-36.
179. Soloperto A, Boccaccio A, Contestabile A, Moroni M, Hallinan GI, Palazzolo G, et al. Mechano-sensitization of mammalian neuronal networks through expression of the bacterial mechanosensitive MscL channel. *J Cell Sci*. 2018;jcs. 210393.
180. Booth IR, Blount P. The MscS and MscL families of mechanosensitive channels act as microbial emergency release valves. *Journal of bacteriology*. 2012;194(18):4802-9.
181. Gradinaru V, Thompson KR, Deisseroth K. eNpHR: a *Natronomonas halorhodopsin* enhanced for optogenetic applications. *Brain cell biology*. 2008;36(1-4):129-39.

182. Brown J, Behnam R, Coddington L, Tervo D, Martin K, Proskurin M, et al. Expanding the optogenetics toolkit by topological inversion of rhodopsins. *Cell*. 2018;175(4):1131-40. e11.
183. Chan KY, Jang MJ, Yoo BB, Greenbaum A, Ravi N, Wu W-L, et al. Engineered AAVs for efficient noninvasive gene delivery to the central and peripheral nervous systems. *Nature neuroscience*. 2017;20(8):1172.
184. Deisseroth K. Optogenetics: 10 years of microbial opsins in neuroscience. *Nature neuroscience*. 2015;18(9):1213.
185. Polania R, Nitsche MA, Ruff CC. Studying and modifying brain function with non-invasive brain stimulation. *Nature neuroscience*. 2018:1.
186. Fini M, Tyler WJ. Transcranial focused ultrasound: a new tool for non-invasive neuromodulation. *International Review of Psychiatry*. 2017;29(2):168-77.
187. Lee W, Lee SD, Park MY, Foley L, Purcell-Estabrook E, Kim H, et al. Image-guided focused ultrasound-mediated regional brain stimulation in sheep. *Ultrasound in medicine & biology*. 2016;42(2):459-70.
188. Elias WJ, Lipsman N, Ondo WG, Ghanouni P, Kim YG, Lee W, et al. A randomized trial of focused ultrasound thalamotomy for essential tremor. *New Engl J Med*. 2016;375(8):730-9.
189. Lee W, Kim H-C, Jung Y, Chung YA, Song I-U, Lee J-H, et al. Transcranial focused ultrasound stimulation of human primary visual cortex. *Sci Rep-Uk*. 2016;6:34026.
190. Guo H, Hamilton M, Offutt SJ, Gloeckner CD, Li T, Kim Y, et al. Ultrasound produces extensive brain activation via a cochlear pathway. *Neuron*. 2018.
191. Boyden ES. Optogenetics and the future of neuroscience. *Nature neuroscience*. 2015;18(9):1200.
192. Chen R, Romero G, Christiansen MG, Mohr A, Anikeeva P. Wireless magnetothermal deep brain stimulation. *Science*. 2015:1261821.
193. Chen S, Weitemier AZ, Zeng X, He L, Wang X, Tao Y, et al. Near-infrared deep brain stimulation via upconversion nanoparticle-mediated optogenetics. *Science*. 2018;359(6376):679-84.

194. Carvalho-de-Souza JL, Treger JS, Dang B, Kent SB, Pepperberg DR, Bezanilla F. Photosensitivity of neurons enabled by cell-targeted gold nanoparticles. *Neuron*. 2015;86(1):207-17.
195. Marino A, Arai S, Hou Y, Sinibaldi E, Pellegrino M, Chang Y-T, et al. Piezoelectric nanoparticle-assisted wireless neuronal stimulation. *ACS nano*. 2015;9(7):7678-89.
196. Marino A, Genchi GG, Mattoli V, Ciofani G. Piezoelectric nanotransducers: The future of neural stimulation. *Nano Today*. 2017;14:9-12.
197. Wang Y, Guo L. Nanomaterial-enabled neural stimulation. *Frontiers in neuroscience*. 2016;10:69.
198. Munshi R, Qadri SM, Zhang Q, Rubio IC, del Pino P, Pralle A. Magnetothermal genetic deep brain stimulation of motor behaviors in awake, freely moving mice. *Elife*. 2017;6:e27069.
199. Kaberniuk AA, Shemetov AA, Verkhusha VV. A bacterial phytochrome-based optogenetic system controllable with near-infrared light. *Nature methods*. 2016;13(7):591.
200. Redchuk TA, Omelina ES, Chernov KG, Verkhusha VV. Near-infrared optogenetic pair for protein regulation and spectral multiplexing. *Nature chemical biology*. 2017;13(6):633.
201. Ferrara K, Pollard R, Borden M. Ultrasound microbubble contrast agents: fundamentals and application to gene and drug delivery. *Annu Rev Biomed Eng*. 2007;9:415-47.
202. Cosgrove D. Ultrasound contrast agents: an overview. *European journal of radiology*. 2006;60(3):324-30.
203. Ibsen S, Tong A, Schutt C, Esener S, Chalasani SH. Sonogenetics is a non-invasive approach to activating neurons in *Caenorhabditis elegans*. *Nat Commun*. 2015;6:8264.
204. Quaia E. Microbubble ultrasound contrast agents: an update. *Eur Radiol*. 2007;17(8):1995-2008.
205. Yang H, Cai W, Xu L, Lv X, Qiao Y, Li P, et al. Nanobubble-Affibody: Novel ultrasound contrast agents for targeted molecular ultrasound imaging of tumor. *Biomaterials*. 2015;37:279-88.
206. Skachkov I, Luan Y, van der Steen AF, de Jong N, Kooiman K. Targeted microbubble mediated sonoporation of endothelial cells in vivo. *IEEE Trans Ultrason Ferroelectr Freq Control*. 2014;61(10):1661-7.

207. Yu H, Lin Z, Xu L, Liu D, Shen Y. Theoretical study of microbubble dynamics in sonoporation. *Ultrasonics*. 2015;61:136-44.
208. McMahon D, Poon C, Hynynen K. Evaluating the safety profile of focused ultrasound and microbubble-mediated treatments to increase blood-brain barrier permeability. *Expert Opin Drug Deliv*. 2019.
209. Dong Q, He L, Chen L, Deng Q. Opening the Blood-Brain Barrier and Improving the Efficacy of Temozolomide Treatments of Glioblastoma Using Pulsed, Focused Ultrasound with a Microbubble Contrast Agent. *Biomed Res Int*. 2018;2018:6501508.
210. Tsai HC, Tsai CH, Chen WS, Inserra C, Wei KC, Liu HL. Safety evaluation of frequent application of microbubble-enhanced focused ultrasound blood-brain-barrier opening. *Sci Rep*. 2018;8(1):17720.
211. Song KH, Harvey BK, Borden MA. State-of-the-art of microbubble-assisted blood-brain barrier disruption. *Theranostics*. 2018;8(16):4393-408.
212. Song KH, Fan AC, Hinkle JJ, Newman J, Borden MA, Harvey BK. Microbubble gas volume: A unifying dose parameter in blood-brain barrier opening by focused ultrasound. *Theranostics*. 2017;7(1):144-52.
213. Choi JJ, Feshitan JA, Baseri B, Wang S, Tung YS, Borden MA, et al. Microbubble-size dependence of focused ultrasound-induced blood-brain barrier opening in mice in vivo. *IEEE Trans Biomed Eng*. 2010;57(1):145-54.
214. Maresca D, Lakshmanan A, Lee-Gosselin A, Melis JM, Ni YL, Bourdeau RW, et al. Nonlinear ultrasound imaging of nanoscale acoustic biomolecules. *Appl Phys Lett*. 2017;110(7):073704.
215. Lakshmanan A, Farhadi A, Nety SP, Lee-Gosselin A, Bourdeau RW, Maresca D, et al. Molecular Engineering of Acoustic Protein Nanostructures. *ACS Nano*. 2016;10(8):7314-22.
216. Yang Y, Qiu Z, Hou X, Sun L. Ultrasonic Characteristics and Cellular Properties of Anabaena Gas Vesicles. *Ultrasound Med Biol*. 2017;43(12):2862-70.
217. Velikyán I, Lindhe O. Preparation and evaluation of a (^{68}Ga) -labeled RGD-containing octapeptide for noninvasive imaging of angiogenesis: biodistribution in non-human primate. *Am J Nucl Med Mol Imaging*. 2018;8(1):15-31.

218. Yang PF, Phipps MA, Newton AT, Chaplin V, Gore JC, Caskey CF, et al. Neuromodulation of sensory networks in monkey brain by focused ultrasound with MRI guidance and detection. *Sci Rep.* 2018;8(1):7993.
219. Shimizu J, Fukuda T, Abe T, Ogihara M, Kubota J, Sasaki A, et al. Ultrasound safety with midfrequency transcranial sonothrombolysis: preliminary study on normal macaca monkey brain. *Ultrasound Med Biol.* 2012;38(6):1040-50.
220. Tokuno H, Hatanaka N, Takada M, Nambu A. B-mode and color Doppler ultrasound imaging for localization of microelectrode in monkey brain. *Neurosci Res.* 2000;36(4):335-8.
221. de Hemptinne C, Swann NC, Ostrem JL, Ryapolova-Webb ES, San Luciano M, Galifianakis NB, et al. Therapeutic deep brain stimulation reduces cortical phase-amplitude coupling in Parkinson's disease. *Nat Neurosci.* 2015;18(5):779-86.
222. Li Q, Qian ZM, Arbutnott GW, Ke Y, Yung WH. Cortical effects of deep brain stimulation: implications for pathogenesis and treatment of Parkinson disease. *JAMA Neurol.* 2014;71(1):100-3.
223. Gradinaru V, Mogri M, Thompson KR, Henderson JM, Deisseroth K. Optical deconstruction of parkinsonian neural circuitry. *Science.* 2009;324(5925):354-9.
224. Miyamoto Y, Katayama S, Shigematsu N, Nishi A, Fukuda T. Striosome-based map of the mouse striatum that is conformable to both cortical afferent topography and uneven distributions of dopamine D1 and D2 receptor-expressing cells. *Brain Struct Funct.* 2018;223(9):4275-91.
225. Chen YH, Huang EY, Kuo TT, Ma HI, Hoffer BJ, Tsui PF, et al. Dopamine Release Impairment in Striatum After Different Levels of Cerebral Cortical Fluid Percussion Injury. *Cell Transplant.* 2015;24(10):2113-28.
226. Schwarcz R, Creese I, Coyle JT, Snyder SH. Dopamine receptors localised on cerebral cortical afferents to rat corpus striatum. *Nature.* 1978;271(5647):766-8.
227. da Silva JA, Tecuapetla F, Paixao V, Costa RM. Dopamine neuron activity before action initiation gates and invigorates future movements. *Nature.* 2018;554(7691):244-8.
228. Widge AS, Malone DA, Jr., Dougherty DD. Closing the Loop on Deep Brain Stimulation for Treatment-Resistant Depression. *Front Neurosci.* 2018;12:175.